

1975

KINETICS OF THE TRANSESTERIFICATION
REACTIONS OF DIMETHYL-
TEREPHTHALATE WITH ETHYLENE
GLYCOL.

JEAN. YAMANIS
University of Windsor

Follow this and additional works at: <http://scholar.uwindsor.ca/etd>

Recommended Citation

YAMANIS, JEAN., "KINETICS OF THE TRANSESTERIFICATION REACTIONS OF DIMETHYL-TEREPHTHALATE WITH ETHYLENE GLYCOL." (1975). *Electronic Theses and Dissertations*. Paper 2558.

This online database contains the full-text of PhD dissertations and Masters' theses of University of Windsor students from 1954 forward. These documents are made available for personal study and research purposes only, in accordance with the Canadian Copyright Act and the Creative Commons license—CC BY-NC-ND (Attribution, Non-Commercial, No Derivative Works). Under this license, works must always be attributed to the copyright holder (original author), cannot be used for any commercial purposes, and may not be altered. Any other use would require the permission of the copyright holder. Students may inquire about withdrawing their dissertation and/or thesis from this database. For additional inquiries, please contact the repository administrator via email (scholarship@uwindsor.ca) or by telephone at 519-253-3000ext. 3208.

KINETICS
OF THE TRANSESTERIFICATION REACTIONS OF
DIMETHYL TEREPHTHALATE WITH ETHYLENE GLYCOL

A Dissertation
Submitted to the Faculty of Graduate Studies through the
Department of Chemical Engineering in Partial Fulfillment
of the Requirements for the Degree of
Doctor of Philosophy at the
University of Windsor

by

Jean Yamanis

Windsor, Ontario
1975

© Jean Yamanis 1975
All Rights Reserved

550985

ia

Στούς Ἀγαπημένους μου Γονεῖς, Ζύζυγο καί Κόρη

To my Beloved Parents, Wife and Daughter

ABSTRACT

The objective of the present study was to establish models for the kinetics of the transesterification reactions of dimethyl terephthalate (DMT) with ethylene glycol (EG) in the presence of cation exchange resins. The study was later extended to include modeling of the kinetics of these reactions in the presence of homogeneous catalysts.

Experimental methanol data for the above reactions in the presence of Amberlite IR-120(H⁺) were obtained from a batch reactor. These preliminary data were adequately described by the following second order model

$$-\frac{1}{W} \frac{dN_A}{dt} = k C_A C_B$$

for the conversion of DMT.

Further experimental work involved the cation exchange resin Amberlyst 15, as catalyst. This part of the investigation was aided by specially developed analytical techniques. Chemical analysis of the reaction mixture was achieved by gas-liquid chromatography after hydroxy compounds were silylated. Silylation was found to be necessary in order to obtain reproducible results for the glycol esters of terephthalic acid. Five compounds were determined in the reaction liquid mixture while a sixth compound, methanol, was determined in the distillate by GLC.

Data for the Amberlyst 15 system were to be obtained from a differential recycle reactor specifically designed and built for this study. This reactor had an on-off control of the output stream which gave rise to reactor volume variability. A mathematical analysis showed that, for the first and second order kinetics considered, this reactor would attain steady state even though the reactor volume was variable. Preliminary data of transesterification indicated that the recycle reactor indeed

came to steady state. However, a shift to a batch reactor was made in order to obtain information about product distribution fast.

The batch reactor transesterification data obtained in the presence of Amberlyst 15 showed that, at the temperature of 146°C, EG dehydrates to a very significant extent. The likely product of EG dehydration, ethylene oxide, participates in several reactions the products of which render the process unselective and inefficient. For this reason further experimentation with the system was terminated.

Kinetic data of the transesterification reactions in the presence of homogeneous catalysts were obtained from the literature. Analysis of these data, which are time profiles of reaction produced methanol, was prompted by the inadequacies of previously proposed kinetic models for these reactions. The analysis led to the conclusion that oligomerization reactions are negligible for molar ratios of EG to DMT greater or equal to two and in the temperature range of 175 to 197°C. For these conditions the following two models were found to describe the data exceptionally well:

Methyl-Ester Group Model:
$$-\frac{dN_E}{dt} = 2k_1 N_C C_E C_B$$

Molecular Species Model:
$$\frac{dN_m}{dt} = 4k_1 N_C N_B (N_A + 0.5N_R) / V^2$$

The first model, based on the simplified reaction of a methyl-ester group with ethylene glycol, supplies information about methyl-ester group conversion only. The second model, based on series-parallel reactions of molecular species, provides information about methanol production and product distribution. The two models give the same information about methanol production but the second is more comprehensive.

ACKNOWLEDGEMENTS

The author wishes to express his sincere gratitude to Dr. R. Vilenchich and Dr. M. Adelman for their able technical advice. Dr. Vilenchich is also acknowledged for suggesting the research topic.

In addition, the author wishes to thank Dr. M. C. de Matherbe for his frequent advice. Thanks are also extended to the Faculty Members of the Chemical Engineering Department of this University.

Mr. G. Ryan and the staff of the Electronics Research and Design Shop of this University are acknowledged for constructing and repairing equipment needed in the experimental work.

Imperial Oil Limited is gratefully acknowledged for providing the support funds for this investigation.

Last but not least, I wish to express my feelings of appreciation for my wife, Donna, who behaved superbly in preserving harmony in our home despite my long daily hours of endeavour.

CONTENTS

ABSTRACT	iv
ACKNOWLEDGEMENTS	vi
TABLE OF CONTENTS	vii
LIST OF FIGURES	ix
LIST OF TABLES	xiii
I. INTRODUCTION	1
II. REVIEW OF HOMOGENEOUS KINETICS	4
III. PRELIMINARY INVESTIGATION WITH AMBERLITE IR-120	14
A. Experimental	14
B. Analysis of Preliminary Data	15
IV. CHEMICAL ANALYSIS	21
A. Gas Chromatographic Analysis of the Liquid Product	21
1. Experimental	22
a. Chromatographic Equipment and Operating Conditions	22
b. Reagents and Preparation of MHET	23
c. Silylation Procedure	24
2. Correlation of Data and Discussion	27
B. Gas Chromatographic Analysis of Distillate	30
1. Experimental	31
2. Correlation of Calibration Data	33
C. Product Characterization Analysis	34
1. Total Carboxylic Groups	35
2. Total Free Carboxylic Groups	35
3. Glycols in Saponified Product	36

V. EXPERIMENTAL EQUIPMENT AND PROCEDURES	37
A. Differential Recycle Reactor	37
1. Recycle Reactor Design	39
a. The Reactor and Methanol-Stripper Loop	41
b. The Feed Flow System	46
c. The Flow Control Element	48
2. Reactor Operation Procedure	51
B. Batch Reactor	54
1. Batch Reactor Design	55
2. Batch Reactor Operation	57
VI. TRANSESTERIFICATION CATALYZED BY AMBERLYST 15	59
A. Recycle Reactor Performance	59
B. Batch Reactor Results	62
1. Effects of Transport Processes	62
2. Distribution of Terephthalate Esters	65
3. Discussion	70
VII. MATHEMATICAL ANALYSIS OF THE DIFFERENTIAL RECYCLE REACTOR	79
A. Volume Mathematical Functions	79
B. Differential Equations	82
C. Transient Response	84
1. Irreversible First Order Reaction	85
2. Irreversible Second Order Reaction	88
D. Discussion	90
VIII. OLIGOMERIZATION REACTIONS	96
A. Oligomerization Model	97

B.	Oligomerization Model. Non-Isothermal Data	100
C.	Polycondensation Equilibrium Constant and its Implications	105
D.	Oligomerization Model. Isothermal Data	107
IX.	METHYL-ESTER GROUP REACTION	115
A.	Methyl-Ester Group Model	115
B.	Testing of Methyl-Ester Group Model	117
X.	MOLECULAR SPECIES REACTIONS	125
A.	Molecular Species Model	125
B.	Testing of Molecular Species Model	129
C.	Product Distribution.	134
XI.	DISCUSSION and CONCLUSIONS	138
	REFERENCES	142
	NOMENCLATURE	145
	APPENDIX A. Gas Chromatographic Analysis Calibration Data	149
	APPENDIX B. Feed Flow Set-ups	153
	APPENDIX C. Experimental Data	156
	1. Preliminary Data for Amberlite IR-120	156
	2. Batch Reactor Data for Amberlyst 15	156
	APPENDIX D. Experimental Data for Homogeneous Catalysis	175
	APPENDIX E. Analytical Integration of Methyl-Ester Group Model	182
	VITA AUCTORIS	186

FIGURES

<u>Figure</u>	<u>Page</u>
I.1 Production of Polyethylene Terephthalate	2
III.1 Second Order Integral Values vs. Time	18
III.2 Second Order Integral Values vs. Time	19
IV.1 NMR Spectrum of Methyl-(2-Hydroxyethyl) Terephthalate	25
IV.2 Chromatogram of a Synthetic Mixture	26
IV.3 Chromatogram of a Distillate Sample (Run R-116B)	32
V.1 Schematic of Recycle Reactor	38
V.2 Schematic of Recycle Reactor Set-up	40
V.3 Fixed-Bed Reactor	42
V.4 Packed Tower	43
V.5 Downcomer	45
V.6 Composite Flow Control Element	49
V.7 Effects of Flow Control Element Design	52
V.8 Schematic of Batch Reactor	56
V.9 Sampling Probe	56
VI.1 Recycle Reactor Performance	60
VI.2 Two-level Factorial Experiment	63
VI.3 Results of Two-level Factorial Experiment	64
VI.4 Effects of Resin Particle Size	66
VI.5 Chromatogram of a Transesterification Sample (Run R-113B)	67a
VI.6 Terephthalate Ester Profiles of Run R-113B	68
VI.7 Partial Yield vs. Time for Run R-113B	69
VI.8 Partial Yield vs. Time for Run R-116B	71

<u>Figure</u>	<u>Page</u>
VI.9 Partial Yields vs. Time for Run R-117B	72
VII.1 Schematic of Recycle Reactor with On-Off Control of Outlet Stream	80
VII.2 Graph of Reactor Liquid Volume	81
VII.3 Transient Response for First Order Kinetics	91
VII.4 Transient Response for Second Order Kinetics	92
VII.5 Concentration Fluctuations during Transient Period for First Order Kinetics	94
VII.6 Concentration Fluctuations during Transient Period for Second Order Kinetics	95
VIII.1 Graph of First Glycol Function	101
VIII.2 Graph of Second Glycol Function	101
VIII.3 Rate Constant vs. Reciprocal Absolute Temperature	103
VIII.4 Polycondensation Equilibrium Constant	106
VIII.5 Differential Analysis of Oligomerization Model	108
VIII.6 Graph of Integrand	110
VIII.7 Oligomerization Model Applied to Fontana's Data	112
VIII.8 Oligomerization Model Applied to Peebles and Wagner's Data	113
VIII.9 Oligomerization Model Applied to Tomita and Ida's Data	114
IX.1 Methyl-Ester Group Model Applied to Fontana's Data	118
IX.2 Methyl-Ester Group Model Applied to Tomita and Ida's Data	120
IX.3 Methyl-Ester Group Model Applied to Peebles and Wagner's Data	121
X.1 Molecular Species Model Applied to Fontana's Data	131
X.2 Molecular Species Model Applied to Tomita and Ida's Data	132

<u>Figure</u>		<u>Page</u>
X.3	Molecular Species Model Applied to Peebles and Wagner's Data	133
X.4	Product Distribution (Curves 1, 2, 3 are DMT, MHET and BHET, respectively)	137
B.1	Pressurized Tank Feed System	154
B.2	By-Pass-Loop Feed System	154

TABLES

<u>Table</u>	<u>Page</u>
IV.1 Relative Retention	27
IV.2 Regression Statistics	29
IV.3 Experimental Error	30
V.1 Flow Control Element Data	51
VI.1 Ethylene Glycol Products	74
VI.2 Undesirable Transesterification Products	77
VIII.1 Results of Rate Constant Regression	104
VIII.2 Non-Linear L.S. Analysis of Rate Model	104
IX.1 Statistics for the Methyl-Ester Group Model	122
IX.2 Rate Constants for the Methyl-Ester-Group Model	123
X.1 Statistics for the Molecular Species Model	134
X.2 Rate Constants for the Molecular Species Model	135
A.1 GLC Calibration Data	150
A.2 GLC Calibration Data	151
A.3 Methanol Calibration Data	152
C.1 Transesterification Data with Amberlite IR-120	157
C.2 Experimental Data of Run R-112B	160
C.3 Experimental Data of Run R-113B	161
C.4 Experimental Data of Run R-114B	162
C.5 Experimental Data of Run R-115B	163
C.6 Experimental Data of Run R-116B	164

TablePage

C.7	Experimental Data of Run R-117B	165
C.8	Experimental Data of Run R-118B	166
C.9	Experimental Component Profiles	167
C.10	Experimental Component Profiles	168
C.11	Experimental Component Profiles for Run R-116B	169
C.12	Experimental Component Profiles	170
C.13	Free and Esterified Glycols	171
C.14	Mass of 2-Methoxy-ethanol	171
C.15	Total Carboxylic Groups	172
C.16	Total Free Carboxylic Groups	173
C.17	Methanol Profile for Run R-116B	174
D.1	Fontana's Non-Isothermal Data	177
D.2	Fontana's Near-Isothermal Data	178
D.3	Tomita and Ida's Data Set #1	179
D.4	Tomita and Ida's Data Set #2	179
D.5	Tomita and Ida's Data Set #3	180
D.6	Tomita and Ida's Data set #4	180
D.7	Peebles and Wagner's Data	181

I. INTRODUCTION

Bis-(2-hydroxyethyl) terephthalate (BHET) is the monomer from which polyethylene terephthalate, the polyester polymer on which important fibres are based, is produced by condensation polymerization.

Until a few years ago the production of monomer was exclusively based on dimethyl terephthalate from which it was obtained by transesterification of dimethyl terephthalate (DMT) with ethylene glycol (EG). The transesterification of DMT with EG is usually referred to as the precondensation stage, while the step producing polyethylene terephthalate (PET) is referred to as the polycondensation stage. A description of a continuous process is given in [1].

In the mid-1960's some producers started producing the monomer by direct esterification of pure terephthalic acid (TPA) with ethylene glycol [2], while in the early 1970's processes were being developed for producing BHET from TPA and ethylene oxide [3].

The two routes of monomer production are schematically shown in Fig. I.1. The DMT route involves one step more than the TPA route and, therefore, is a little more expensive than the latter. However, the economics of the pure-acid process are not dramatically favourable [2] and this, coupled with the fact that major DMT plants were built until recently indicates that the transesterification route is not going to lose its significance, in the near future at least. Therefore, efforts aimed at improving and elucidating basic chemical processes along this path are deemed well justified, and the present study deals with some aspects of the kinetics of the transesterification reactions in the presence of heterogeneous and homogeneous catalysts.

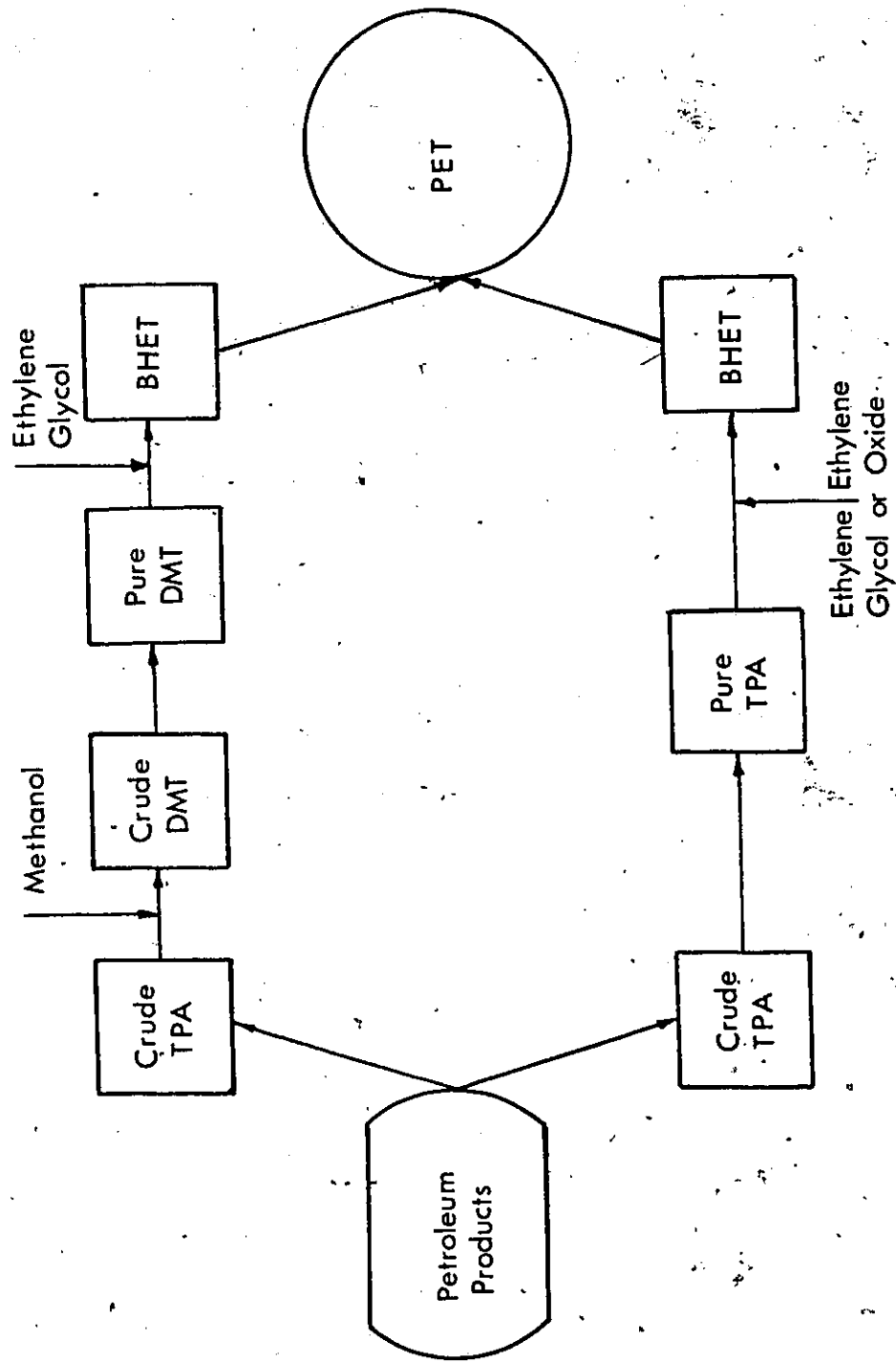


Fig. I.1 Production of Polyethylene Terephthalate

Isagulyants [4] and Wlenchich [5] had shown that cation exchange resins, in the hydrogen form, catalyzed the transesterification reactions. However, it was not known whether they were efficient catalysts, and the objective of the research in this area was to obtain some answers, in terms of kinetic models, to this question. The catalysts investigated were Amberlite IR-120 and Amberlyst 15, in the hydrogen form. The investigation was prompted by the following potential advantages offered by the resins:

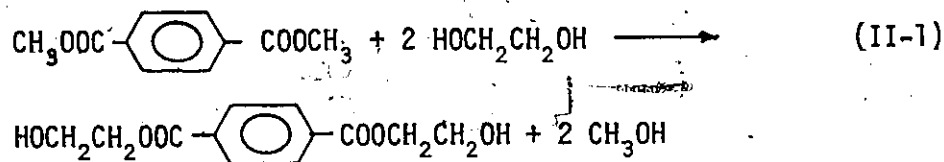
- removal of catalyst from the reaction product, by a simple filtration for example, thus avoiding contamination of the latter, and
- economic savings effected by repeated use of the resin, which shows good stability of activity.

The experimental investigation of the transesterification reactions called for adequate analytical techniques in order to follow the transesterification process, and the author devoted considerable time in developing original and reliable procedures for gas chromatographic analysis of the product. In addition, the differential recycle reactor, which was designed and built for studying the reactions posed problems about its behaviour the answers to which were obtained by means of a mathematical analysis of the transient response of the reactor.

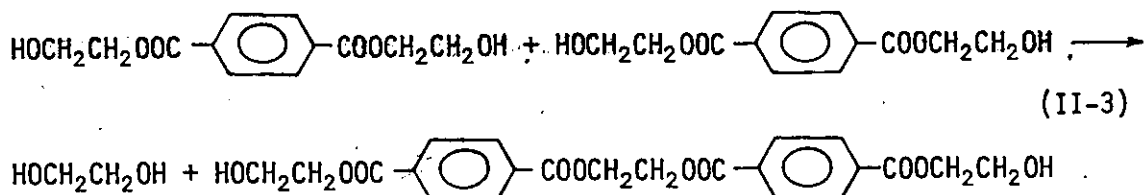
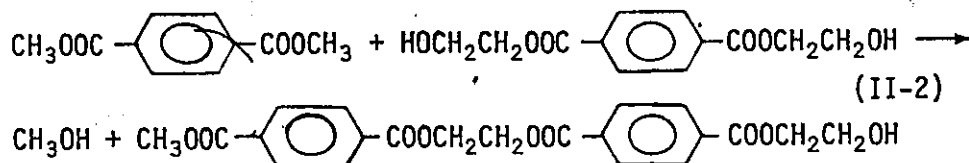
The effects of homogeneous catalysts were not experimentally investigated by the author. Instead, the data of previous investigators were used in building adequate kinetic models for the transesterification reactions catalyzed by homogeneous catalysts. This modeling endeavour was prompted by the inadequacy of previously proposed models, which became apparent from a critical evaluation of the literature.

II REVIEW OF HOMOGENEOUS KINETICS

The monomer bis(2-hydroxyethyl) terephthalate (BHET) is the main product of the precondensation stage, and is formed by the following overall reaction;

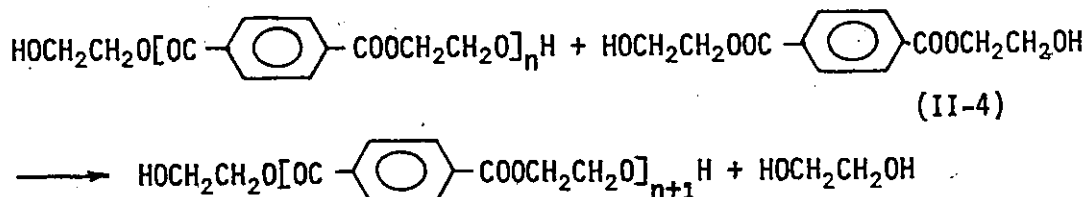


Other reactions that proceed to some extent in this stage are of the form

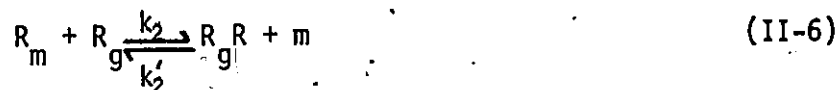


Reactions (II-2) and (II-3) along with a host of similar reactions produce a mixture of oligomers [6,7], which are the by-products of the precondensation stage.

The polycondensation reaction that produces the polyester can be depicted as follows:



The multiplicity of chemical reactions taking place in the precondensation stage can be put into a compact form if these reactions are written in terms of participating functional groups. These reactions were proposed by Challa [8] and are given by



where

$R_m = -COOCH_3$ methyl-ester end group

$R_g = -COOCH_2CH_2OH$ 2-hydroxyethyl-ester end group

$R_g R = -COOCH_2CH_2COO-$ ethylene diester group (interunit group)

$g =$ ethylene glycol

$m =$ methanol

$R =$ monomer or polymer molecule

Reactions (II-5), (II-6) and (II-7) are, ester interchange, transesterification and polymerization reactions respectively.

The first kinetic study of the precondensation reactions was carried out by Griehl and Schnock [9]. They used a slight excess of ethylene glycol and followed the progress of the reaction by determining the amount of methanol distilled. They found that their data could be

described by a first order model, i.e.,

$$-\frac{dC_A}{dt} = k N_C C_A \quad (\text{II-8})$$

where C_A is DMT concentration and N_C is the amount of catalyst in moles.

It should be pointed out that the reaction volume of this system varies with time and, therefore, the use of the rate form defined in Eq. (II-9)

$$-\frac{dC_A}{dt} \quad (\text{II-9})$$

for the reaction rate is, strictly speaking, incorrect. The same form was also assumed by all but one subsequent investigators as will be seen later. The correct expression [10] for variable volume systems is

$$-\frac{1}{V} \frac{dN_A}{dt} \quad (\text{II-10})$$

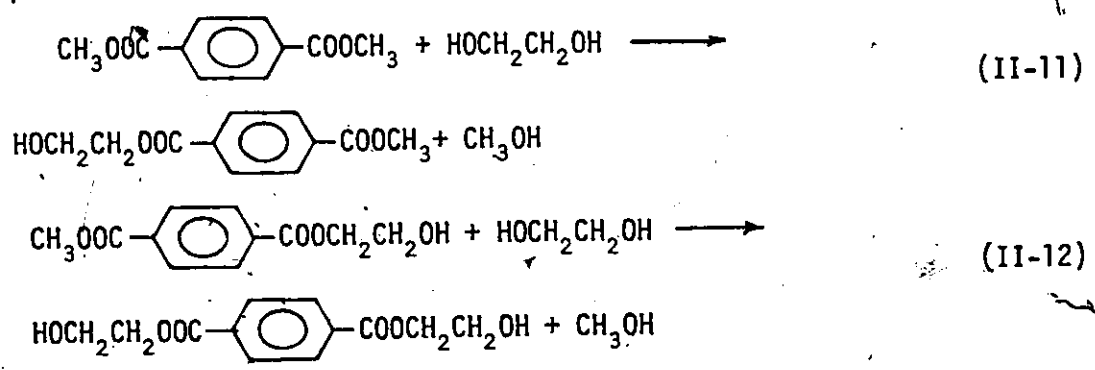
Also, equation (II-8) implies that ethylene glycol does not have any effect on the rate.

The above observations together with the questionable experimental procedure used by Griehl and Schnock create serious doubts as to the usefulness of the data by these investigators.

Mihail et al. [11] determined the amount of methanol evolved during the precondensation stage catalyzed by various catalysts. They found that their data could not be described by a rate expression of either first order in DMT alone or first order in ethylene glycol alone or an overall second order rate expression with one order each for DMT and ethylene glycol. They concluded that the reaction order must be

fractional. They also assumed a constant volume rate form, i.e., (II-9) and their data may be questionable since they used very small quantities of reactants (complete conversion of all the DMT would have produced 2g of methanol). Mihail and coworkers as well as Griehl and Schnock tried to analyze their data by tacitly assuming that oligomerization reactions do not take place in the precondensation stage.

Peebles and Wagner [12] reanalyzed the transesterification reaction because they thought it likely that the reaction follows a mechanism of two competitive, consecutive second order reactions. They were the first investigators to implicitly acknowledge the possibility that side reactions such as (II-2) and (II-3) take place, but to avoid the complications arising from consideration of these reactions they used an excess of ethylene glycol, and assumed that these reactions would be suppressed and would, therefore, be negligible. In their limited experiments, they followed the course of transesterification by measuring the amount of methanol evolved. The analysis of their experimental data was performed according to the following representation of the reactions



and the authors presented an extensive mathematical development which, they claimed, gave due consideration to the fact that the volume of this

reaction mixture changes with conversion.

Actually Peebles and Wagner presented their mathematical development as a novel approach to the analysis of competitive, consecutive second order systems with variable volume while the transesterification reactions were presented as an example of the applicability of their analysis. For the reaction system



where A, B, R, S and m are DMT, ethylene glycol, methyl 2-hydroxyethyl terephthalate (MHET), bis-(2-hydroxyethyl) terephthalate (BHET) and methanol, respectively, they defined the following reaction rate

$$-\frac{dC_B}{dt} = (1-vC_{B_0})[k_1 C_A C_B + k_2 C_R C_B] \quad (\text{II-15})$$

and

$$-\frac{dC_A}{dt} = (1-2vC_{A_0})k_1 C_A C_B \quad (\text{II-16})$$

where v is the molar volume of the distillate and the terms in parentheses are alleged correction factors which must be applied to the rate constants.

It is clear that the authors have used the rate form applicable only to a constant volume system when their objective was to analyze a variable volume system. In addition, the applied correction factors do not make up for the rate form used as the following analysis shows in terms of Eq. (II-16). The correct rate equation for component A in a variable volume system is

$$-\frac{1}{V} \frac{dN_A}{dt} = k_1 C_A C_B \quad (\text{II-17})$$

while Eq. (II-16) when expanded becomes

$$-\frac{1}{V} \frac{dN_A}{dt} + \frac{N_A}{V^2} \frac{dV}{dt} = k_1 C_A C_B - 2vC_{A_0} \frac{k_1 C_A C_B}{V} \quad (\text{II-18})$$

By using Eq. (II-17), the following equality

$$\frac{N_A}{V^2} \frac{dV}{dt} = -2vC_{A_0} k_1 C_A C_B \quad (\text{II-19})$$

must hold for Eq. (II-16) to be valid. Simplification of Eq. (II-19)

leads to

$$\frac{dV}{dt} = -2vC_{A_0} k_1 N_B \quad (\text{II-20})$$

But since the volume was defined by

$$V = V_0 - vN_{A_0} + vN_A \quad (\text{II-21})$$

Eq. (II-20) becomes

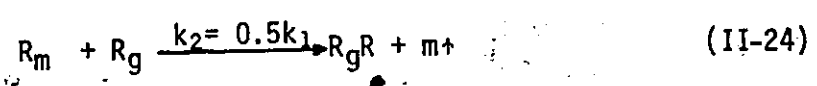
$$-\frac{1}{V} \frac{dN_A}{dt} = 2C_{A_0} k_1 C_B \quad (\text{II-22})$$

which, of course is not the same as equation (II-17). Consequently Eq. (II-19) does not hold and, therefore, the rate expressions assumed by Peebles and Wagner do not include adequate correction for the volume variability. In addition, the models did not account for the variation of catalyst concentration, which is the result of the change in volume.

Peebles and Wagner found that their mathematical formulas did not describe their methanol data. However, in view of the inadequate mathematical treatment the validity of their hypothesized reaction model remained essentially untested. It should be noted at this point that

their transesterification data suffer from significant experimental error (at times more than $\pm 5\%$).

In a later study of the transesterification reactions Fontana [13] criticized the kinetic analysis of Peebles and Wagner for their simplifying assumption that "reactions of all higher species could be neglected". Fontana based his criticism not on experimental evidence of the occurrence of oligomerization reactions but on the results of his analysis and what he called an adequate fit of his model to the data. He assumed that oligomerization reactions do occur and a reaction model composed of Eqs. (II-5) and (II-6) which were considered irreversible, i.e.,



where the symbols stand for the quantities defined previously. He further interpreted an assumed value of the polycondensation equilibrium constant to mean that the rate constant ratio k_2/k_1 is equal to 0.5 and independent of temperature. This interpretation allowed him to derive the following product distribution

$$R_g = (g_0^{0.75} g_0^{-0.25} - g) / 0.75 \quad (II-25)$$

and the model

$$\frac{dm}{dt} = 2k_1 \frac{R_m (g + 0.25 R_g) C}{V^2} \quad (II-26)$$

where C is the amount of catalyst in moles, R_m and R_g are methyl ester and glycol ester end-groups in equivalents, respectively, and g is ethylene glycol in moles.

Fontana's kinetic data were based on methanol vs. time profiles obtained from a non-isothermal batch reactor, except for one run which was near-isothermal up to about 80% conversion. He analyzed his integral, non-isothermal data by the differential method which for any kinetic run yielded several values for k_1 . These values were then plotted against reciprocal absolute temperature and the straight lines obtained were viewed as justification of his assumptions. In his analysis Fontana ignored the essential requirement of using isothermal data [14, 15] in establishing a kinetic model and used the error-prone differential method of analysis. It will be shown that his reaction and kinetic models are, in the light of the available experimental data, entirely inadequate. However, the reaction model is used in a search for an adequate kinetic model for the homogeneously catalyzed transesterification reactions.

In a study of the catalytic properties of metal acetylacetonates in the transesterification of DMT, Yampol'skaya and coworkers [16] used an excess of ethylene glycol and found the rate to be first order with respect to dimethyl terephthalate. Sorokin and Chebotareva [17] have been the only investigators to have tried to analyze the product chemically. They identified the mixed ester, methyl-2-hydroxyethyl terephthalate, and the glycol diester, bis-(2-hydroxyethyl) terephthalate, but they were able to determine only the profiles of ethylene glycol and DMT. Their analysis showed that, at the very early conversion stage, only the mixed ester was present while at a later stage both the mixed and glycol diesters were present. This experimental evidence confirms the expectation that the ester interchange of dimethyl terephthalate

takes place in a series fashion. Sorokin and Chebotareva reported a rate expression with an overall order of four, first order with respect to catalyst and ethylene glycol and second order with respect to DMT. However, their reported analysis is rather incomplete and it is not possible to make any critical comments about their model. It is also rather unfortunate that they do not report any data, graphical or numerical.

Tomita and Ida [18] obtained DMT conversion data by determining only the amount of methanol evolved. They used a batch reactor and only an initial molar ratio of ethylene glycol to DMT equal to two. In analyzing their data they claimed, without experimental evidence, that oligomerization reactions take place only at molar ratios less than two and stated that the reactivity of methyl ester groups on DMT are equal. The latter argument, they said, was based on studies of model compounds while Challa's experimental work on the system under discussion had yielded the same conclusion directly. Tomita and Ida proposed to improve Peebles and Wagner's treatment by including the catalyst concentration in the kinetic model which had already been considered by Fontana. They assumed the following reaction model



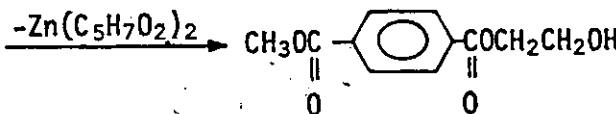
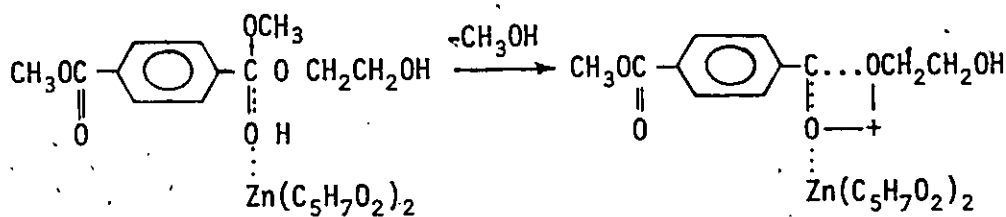
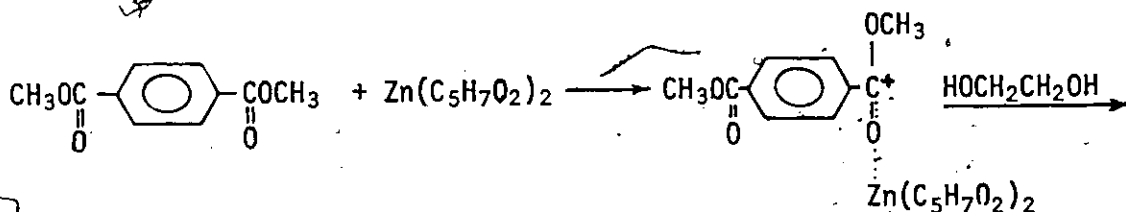
and a rate equation of the form (Eq. (8) of [18])

$$\frac{dC_A}{dt} = k \frac{V}{a_y} \frac{N_A^2}{y^2} = k \frac{N_C}{y} \frac{N_A^2}{y^2} \quad (\text{II-28})$$

The latter is, of course, inappropriate because it is based on the rate

form applicable to a constant volume system, i.e., form (II-9) instead of (II-10). However, Tomita and Ida's model passed the integral analysis test, and this apparently led them to believe that they had indeed assumed an acceptable model. It must also be pointed out that tests of their model were restricted to data obtained at an initial molar ratio of ethylene glycol to dimethyl terephthalate equal to two.

Finally, various catalysts were studied by the previously mentioned investigators. These catalysts were mainly zinc, manganese, magnesium, calcium, tin, and antimony acetates, lead oxide, and zinc, cadmium, manganese and copper acetylacetonates, and zinc stearate. Yampol'skaya [16] reports the following mechanism for the action of acetylacetonates:



III PRELIMINARY INVESTIGATION WITH AMBERLITE IR-120

In a preliminary study [19] of the transesterification reactions between dimethyl terephthalate and ethylene glycol in the presence of cation exchange resins, Amberlite IR-120, in the hydrogen form, was used as catalyst and the investigation was carried out in a batch reactor.

A. Experimental

The cation exchange resin, Amberlite IR-120, had a total capacity of 4.6 milliequivalents of hydrogen ion per gram dry resin and a bead size range of 16-50 mesh. The hydrogen form of the resin was obtained by regeneration with 5% sulfuric acid.

The reactants used in the study were dimethyl terephthalate (m.p. 140-142°C) and ethylene glycol (Fisher "purified" reagent).

A series of experimental runs was carried out with different initial molar ratios of reactants and a known amount of catalyst in a batch reactor.

The batch reactor, a three-necked 200 ml distilling flask, was fitted with a jacketed Vigreux column for separating methanol from the vapour phase. The methanol condenser was connected to the Vigreux column with a 75° connecting tube having a thermometer opening at the top and to the receiver by means of a 105° two-way connecting tube of which the suction opening was fitted with a short tube filled with calcium chloride. All joints were of ground glass. Mixing was induced by a stirrer and reactor temperature was regulated at 142°C by a thermostat controlled bath accurate to $\pm 0.1^\circ\text{C}$.

In a typical run, the reactor charged with DMT and ethylene glycol

was immersed in the bath and enough time allowed for the mixture to form a clear melt or solution. Then 5 ml of methanol was added to the reactor to bring about equilibrium in the system and, thus, avoid accumulation of reaction produced methanol in the liquid and vapour phases. The preheated catalyst was introduced to the reactor when distillation of the added methanol was nearly complete. The methanol produced was condensed and collected, and the progress of the reaction was followed by weighing the amount of methanol as a function of time.

Experimental data are given in Table C.11 of Appendix C. They were obtained with mixing rate adjusted so that external mass transfer effects were negligible, but the effect of intraparticle diffusion was not investigated.

B. Analysis of Preliminary Data

In order to overcome difficulties arising from the possible side reactions and the liquid volume change with time, the preliminary kinetic study was restricted to the lower conversion regime. This restriction should render the effects of side reactions and volume change relatively insignificant.

The following assumptions were made in the data analysis

- a) reaction volume change was negligible
- b) side reactions were negligible, and
- c) intraparticle diffusion effects were not significant.

Based on the second assumption, the only reaction to be considered in the kinetic analysis was reaction (II-1) which is here rewritten as



where A, B, S and m stand for DMT, ethylene glycol, BHET and methanol, respectively.

A mass balance over reaction (III-1) shows that

$$2(N_{A_0} - N_A) = N_{B_0} - N_B = N_m \quad (\text{III-2})$$

which, in terms of DMT conversion, yields

$$N_B = N_{A_0} (M - 2x) \quad (\text{III-3})$$

$$N_m = 2xN_{A_0} \quad (\text{III-4})$$

where $x = (N_{A_0} - N_A)/N_{A_0}$ and $M = N_{B_0}/N_{A_0}$ is the initial molar ratio of reactants.

The following rate expressions were tested for goodness of fit to the data:

$$\frac{1}{W} \frac{dN_A}{dt} = kG_A \quad (\text{III-5})$$

$$\frac{1}{W} \frac{dN_A}{dt} = kC_A C_B \quad (\text{III-6})$$

$$\frac{1}{W} \frac{dN_A}{dt} = kC_A C_B^2 \quad (\text{III-7})$$

where W is the amount of catalyst in grams. These models may easily be expressed in terms of DMT conversion, and the transformed equations are

$$\frac{dx}{dt} = \frac{kW}{V_0} (1-x) \quad (\text{III-8})$$

$$\frac{dx}{dt} = \frac{kWN_{A_0}}{V_0^2} (1-x)(M-2x) \quad (\text{III-9})$$

$$\frac{dx}{dt} = \frac{kW(N_{A_0})^2}{V_0^3} (1-x)(M-2x) \quad (\text{III-10})$$

where V_0 , the initial reaction volume, is given [13] by

$$V_0 = 0.1915N_{A_0} + 0.0606N_{B_0} \quad (\text{III-11})$$

and x may be calculated from the amount of methanol evolved according to Eq. (III-4).

Since the kinetic data were integral data, the models given by Eqs. (III-8), (III-9) and (III-10) were integrated, by the method of separation of variables, in order to apply the standard kinetic analysis method. For Eq. (III-9) the integral is given by

$$\frac{1}{(1-x)} = 1 + k \left(\frac{2WN_{A_0}}{V_0^2} \right) t \quad (\text{III-12})$$

for M equal to two, and

$$\ln \left[\frac{(M-2x)}{2(1-x)} \right] = \ln \left(\frac{M}{2} \right) + k \left[\frac{WN_{A_0}(M-2)}{V_0^2} \right] t \quad (\text{III-13})$$

for M different from two. Then, plotting of the left-hand side of either Eq. (III-12) or Eq. (III-13) should result in a straight line if the assumed model is adequate. Similar expressions result from the other two models.

Least-squares analysis of the integral equations showed that the second order model, Eq. (III-9) or (III-6), described the data best. Figures III.1 and III.2 show the experimental integral values plotted against time for various experimental conditions.

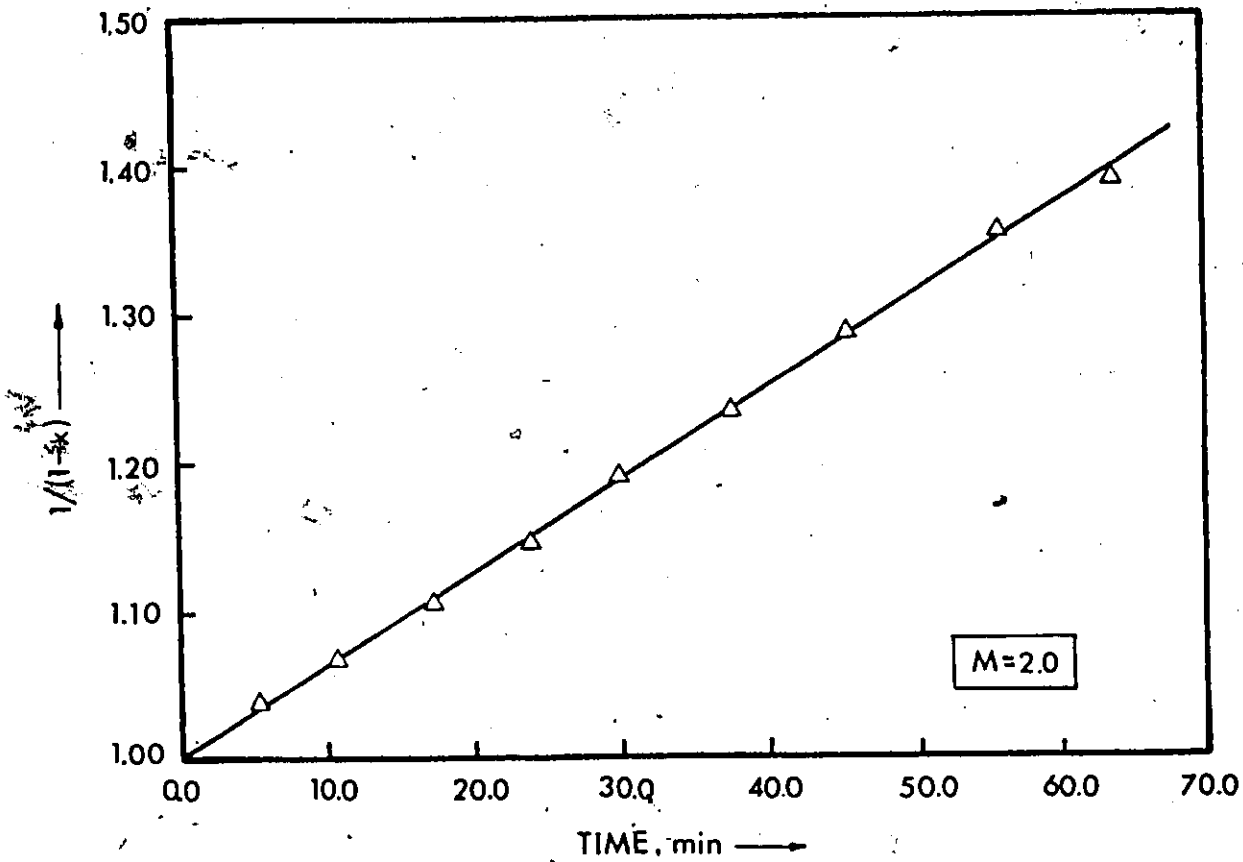


Fig. III.1 Second Order Integral Values vs. Time

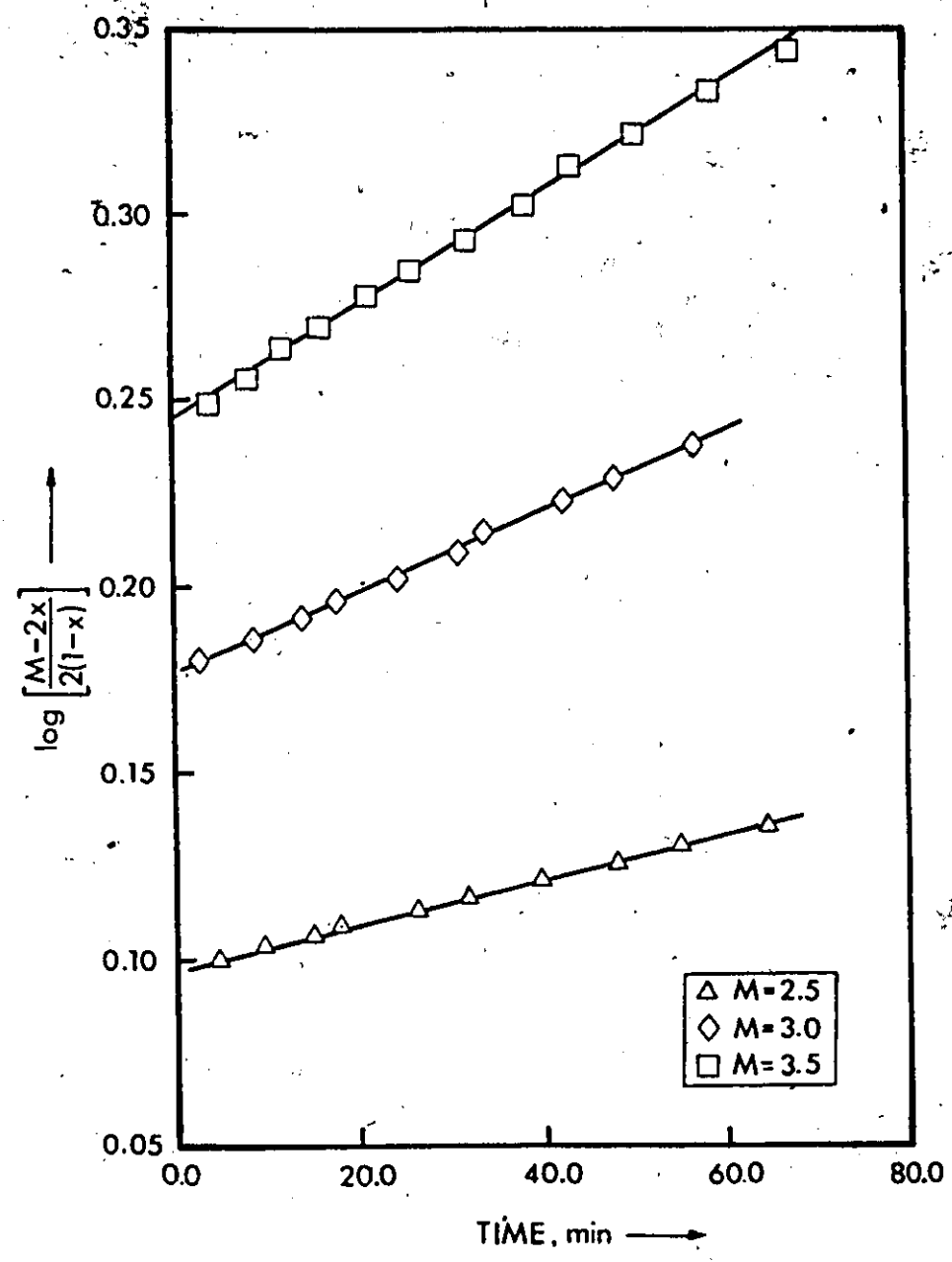


Fig. III.2 Second Order Integral Values vs. Time

The rate constant k was estimated from the least-squares estimate of the slope of the line through the data and was found to have an average value of $3.3 \times 10^{-6} \text{ l}^2 / (\text{mole})(\text{min})(\text{g-resin})$ at 142°C and in the presence of Amberlite IR-120 in the hydrogen form.

IV CHEMICAL ANALYSIS

The literature survey in Chapter II showed that practically none of the previous kinetic investigations of the transesterification reactions involved determination of chemical species other than methanol. The only investigators who attempted such determinations were Sorokin and Chebotareva [15] but their analysis was limited to dimethyl terephthalate and ethylene glycol. Under these restrictions, the kinetic model building process for a complex reaction system, such as the DMT transesterification presumably is, must necessarily rely on external, relevant evidence or reasonable assumptions in order to develop adequate rate expressions.

For the aforementioned reasons, the present author considered chemical analysis of the transesterification products very desirable, and consequently took pains to develop suitable and reliable analytical techniques, mainly in the area of gas-liquid chromatography.

A. Gas Chromatographic Analysis of the Liquid Product

The liquid product is defined as the mixture of transesterification compounds other than methanol, which, because of low volatility, are in the liquid phase at the usual transesterification temperatures. Although complete chemical analysis of the reaction product would be virtually impossible the author believed that determination of as many chemical components as possible was necessary in order to establish adequate kinetic models for the precondensation reactions catalyzed by cation exchange resins.

It was decided that the required wide range analysis of the liquid

product could, best be achieved by gas-liquid chromatography (GLC). Some of the compounds which can be and were [20] determined by GLC are: DMT, EG, methyl-(2-hydroxyethyl) terephthalate (MHET), BHET, and diethylene glycol, a polymerization product of ethylene glycol.

1. Experimental

Preliminary gas chromatographic analyses of bis-(2-hydroxyethyl) terephthalate using Carbowax 20M, Ucon 50 HB 2000, Silicone oil DC-200, Silicone oil DC-550 and Apiezon L as liquid phases on various solid supports under varied experimental conditions were not successful either because the compound did not elute or because reproducibility was poor. To overcome these difficulties, silylation [21-24] of the hydroxyl groups before GLC analysis was undertaken and this technique led to excellent results.

a. Chromatographic Equipment and Operating Conditions

The gas-liquid chromatographic analysis was carried out using a Varian Aerograph, model 1520(c), gas chromatograph equipped with a linear temperature programming module and dual flame ionization detectors.

The column used was 2 ft by 1/8 in. O.D. packed with 10% Apiezon L on Chromosorb G A/W DMCS, 100-120 mesh. The flow rate of the nitrogen carrier gas was set at 31 cc/min measured at the column exit and at room temperature.

The temperatures of the injector port and of the ionization detector region were kept at 280°C and 300°C respectively, while that of the oven was held at 90°C for 60 seconds after sample injection and then linearly raised to 270°C at the rate of 20°C/min. A piece of aluminum

foil placed between the Teflon lined septum used and the injection port slowed down degradation of the septum considerably, and chromatograms were free from septum decomposition product interference.

b. Reagents and Preparation of MHET

High purity dimethyl terephthalate (99.9 + %) and ethylene glycol (99 + mol%) were obtained from Aldrich Organic Chemicals. Bis-(2-hydroxyethyl) terephthalate was obtained from E.I. DuPont de Nemours and Co., and it was further purified by recrystallization from methanol. Diethylene glycol and 1,4-dioxane were supplied by Fisher Scientific Co., while the silylating reagents, i.e., trimethylchlorosilane and hexamethyldisilazane were procured from Pierce Chemical Co. Methyl-(2-hydroxyethyl) terephthalate was prepared from BHET by partial alcoholysis.

The procedure for partial alcoholysis of BHET, though similar to that reported by Kudrna and Pavelcova [25], was established using sequential factorial experiments. To a preheated 0.7M solution of BHET in methanol, enough 0.1M methanolic NaOH was added to yield a final concentration of 0.007M NaOH and the reaction was allowed to proceed for 80 seconds at the reaction temperature of 40°C. The alcoholysis was frozen by neutralizing the alkali with 0.01M aqueous HCl, which caused precipitation of the DMT produced. The precipitate was filtered off and discarded while the filtrate was evaporated down to a melt which was dissolved in CHCl_3 at 60°C. The first crop of crystals from CHCl_3 at room temperature was mainly BHET while the second crop at 0°C was mainly MHET. The latter was recrystallized from isopropyl ether, and the crystals were dried at 50°C. The product thus obtained had a

melting point of 80-81°C, which was in close agreement with that reported by Zahn and Krzikalla [26], and it was identified by NMR spectroscopy (Fig. IV.1). The purity of the product was found to be 99% by determining the BHET impurity by means of the GLC bracketing technique.

c. Silylation Procedure

The solvent used to dissolve both synthetic mixtures of the quantitatively determined compounds and the transesterification product was a solution of 1.34 g of bibenzyl (the internal standard) in 100 ml 1,4-dioxane. Synthetic mixtures were dissolved in 5 ml while the transesterification product was dissolved in an appropriate volume of solvent (as determined by total sample mass and conversion stage). Silylation of dissolved compounds was achieved by using hexamethyldisilazane (HMDS) and trimethylchlorosilane (TMCS) taken in the volume ratio of 2:1. To this end, 0.4 ml of solution were transferred to a screw cap septum vial containing a mixture of 0.8 ml HMDS and 0.4 ml TMCS. The vial was then sealed using Teflon-rubber laminated discs, and its contents were simmered for a few minutes on a low temperature hot plate. After cooling, the vial was centrifuged in order to separate the precipitate, presumably ammonium chloride, and the clear supernatant liquid was sampled using a 5 µl syringe. Chromatograms (Fig. IV.2) were obtained by injecting one microlitre of silylated sample under the previously stated conditions. Table IV.1 lists relative retention times.

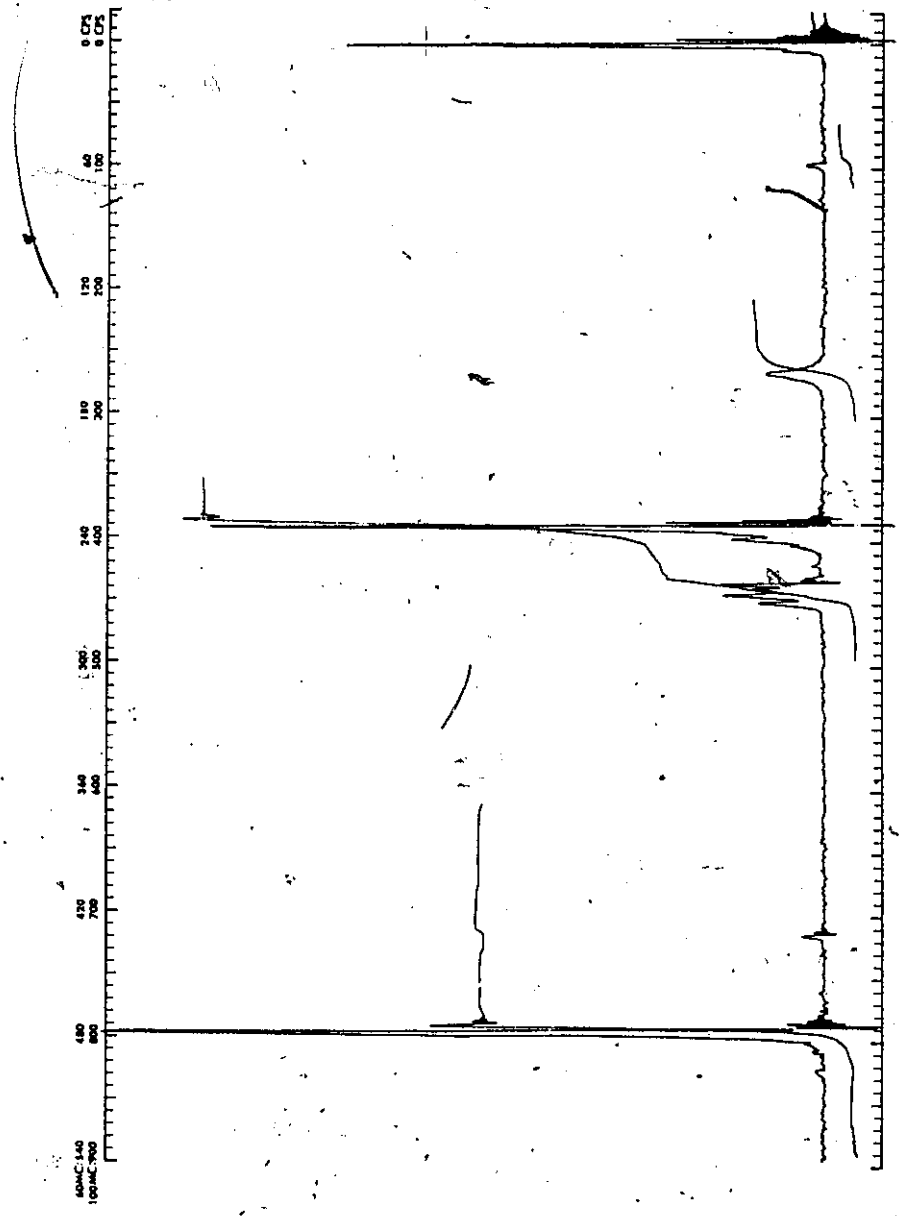


Fig. IV.1 NMR Spectrum of Methyl-(2-Hydroxyethyl) Terephthalate

A: Solvent &
Reagents
B: EG-TMS
C: DEG-TMS
D: DNT
E: Bibenzyl
F: MHET-TMS
G: BHET-TMS

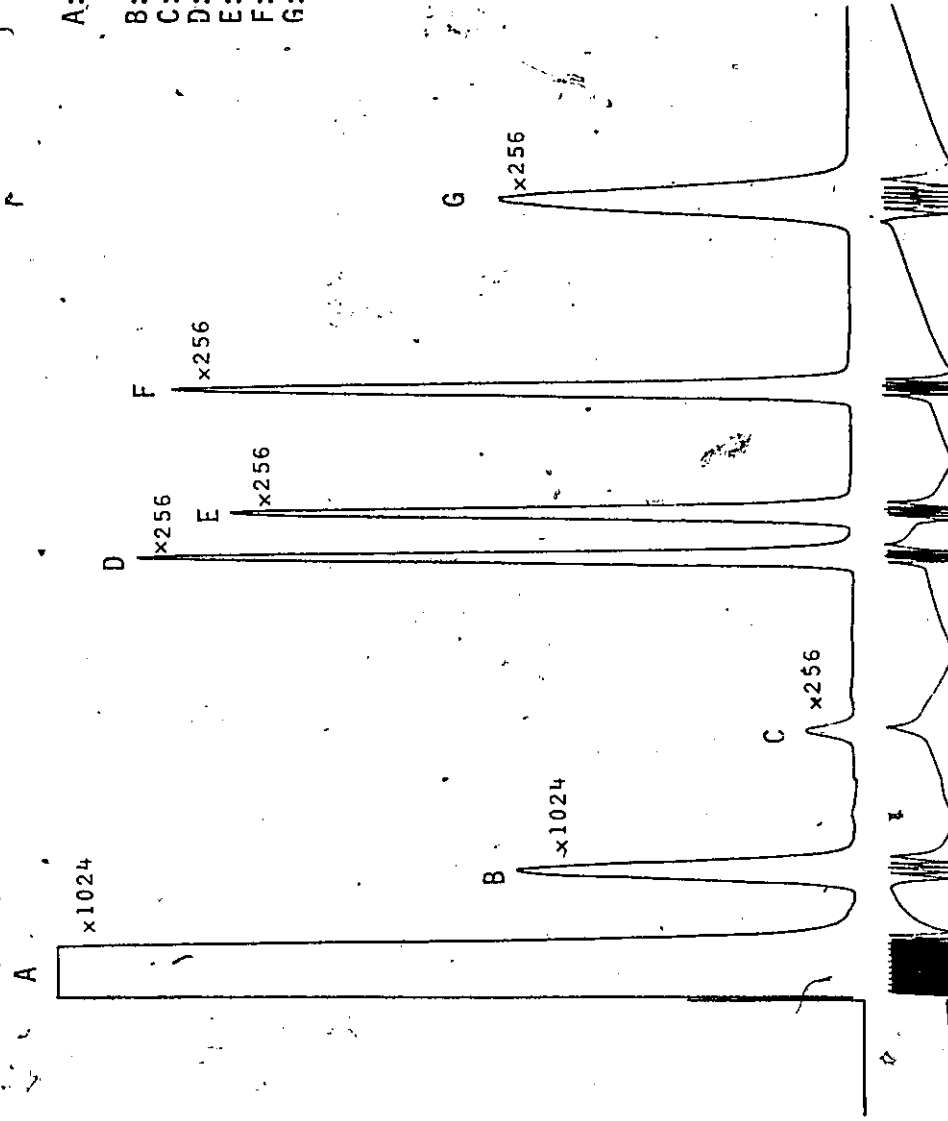


Fig. IV.2 Chromatogram of a Synthetic Mixture

TABLE IV.1
Relative Retention

Compound	Relative ^a Retention
EG - TMS ^b	0.27
DEG - TMS	0.56
DMT	0.97
BB	1.00
MHET - TMS	1.25
BHET - TMS	1.63

a Values refer to retention time of bibenzyl
of 490 seconds

b TMS denotes trimethylsilyl derivative

2. Correlation of Data and Discussion

Calibration curves were established using four synthetic mixtures, whose composition was a randomly chosen combination of the four preassigned levels of each compound. Peak areas were determined using a mechanical integration module (DISC).

In the case of the transesterification product the volume of solvent was not constant, as in the case of synthetic mixtures, but varied in order to dissolve the sample and bring component concentrations within the calibration range. This variability in solvent volume made it necessary to correlate the ratio of component peak area to that of the internal standard with component concentration. However, component concentration could not be determined since the total solution volume

could not be measured. Peak ratios were, therefore, correlated with component mass per millilitre solvent used and the following development justifies the approach. Since peak area is proportional [27] to concentration in injected sample, we have for the i^{th} component

$$A_i = f_i C_i = f_i \left(\frac{m_i}{V_t} \right) b \quad (\text{IV-1})$$

and for the internal standard

$$A_s = f_s C_s = f_s \left(\frac{m_s}{V_t} \right) b \quad (\text{IV-2})$$

where A is peak area, f detector response factor, C concentration in silylated sample, m mass (g) in solution before silylation, V_t total volume of solution before silylation, b a proportionality constant accounting for the dilution by the silylating reagents, and subscript i denotes quantities for i^{th} component while s denotes those for internal standard. Dividing Eq. (IV-1) by Eq. (IV-2) we have:

$$\frac{A_i}{A_s} = \left(\frac{f_i}{f_s} \right) \frac{m_i}{m_s} \quad (\text{IV-3})$$

and since

$$m_s = C'_s V_s \quad (\text{IV-4})$$

where C'_s is the concentration (g/ml) of internal standard in the solvent, a fixed quantity, and V_s the solvent used to dissolve the sample, Eq. (IV-3) becomes

$$\frac{A_i}{A_s} = \left(\frac{f_i}{f_s C'_s} \right) \frac{m_i}{V_s} \quad (\text{IV-5})$$

The bracketed term in Eq. (IV-5) is constant and, therefore, peak area ratios correlate with component mass per millilitre solvent used according to the simple model of a line through the origin.

Least squares analysis of the experimental data (given in Appendix A) showed that the model

$$\left(\frac{A_1}{A_S}\right) = B_1 \left(\frac{m_1}{V_S}\right) \quad (\text{IV-6})$$

explained more than 99.8% of the variation in the data and, therefore, correlated the data very well. Table IV.2 gives some regression statistics while Table IV.3 gives estimates of the experimental error in the peak area ratios. Unknown compositions were calculated from Eq. (IV-6) using the least squares estimates of the B_1 's and the experimental values of peak area ratios and solvent volume used.

TABLE IV.2
Regression Statistics

Compound	Correlation Coefficient	Regression Coefficient	
		Least Squares Estimate	95% Confidence Interval
EG - TMS	0.9984	31.78	$31.36 < B < 32.20^a$
DEG - TMS	0.9989	78.30	$77.43 < B < 79.17^b$
DMT	0.9998	38.15	$37.91 < B < 38.39^a$
MHET - TMS	0.9990	43.41	$43.41 < B < 43.82^b$
BHET - TMS	0.9971	46.46	$45.72 < B < 47.20^b$

a Based on 21 degrees of freedom

b Based on 22 degrees of freedom

TABLE IV.3
Experimental Error

Compound	Mean Peak Area Ratio	Experimental Error, δ
EG - TMS	0.499	0.017
DEG - TMS	0.245	0.007
DMT	0.635	0.011
MHET - TMS	0.713	0.018
BHET - TMS	0.779	0.032

The previously mentioned silylating procedure and the volumes of silylating reagents taken assured a minimum 13:1 excess of silylating groups to those to be silylated. Factorial experiments at half and double this ratio did not show any significant effects.

Experiments showed that silylation was very fast and under the experimental conditions it was complete within one or two minutes.

Retention times and calibrations were checked periodically and found to be stable. Analysis of the instrumentation set-up showed that in all probability half of the already low experimental error was caused by the inaccuracy of the mechanically activated integrator system.

B. Gas Chromatographic Analysis of Distillate

The distillate is defined as the mixture of methanol and other relatively volatile components which might possibly distill over during the precondensation stage. Of all the previous investigators only Griehl and Schnock [9] referred to the analysis of the distillate. They based this analysis on refractive index variation with ethylene

glycol content. Presumably, the other researchers found the distillate to be virtually pure methanol without reporting so.

In the preliminary kinetic study by the author, it was assumed that the distillate was pure methanol. However, in the later study the following experimental techniques were established for analyzing the distillate by gas-liquid chromatography.

1. Experimental

Since there was no knowledge about the components of the distillate, its analysis was developed according to a trial-and-error procedure. Firstly, a suitable GLC column had to be found which would adequately and completely resolve the sample, and, secondly, some or all of the resolved components had to be identified.

After a few preliminary trials with different columns at various temperatures, it was found that a column with 10% Ucon 50 HB 2000 on Chromosorb G, A/W, DMCS, 100/120 mesh adequately resolved the distillate sample at the column oven temperature of 70°C and carrier gas flow rate of 18 ml/min, measured at the column exit and at room temperature. The carrier gas used was nitrogen.

The gas-liquid chromatographic analysis was carried out using a Varian Aerograph, Model 1200, gas chromatograph equipped with an isothermal temperature module for controlling the oven temperature.

For the distillate analysis, the temperatures of the injector port, the oven and the ionization detector region were kept constant at 200°C, 70°C and 210°C, respectively.

A chromatogram of a typical distillate sample is shown in Fig. IV.3. This clearly indicates the presence of components other than methanol in the sample. Identification of some of these compounds was

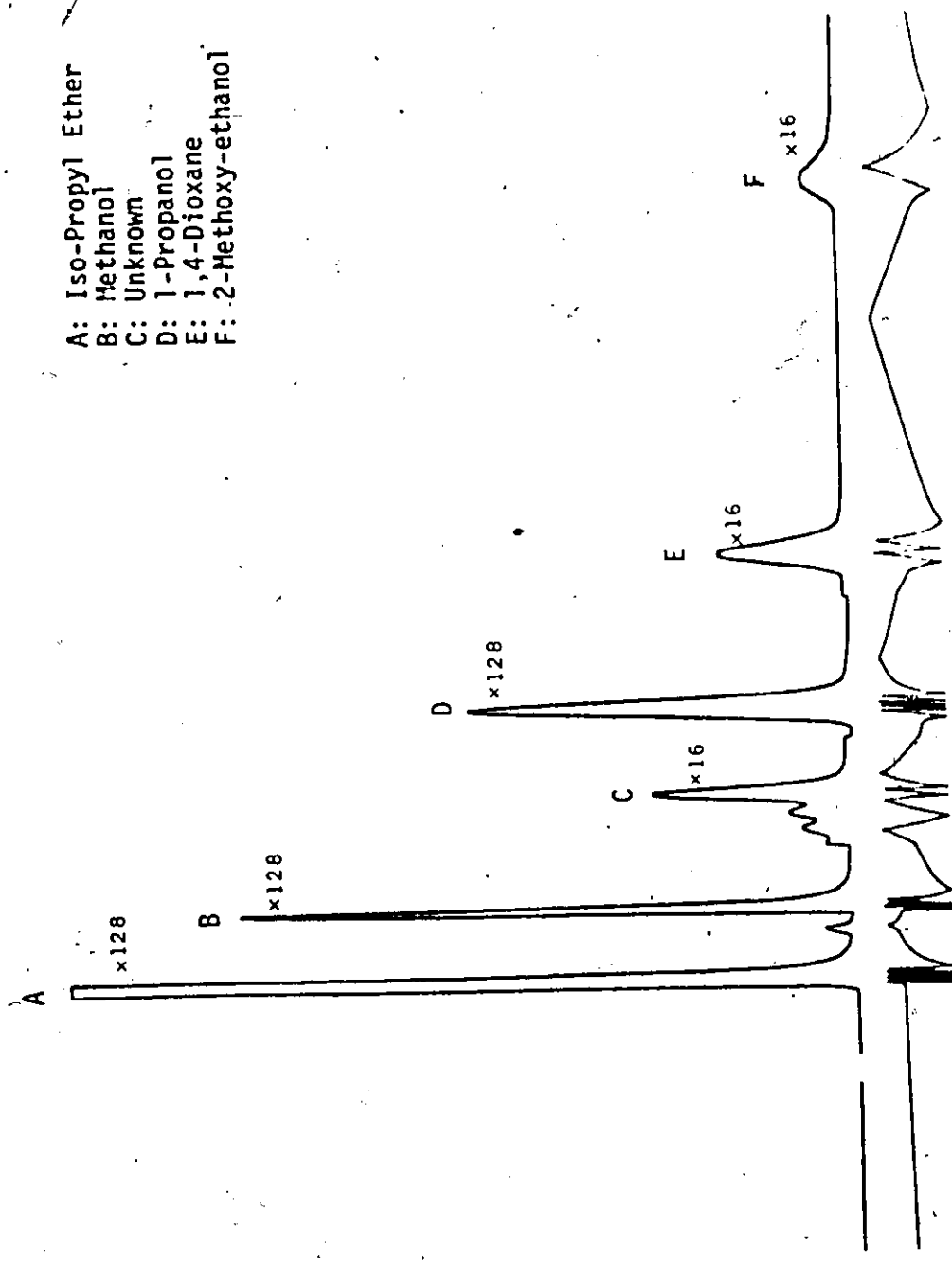


Fig. IV.3 Chromatogram of a Distillate Sample (Run R-1168)

achieved by hypothesizing reactions which ethylene glycol might undergo, and comparing the retention time of the major products of the assumed reactions with retention times on the actual distillate chromatogram and/or adding the pure compound to the distillate, obtaining a chromatogram and comparing it with that of the distillate alone. These are standard gas chromatography identification procedures, and they led to the following identified compounds in the distillate: methanol, dioxane, 2-methoxyethanol, ethylene glycol, while no attempt was made in identifying other compounds indicated in the chromatogram.

Calibration experiments were restricted to methanol and followed the general procedure for the GLC analysis of the distillate. The distillate was sampled with a microlitre syringe, fitted with a Chaney adaptor, by means of which 0.3 ml were dispensed into a preweighed vial. After weighing, the sample was diluted with 3 ml dilutant which was made of 5 ml 1-propanol diluted to 100 ml with isopropyl ether. One microlitre of the diluted sample was injected into the chromatograph and a chromatogram obtained under the previously stated conditions.

High purity methanol 99.9 mol% and purified iso-propyl ether were procured from Fisher Scientific Co., while reagent grade n-propyl alcohol was obtained from Anachemia Chemicals Ltd.

2. Correlation of Calibration Data

The calibration curve for methanol was established by using three different standards of methanol. Peak areas were measured by a Disc integrator.

The experimental procedure was established in a manner which

ensured that the mass of internal standard was constant and, therefore, Eq. (IV-3) becomes

$$\frac{A_i}{A_s} = \left(\frac{r_i}{r_s m_s} \right) m \quad (\text{IV-7})$$

and since the bracketed term is constant, Eq. (IV-7) shows that peak area ratios plotted against methanol mass should result in a straight line through the origin.

Least squares analysis of the calibration data (given in Appendix A) showed that the model

$$\left(\frac{A_i}{A_s} \right) = \beta m_i \quad (\text{IV-8})$$

described the data very well and explained 99.98% of the variation of the data. The 95% confidence interval for the regression coefficient is

$$4.085 < \beta < 4.177 \quad (\text{IV-9})$$

with seven degrees of freedom, while the experimental error is estimated to be $\hat{\sigma} = 0.014$

C. Product Characterization Analysis

In the course of the investigation of the transesterification reactions it was found necessary to obtain additional information about the composition of the liquid product. This was necessitated by the inability to establish meaningful material balances in terms of a few chemical species and was achieved by especially treating the liquid product and, subsequently determining either functional groups by wet analysis or selected compounds by means of gas chromatography. The following procedures and analyses were applied to the liquid product of run R-113B-702 only.

1. Total Carboxylic Groups

2.5 g of liquid product or left-over mass was dissolved in a mixture of 40 ml 2-propanol, 10 ml 1,4-dioxane and 5 ml methanol at 65°C, while a blank of the same total solvent volume was kept at room temperature. When the sample was dissolved 50 ml of aqueous 1N NaOH was added to both the sample and the blank, and saponification of the liquid product was carried out in thermostated water bath maintained at 65°C for 2½ hours. Then enough distilled water was added to dissolve the precipitated salts, an equal volume of water was added to the blank, and the remaining sodium hydroxide was titrated with 0.5N HCl to the phenolphthalein end-point. The difference between added and unreacted NaOH, corrected according to the blank, was used up in saponifying the sample esters. This difference is equal to total milliequivalents of carboxylic groups in the sample. From the latter the amount of DMT in the original sample could be obtained and compared with the amount of DMT weighed.

2. Total Free Carboxylic Groups

1.0 g of left-over mass was dissolved at room temperature in 75 ml 1,4-dioxane and 25 ml methanol and a blank of the same volume was prepared. The sample solution was cooled down to 0°C in an ice bath and titrated with methanolic 1N NaOH to phenolphthalein end-point. The blank was similarly titrated. The difference between the NaOH volumes used for the sample and the blank represents milliequivalents of free carboxylic groups in the sample.

3. Glycols in Saponified Product

2.5 g of left-over mass were saponified according to the procedure given in section IV.C.1 and upon cooling the white precipitate was filtered off with a Buchner funnel and washed with 25 ml 2-propanol. The filtrate was neutralized with 2N HCl and was further treated to prepare samples for GLC analysis. This treatment was aimed at removing the water, added in the saponification step, which is objectionable in the silylation step.

To the neutralized filtrate 50 ml 2-propanol were added, and the resultant solution was evaporated down to 25 ml on a low temperature hot plate. The concentrated solution, thus, obtained was diluted with 25 ml 1,4 - dioxane, and the precipitate formed upon dilution was filtered off and washed with dioxane. After dissolving 1.34 g of bibenzyl (the internal standard) in the filtrate, its volume was made up to 100 ml and the resultant solution was ready for silylation and chromatographic analysis according to section IV.A.

V EXPERIMENTAL EQUIPMENT AND PROCEDURES

The investigation of the kinetics using Amberlite IR-120 was interrupted in order to embark on a more ambitious project. The aim of this project was the establishment of a conclusive model describing the surface phenomena of the transesterification reactions catalyzed by cation exchange resins.

In the pursuit of the above objective a continuous flow reactor was to be used in obtaining kinetic data. The data acquisition program was to draw heavily on statistical experimental designs and extensive chemical analysis of the transesterification products, while model discrimination techniques were to be used in developing the kinetic model(s).

Because of the gel-like structure of Amberlite IR-120 which might not allow utilization of internal exchange capacity, it was decided to study the transesterification reactions catalyzed by Amberlyst 15. The latter is a macroreticular resin with average pore diameter of about 180 Angstrom units, average surface area of 47 m²/g dry resin and total exchange capacity of 4.8 meq/g dry resin [28].

A. Differential Recycle Reactor

The limitations of a batch reactor system, mainly due to the complications caused by its transient nature, made use of a continuous flow reactor very desirable. Actually, it was decided to go one step further, that is, to design and build a differential recycle or recirculation reactor, a schematic of which is shown in Fig. V.1. The differential character of this reactor is established by adjusting the recycle volumetric rate, V_r , to be much larger than the feed flow, V_o .

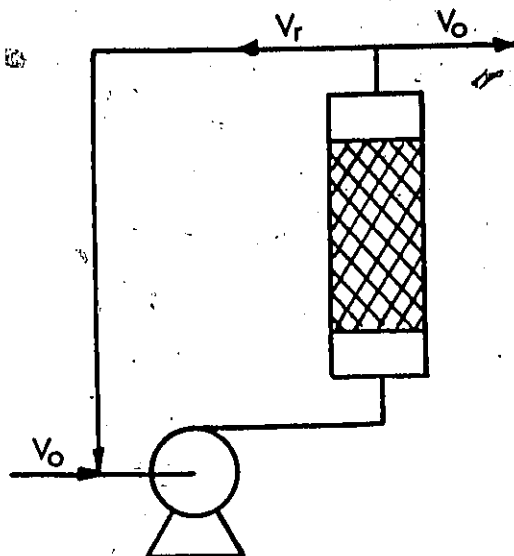


Fig. V.1 Schematic of Recycle Reactor

Use of differential recycle reactors in kinetic studies of heterogeneously catalyzed reactions was proposed by Dohse [29] and Hougen [30], and various designs have been advanced by Perkins and Rase [31], Boreskov [32], Korneichuk [33], Butt et al. [34] and others. The experimental researches of Perkin and Rase and Butt et al. have demonstrated that this reactor does offer significant advantages in obtaining accurate reaction rate data for kinetic model building. The attractive features of a differential recycle reactor are [31, 35]:

- a direct measure of the reaction rate is obtained with each experimental run at steady state,
- the large changes in concentration across the reactor loop minimize the effects of errors in analysis of inlet and outlet stream compositions, giving accurate and precise rate measurements, and
- good temperature control is obtained with appropriate recirculation rate

while its disadvantages are a prolonged transient period and possible difficulties in ascertaining whether steady state conditions have obtained. The latter would be experienced in cases where fast chemical analysis is not possible.

1. Recycle Reactor Design

The design of the recycle reactor dealt with the following major components: the reactor and methanol-stripper loop, the feed flow system and control elements.

Originally, the design was guided by a strong sense of economizing and use of available equipment. For example, in order to use available temperature control apparatus and avoid waste of chemicals, arising from a long transient operation of a large reactor, it was decided to keep the reactor size small. This in turn dictated the size of all other equipment and of the streams. Figure V.2 shows a schematic of the fairly elaborate experimental set-up which was built and found to function smoothly.

The materials of construction used were stainless steel 304 and 316, aluminum alloys, glass, Teflon, Viton and mild steel. Both feed and head tanks were Teflon coated to avoid contamination of reactants with possible corrosion products.

Since dimethyl terephthalate and transesterification products are solids at room temperature, it had to be ensured that the temperature of every inch of tubing and every piece of equipment was high enough to prevent solidification. Heating of the tubing, the packed tower and the pumps was achieved by means of heating tapes while heating of the feed and head tanks as well as the oil baths by suitable tubular heating

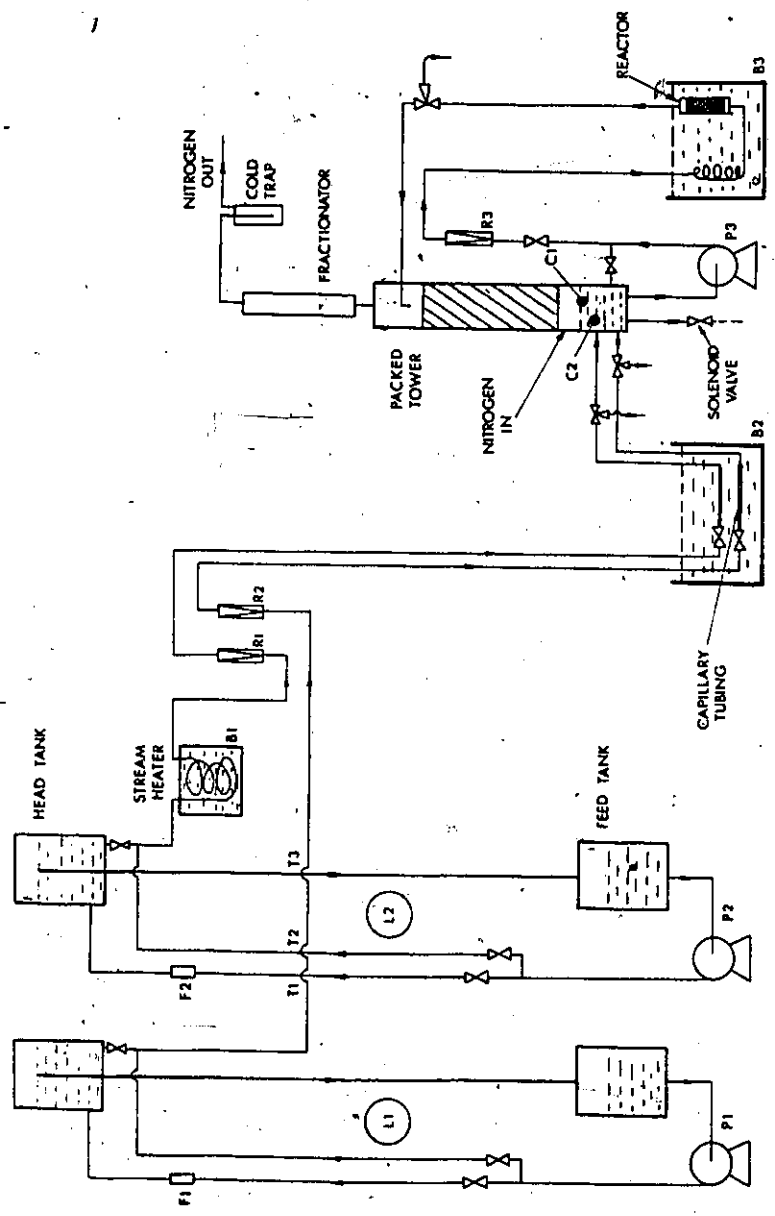


Fig. V.2 Schematic of Recycle Reactor Set-up

elements. With the exception of the oil baths which were controlled by relays, temperature control of other equipment was achieved by variable transformers. Thermocouples were extensively used to monitor both wall and stream temperatures.

a. The Reactor and Methanol-Stripper Loop

The reactor itself was made out of standard pipe fittings, and a schematic is shown in Fig. V.3.- Both 1" and 1 1/2" pipe fittings were used, which coupled with nipples of various lengths resulted in an assortment of reactors, the largest of which could accommodate about 150 grams of dry Amberlyst 15. The lower end of the reactor cylinder was mechanically fitted with a piece of 200 mesh stainless steel 316 screen, while the upper cap was similarly fitted. The screens, of course, were used to confine the resin particles in the reactor. Two 1/16" miniature thermocouples, with stainless steel sheaths, were used to monitor the temperature of the inlet stream and the catalyst bed close to its upper end. The reactor, along with a temperature equilization coil for the incoming stream, was immersed in a paraffinic oil bath.

In order to somewhat reduce the complexity of the transesterification reactions, it was decided to provide a means of effectively removing the methanol produced from the reactor system. The removal of methanol would make the reactions irreversible, and, thus, facilitate the kinetic analysis. To this end, a packed tower was designed (Fig. V.4) and installed in the recycle loop of the reactor (Fig. V.2). The effluent stream of the reactor loaded with methanol would be directed to the top of the tower and flow downwards by gravity, and in the process be stripped of its methanol content by an uprising stream of nitrogen gas.

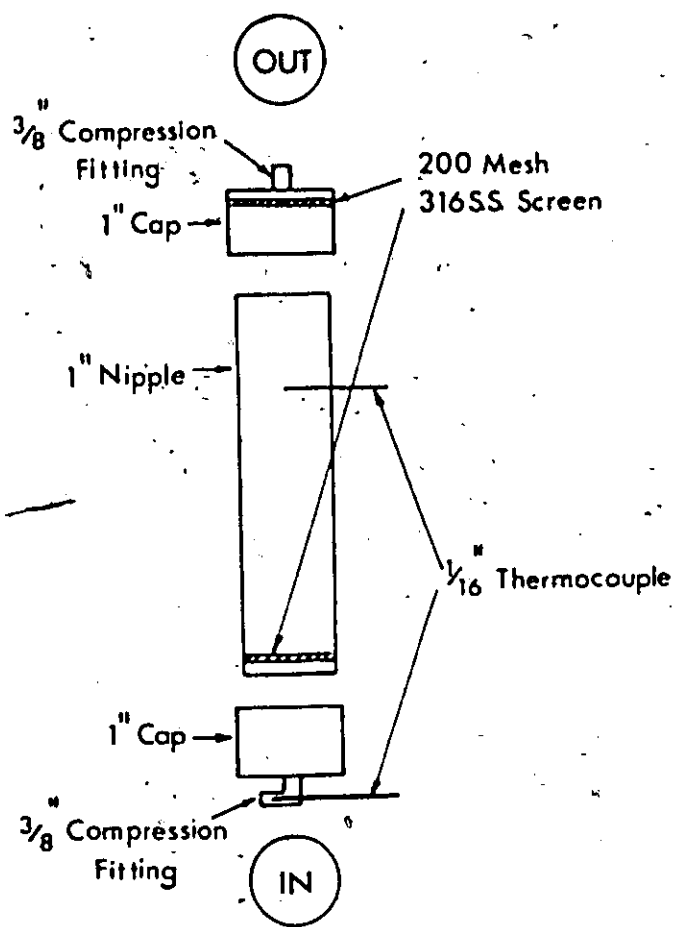


Fig. V.3 Fixed-Bed Reactor

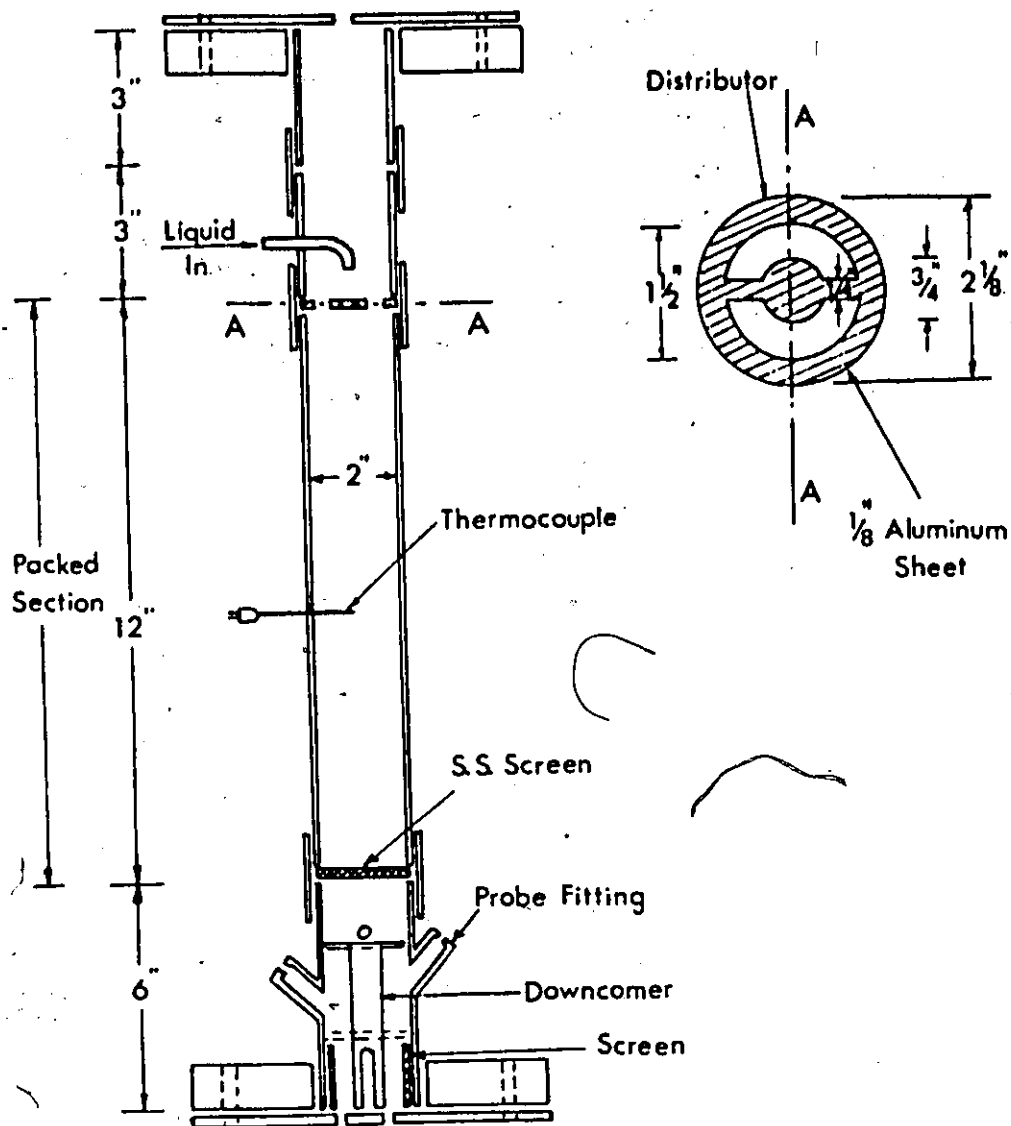


Fig. V.4 Packed Tower

The packed tower was made from 2" aluminum pipe fittings for the cylinder and aluminum plate for the blind flanges. The packing was 1/4" Raschig rings made of glass, and was supported by a piece of 4 mesh stainless steel screen. The distributor served to spread the incoming liquid over the packing. The lower end of the tower had two special fittings which were used to support the liquid-level sensors (C1 and C2 in Fig. V.2). These sensors were part of a liquid-level control system which regulated the pool of liquid in the bottom of the packed tower. This control system, which is an on-off system, requires smooth free liquid surface in order to function properly, and the downcomer and cylindrical stainless steel screen at the bottom of the tower were used to fulfill the requirement. The downcomer (Fig. V.5) was used to collect and direct the liquid leaving the packing section, and, thus, avoid false activation of the controller caused by erratic liquid drippings from the support plate. The cylindrical screen was used to diffuse the turbulent by-pass flow from the recycle pump (P3 Fig. V.2).

The behaviour of the reactor depends to a large extent on the inlet and outlet streams and their control. In other words, the reactor may be expected to operate smoothly only if the streams are reliably and well controlled because it is only then that steady state conditions, a prerequisite of making kinetic measurements, may obtain.

If the methanol removal equipment was not necessary in the system the outlet stream hardware could have been a simple overflow arrangement and control of the feed flow would have sufficed to control both streams. However, the presence of the methanol stripper excluded that arrangement and necessitated control of both streams. It was then decided to control

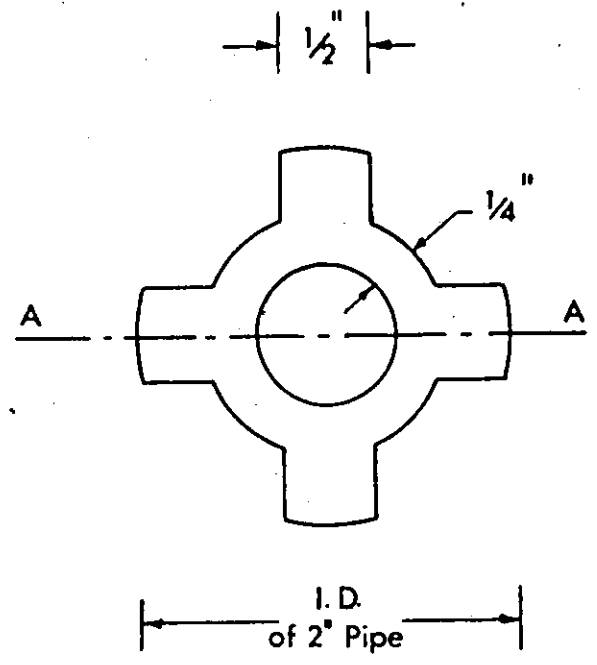
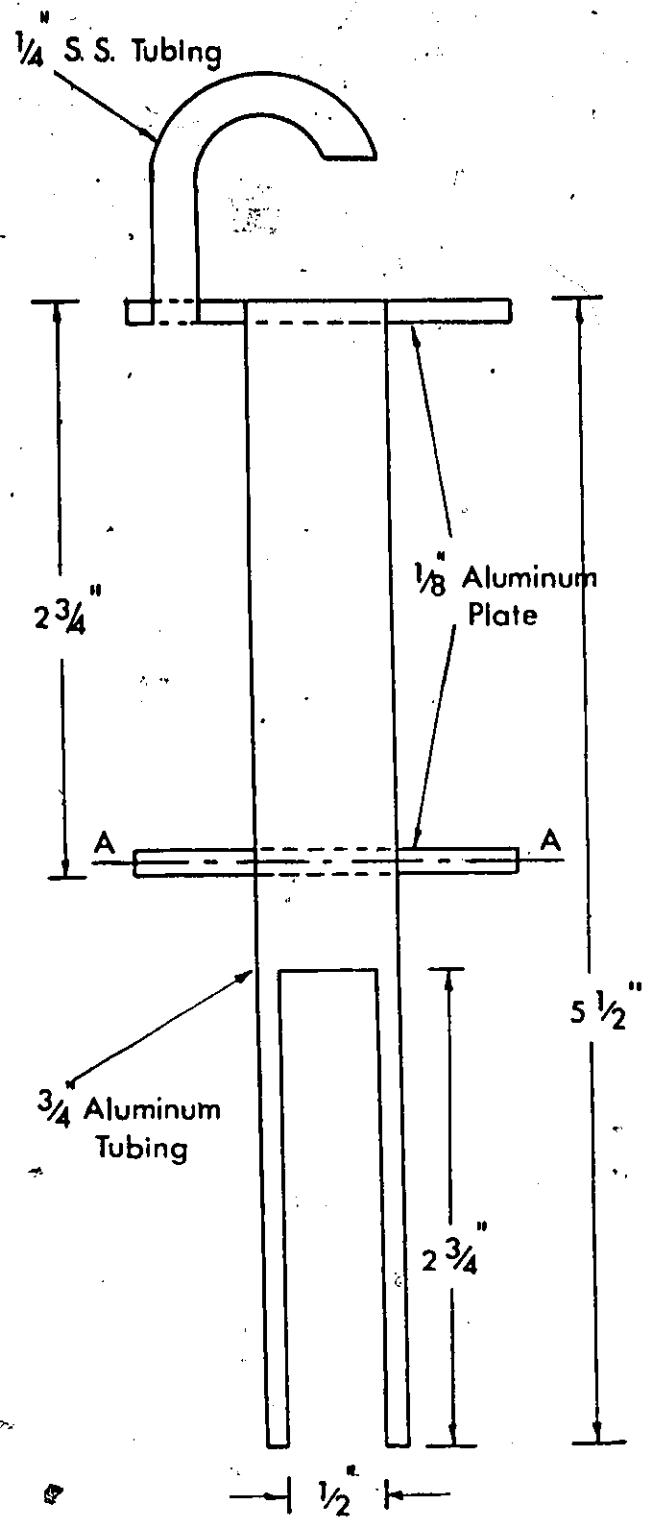


Fig. V.5 Downcomer

the outlet stream by means of a liquid-level controller and solenoid valve arrangement. According to this method of control the volume of the liquid pool at the bottom of the packed tower would increase until the free liquid surface reached the "high" probe (C1 in Fig. V.2) at which time the controller would open the solenoid valve, thus, allowing liquid discharge. The liquid outflow would then go on until the free liquid surface was lowered to just below the "low" (C2 in Fig. V.2) probe when the controller would interrupt the liquid discharge by closing the solenoid valve. The operation of the controller actually used (DYNA-SENSE Electronic Liquid Level Controller, Model No. 7188, by Cole-Parmer) relied on electrical conductivity of the liquid being controlled. This on-off mode of control of the outlet stream made the volume of the recycle reactor variable, and the effects of this variability are explored in the mathematical analysis of the reactor given in chapter VII.

The nitrogen stream loaded with vapours from the packed tower stripping operation was to enter the fractionator (Fig. V.2), atop the tower, where vapours other than methanol would be condensed and returned to the reactor loop. The fractionator was made out of a jacketed Vigreux column, the jacket of which would be maintained at about 100°C by means of recirculated and thermostated water. Subsequently, the nitrogen stream with methanol vapours would pass through a cold trap, maintained at the freezing point of methanol, where methanol vapours would be condensed and collected.

b. The Feed Flow System

The design of the feed flow system was guided by the following

basic requirements: stable driving force, steady resistance to flow along the line and stable characteristics of the flow control element. Building the system which would ensure the above features required considerable time, several modifications (a brief presentation of which is given in Appendix B) and persistence on the part of the author.

The stable pressure head was achieved by using a feed and a head tank combination (Fig. V.2). Liquid from the feed tank would be pumped to the head tank via tubing T1 and in the process be filtered by the fine filter F2 (particles 15μ or larger would be removed). The liquid level in the head tank was maintained constant by the overflow tubing T3 which returned excess liquid back to the feed tank. The loop thus established would keep both the level and the temperature of the feed liquid constant. Tubing T2 was to divert the delivery stream to the feed flow system directly in order to purge the latter of air pockets (using the high velocity created by the pump).

The above feed loop arrangement established the constancy of the one end of the driving force and similar stability had to be secured for the other, that is, the point of introduction of the feed stream into the recycle reactor loop. Experience indicated that the point of introduction should not be in the delivery side of the recycle pump (P3), because slight, perhaps unavoidable pressure fluctuations would adversely affect the stability characteristics of the feed streams. It was therefore decided to place the feed streams just above the downcomer plate at the lower end of the packed tower where the pressure was expected to be stable, and which was later confirmed.

With stable pressures at the end points, stable driving force would be obtained by a stable temperature profile along the feed line, which would secure the required stability of the stream physical properties. This was, as for other parts of the system, achieved by electric heating tapes, controlled by variable transformers, and adequate fiberglass insulation. Good temperature control would also secure steady resistance to flow along the line.

The feed loops, L1 for DMT and L2 for ethylene glycol are the same except that pump P1 was high temperature one whereas pump P2 for glycol was a magnetically driven pump with a maximum temperature limit of about 250°F. Actually, this pump was found to decouple even at lower temperatures and as a result the temperature of the glycol feedstock had to be kept at about 220°F, which was about 80°F lower than the required stream temperature. This necessitated the introduction of a stream heater, B1, for heating the glycol stream up to the required temperature. The heater was a paraffinic oil bath the temperature of which was controlled by means of a proportional controller (Thermoelectric Model 32422) whose sensor was immersed in the glycol stream just downstream from the heater.

c. The Flow Control Element

The flow control elements, which were used in setting and regulating the feed stream flow rates, were made from a fine metering valve and a piece of glass capillary tubing in series. This composite flow control element is shown in Fig. V.6, and its use was

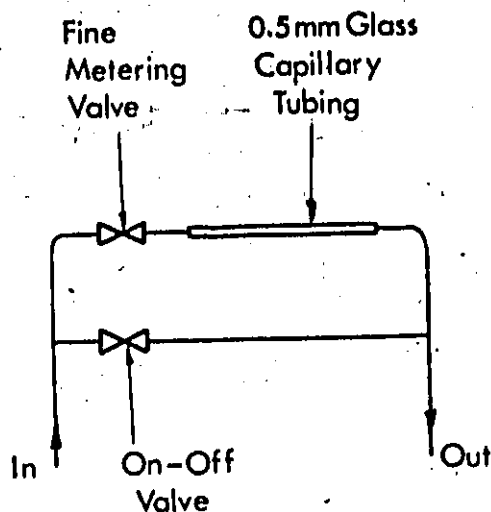


Fig. V.6 Composite Flow Control Element

adopted because of the following reasons: a) the use of the valve alone would have to be set at very low flow coefficient (C_V) values in order to regulate the flow rate in the range of 4-15 g/min desired (Fig. V.7) and experience indicated that such low settings were troublesome, b) the flow rate was strongly dependent on the flow coefficient so that uncontrollable factors affecting the latter would influence the former, and c) the use of a capillary tube alone would not be satisfactory because it did not allow on-stream adjustment of flow rate.

The size of the capillary tubing used was chosen by calculating the mass flow rates for given capillary length and diameter at various valve openings of a given valve at the available pressure drop. This calculation was based on the equation:

$$\Delta P_{\text{total}} = \Delta P_{\text{valve}} + \Delta P_{\text{capillary}} \quad (V-1)$$

where it was assumed that ΔP_{total} was the available head with pressure losses along the lines neglected due to the large line diameter and the low flow. Now, we have that

$$\Delta P_{\text{valve}} = \frac{1}{(7.47 \times 60 \times 12)^2} G \frac{Q^2}{C_v^2} \quad (V-2)$$

and, since the flow is laminar,

$$\Delta P_{\text{capillary}} = \frac{128}{g_c \pi} \frac{QL\mu}{D^4} \quad (V-3)$$

where C_v is the valve flow coefficient, Q is the volumetric rate of flow, G and μ are specific gravity and viscosity of the liquid, respectively, and L and D are length and diameter of the capillary tubing, respectively.

Substituting Eqs. (V-2) and (V-3) in Eq. (V-2), there is obtained

$$\Delta P_{\text{total}} = \frac{1}{(7.47 \times 60 \times 12)^2} G \frac{Q^2}{C_v^2} + \frac{128}{g_c \pi} \frac{QL\mu}{D^4} \quad (V-4)$$

from which Q is easily calculated upon specification of the other terms. Here, Q is expressed in cubic feet per second which was transformed to grams per minute, the mass flow rate.

Table V.1 gives physical property values for dimethyl terephthalate and ethylene glycol used in the design of the flow control element, and the capillary dimensions chosen as most suitable from the control and building points of view.

TABLE V.1

Flow Control Element Data

Temperature: 145°C				
Total Head: 50 in.				
	ρ , g/ml	μ , cp	L, in	D, mm
Dimethyl Terephthalate	1.119 ^a	0.981 ^b	5.75	0.5
Ethylene Glycol	1.017 ^a	0.62 ^c	4.75	0.5

a estimated from molar volume [Appendix D]

b Petukhov [36]

c Perry's [37]

The effect of the flow control element design on the mass flow rate is shown in Fig. V.7 for the ethylene glycol stream based on the specifications of Table V.1.

To ensure stable dimensional characteristics the composite flow control elements were immersed in a thermostated paraffinic oil bath maintained at 145°C.

2. Reactor Operation Procedure

The feed tanks were loaded with ethylene glycol and dimethyl terephthalate in pellets and power to all the heating units was turned on. One day was then allowed for DMT to melt and the various parts of

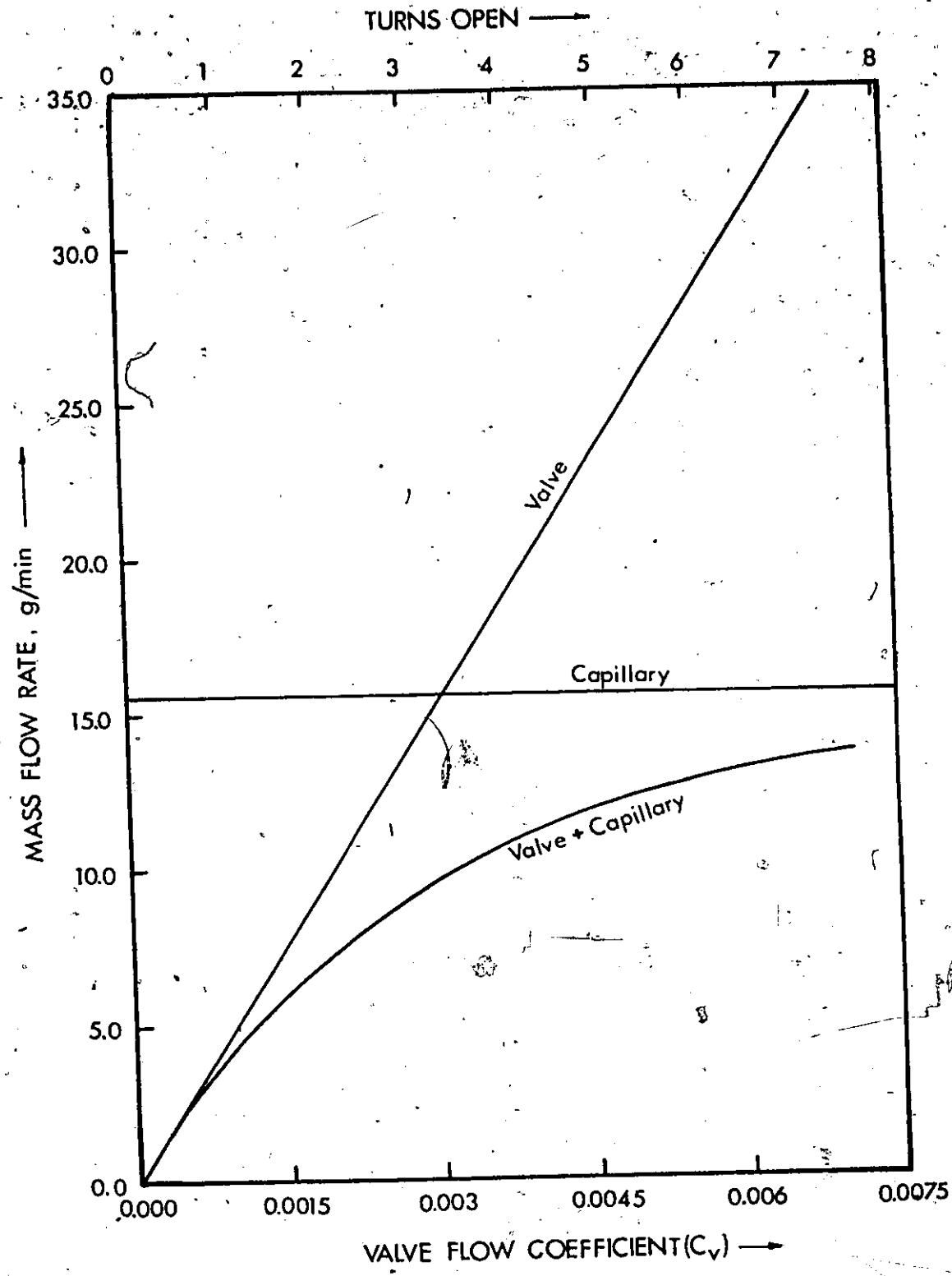


Fig. V.7 Effects of Flow Control Element Design.

the system to reach the set temperatures. Subsequently the feed loop pumps (P1 and P2 Fig. V.2) were turned on and feedstock recirculation in the loop feed tank-line T1 - head tank - line T3 - feed tank was established. After the recirculation had equalized feed stock temperatures in the head and feed tanks, the pump delivery was momentarily switched to line T2 and purging of the feed line was achieved while the stream was diverted to the drain. Flow rates were then set by adjusting the fine metering valve of the control element and accumulation of reactants in the desired molar ratio began in the bottom of the packed tower. Accumulation continued until the liquid surface rose to the "high" probe (C1) of the liquid level controller, which opened the solenoid valve and discharge took place. At that time the reactor loop pump, P3, was turned on and recirculation rate was adjusted by means of a regulating valve and the help of a rotameter.

The last operation marked the beginning of an experimental run. The stream of nitrogen was turned on and adjusted to about 60 cc/min, which was enough to adequately strip the liquid stream of methanol. The operation of the reactor was followed by monitoring feed flow rates and reactor loop recycle rate by means of the rotameters (R1, R2, R3) and the temperatures of streams, of tanks etc. by means of two multiple point strip chart recorders. Occasional adjustments of flow rate were made manually.

The approach to steady state was followed either by determining the rate of methanol production or by analysing the liquid outlet stream. The rate of methanol production was determined from the amount collected in the cold trap over a measured length of time. The composition of the

outlet stream was established by gas chromatographic analysis of stream samples obtained at the exit of the solenoid valve at the end of the liquid discharge cycle. These data were then plotted versus time and a straight line relationship parallel to the time axis indicated that steady state conditions had obtained. Under steady state conditions, feed stream mass flow rates were determined by collecting the streams in preweighed vials over a timed interval. These rates along with the analysis of the outlet stream were used to calculate reaction rates according to the following equation:

$$-r_i = \frac{F_i^o - F_i^f}{W} \quad (V-5)$$

where $-r_i$ is reaction rate for component i , F_i^o and F_i^f are the inlet and outlet molar rates of component i in moles/min and W is the amount of catalyst in grams.

B. Batch Reactor

During the course of the investigation and with the help of the chemical analysis of the liquid product it became evident that other reactions, in addition to the ester interchange reactions, were catalyzed by the cation exchange resin, Amberlyst 15, to a significant extent. This made the use of a batch reactor necessary because only the batch reactor would help establish mass balances and, hopefully, the number of significant reactions.

A new, improved version of batch reactor was, therefore, designed. The improvements were the introduction of a nitrogen gas stream to remove the methanol vapour from the reactor and the use of a special sampling probe which would make multiple sampling of the reaction product during a

run possible. The use of the nitrogen gas necessitated a cold trap for condensing the vapours from the gas stream.

1. Batch Reactor Design

A schematic of the batch reactor set-up, which was made of glass, is shown in Fig. V.8. The reactor itself was a three-necked distilling flask. The centre neck was used for a glass stirrer which was fitted with a Teflon-and-O-ring seal for a leak-free operation. One of the side necks was connected to a Vigreux column the temperature of which was maintained at about 100°C by means of a heating tape. The opposite neck was fitted with a suitably designed probe for sampling the reaction melt. This probe had a separate inlet for a nitrogen gas stream which was used to carry the methanol vapours out and, thus, ensure irreversibility of the transesterification reactions. The vapour laden nitrogen stream was directed through the Vigreux column and an air condenser to a cold trap where the vapours were condensed and collected. The cold trap was made of a test tube, 21 mm I.D. and 20 cm long, and an inlet tube, 6 mm O.D., which extended to about 3 cm from the bottom of the test tube and was supported by a rubber stopper with a length wise groove which allowed cooled-down nitrogen to escape. The trap was immersed into a methanol cold bath maintained at the freezing point of the alcohol by means of liquid nitrogen.

The sampling probe, a schematic of which is shown in Fig. V.9, was made of Pyrex glass. A piece of capillary tubing, 1.0 mm in diameter, was formed as shown and jacketed with a piece of tubing, the free end of which was joined to a ground glass joint. Then a piece of chromel wire

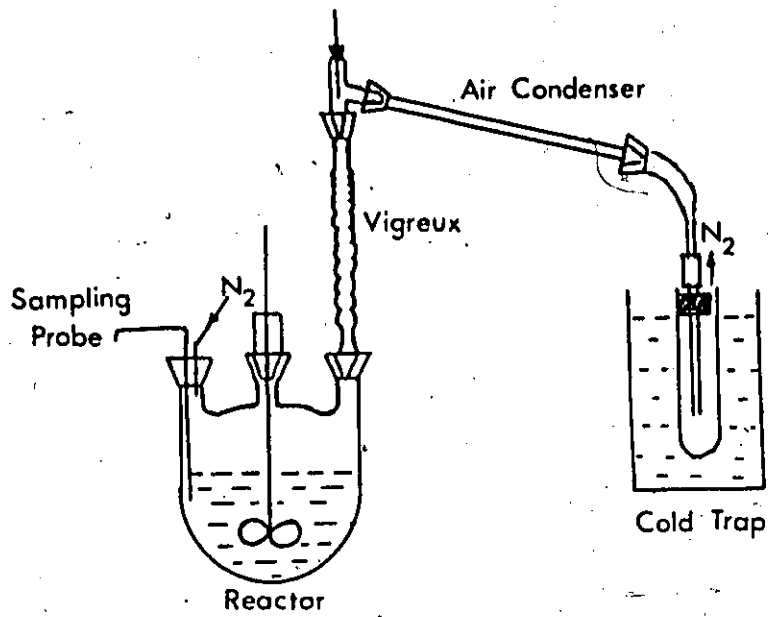


Fig. V.8 Schematic of Batch Reactor

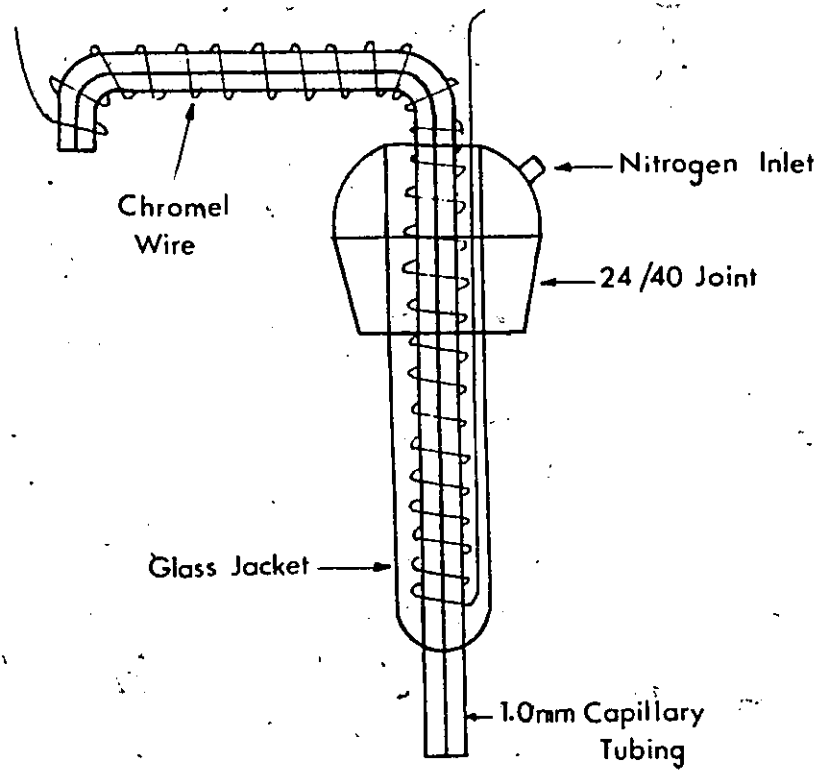


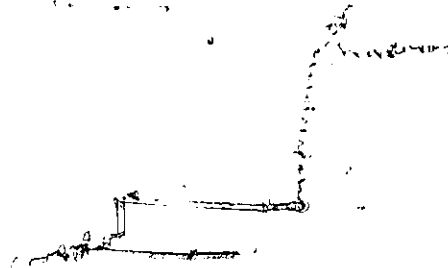
Fig. V.9 Sampling Probe

was wound around the capillary and pushed down the jacket. The chromel wire was used as a heater in maintaining the capillary at a temperature high enough to avoid solidification of the sample. Samples were withdrawn by connecting a sample bottle to the capillary and evacuating with a water pump. To avoid withdrawal of resin particles during sampling, the immersed end of the capillary was covered with a mat of glass wool secured in place with a piece of Teflon tubing.

2. Batch Reactor Operation

Dimethyl terephthalate powder and ethylene glycol were weighted into the reactor at the desired molar ratio, and the loaded reactor was placed in a thermostated paraffinic oil bath accurate to $\pm 0.1^\circ\text{C}$. At that time power to the Vigreux and sampling probe heaters was turned on. After the reactor charge had become a clear melt a preweighed amount of catalyst was placed in an oven, maintained at about the reaction temperature, for about fifteen minutes. The cold bath was then made by pouring liquid nitrogen into methanol in a Dewar flask, and the cold trap precooled for a few minutes while protected from internal moisture condensation by a tube filled with Drierite. Prior to the catalyst addition a few millilitres of methanol were added to the reactor in order to establish equilibrium in the column and the condenser and, thus, prevent loss, as system hold-up, of methanol produced. When distillation of the added methanol had virtually ceased, the preheated catalyst was funneled into the reactor through the sampling probe port. Immediately after the timer and nitrogen gas flow at the rate of about 40 ml/min were started. Periodically liquid samples were withdrawn and at practically the same time the cold trap was replaced with a new, dried

and precooled one. The liquid samples withdrawn were very small, usually less than one gram. The samples thus obtained yielded, when analyzed, component time profiles for each experimental run.



VI TRANSESTERIFICATION CATALYZED BY AMBERLYST 15

The cation exchange resin Amberlyst 15, which was to be used as catalyst in the transesterification of dimethyl terephthalate with ethylene glycol, is marketed in the hydrogen form and in spherical beads in the particle size range of 16 to 50 mesh U.S. standard screens. Therefore, the catalyst required no pretreatment except screening for separating it into desirable particle size fractions. These fractions were obtained by dry screening, and were subsequently dried overnight at 110°C. Some of these fractions would be used in statistically designed experiments, a partial aim of which would be identification of experimental conditions where intraparticle mass transfer effects would be negligible.

A. Recycle Reactor Performance

As was mentioned in Chapter V kinetic data for the precondensation stage reactions were to be obtained from the differential recycle reactor. To this end, the reactor itself would be loaded with the desirable mass and fraction of resin catalyst, and the system would be started up and allowed enough time to reach steady state. The transient state of the reactor was to be followed by analyzing the reactor liquid product periodically and/or determining the rate of methanol production in order to ascertain the establishment of steady state. Typical data for the reactor operation are shown in Fig. VI.1, and they clearly indicate that the reactor system operated very smoothly.

In a few preliminary experiments using the recycle reactor the steady state conversion of DMT across the reactor was about 20%. Yet

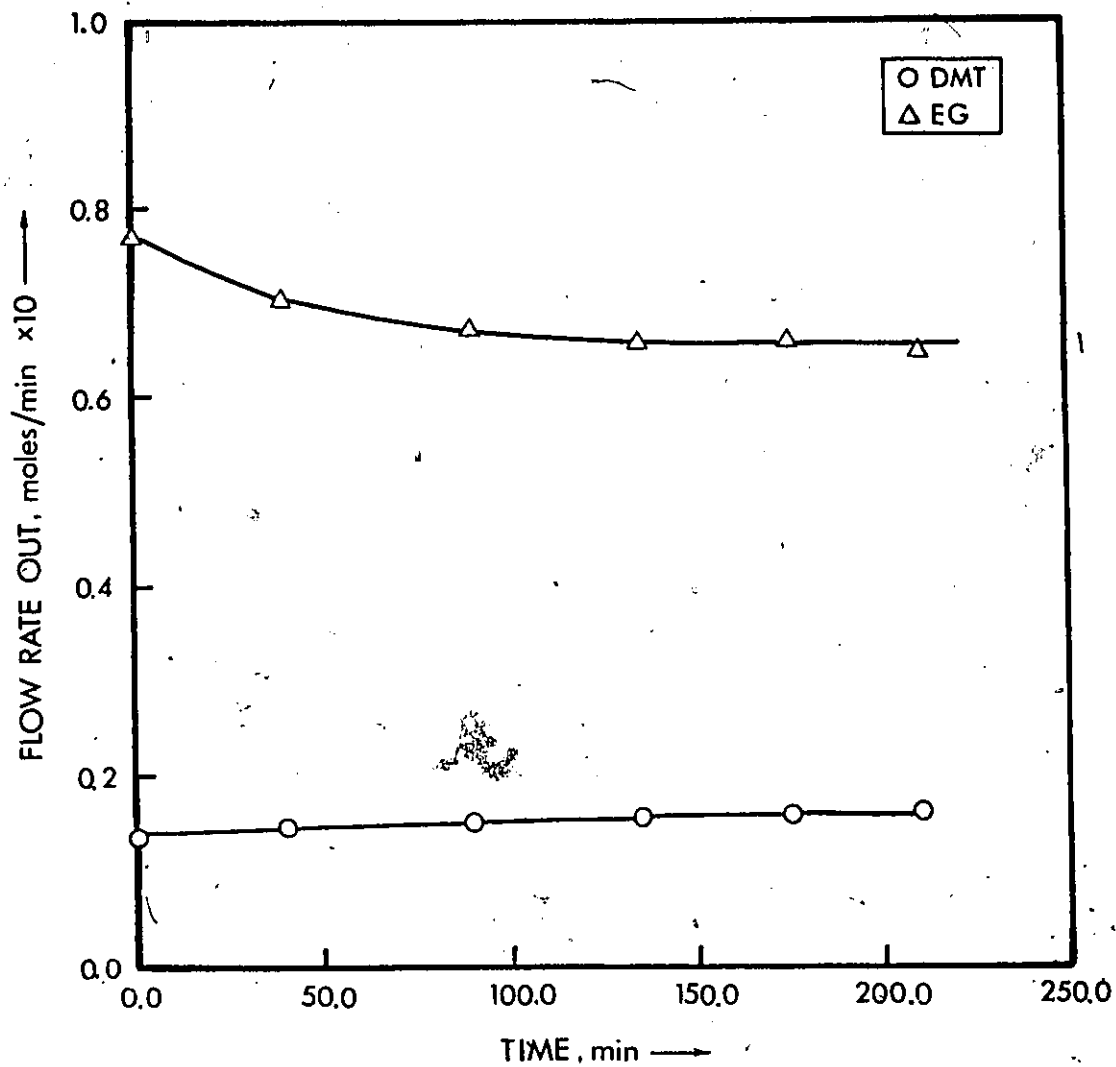


Fig. VI.1 Recycle Reactor Performance

it was observed that the amounts of EG, diethylene glycol, DMT, methyl-(2-hydroxyethyl) terephthalate and bis-(2-hydroxyethyl) terephthalate when summed accounted for only about 90% of the total sample mass. This underestimation was consistent and indicated that additional products, some of which remained in the liquid phase, were formed. Evidence in support of the hypothesis of by-product formation was obtained from the appearance of a new peak on the chromatogram of the liquid product and also the identification of dioxane in the distillate. These findings introduced uncertainties in the overall experimental program and it was decided to carry out some experiments in a batch reactor in order to obtain information about the type and extent of side reactions at various degrees of conversion.

An experiment, aimed at obtaining information about the catalytic properties of the construction materials in the reactor loop, was carried out without catalyst in the reactor. In this experiment the reactor loop was loaded with reactants (molar ratio about 3) enough to keep the liquid level in the packed tower up to the "high" probe (Fig. V.2) under recirculation, and the reactor was operated without either feed or outlet streams. Under these conditions the average distillate production was about 0.04 g/min, which was very small, and it was, therefore, concluded that the construction materials did not have significant catalytic activity.

It was found that the liquid product was dark coloured and this colouring was presumably the result of either resin bleaching or resin degradation, while after long heating periods in the reactor the resin turned black. These resin changes were probably caused by the prolonged exposure of the resin to temperatures exceeding the

recommended maximum safe temperature. It is not known whether these changes were accompanied by reduction in catalytic activity. The latter was, however, found to diminish and virtually disappear after the resin had been kept in the stainless steel reactor for a long time. This was presumably caused by exchange of the active hydrogen ion with metal ions, which were products of corrosion. Corrosion was clearly evident on the sheath of the thermocouple embedded in the reactor after prolonged contact with the catalyst.

B. Batch Reactor Results

As was mentioned earlier the utilization of a batch reactor in the experimental investigation was prompted by a need for information on product distribution. Yet, the batch reactor runs were designed and carried out from a kinetics point of view, in the sense that the data could be used for kinetic model building. These runs yielded information about the effects of transport processes and the effects of reactant molar ratio on product distribution.

1. Effects of Transport Processes

A complete two-level factorial experiment in two factors (Fig. VI.2) was carried out in order to obtain information about product distribution as well as interparticle and intraparticle mass transfer. The two factors were resin particle size and mixing speed, while the reaction temperature was set at 146°C, the initial reactant molar ratio at two, and the catalyst mass at 30.0 grams.

The data for the above factorial experiments are given in Tables C.9 and C.10 of Appendix C while the effects of transport processes on DMT conversion are shown in Fig. VI.3. The figure clearly shows that

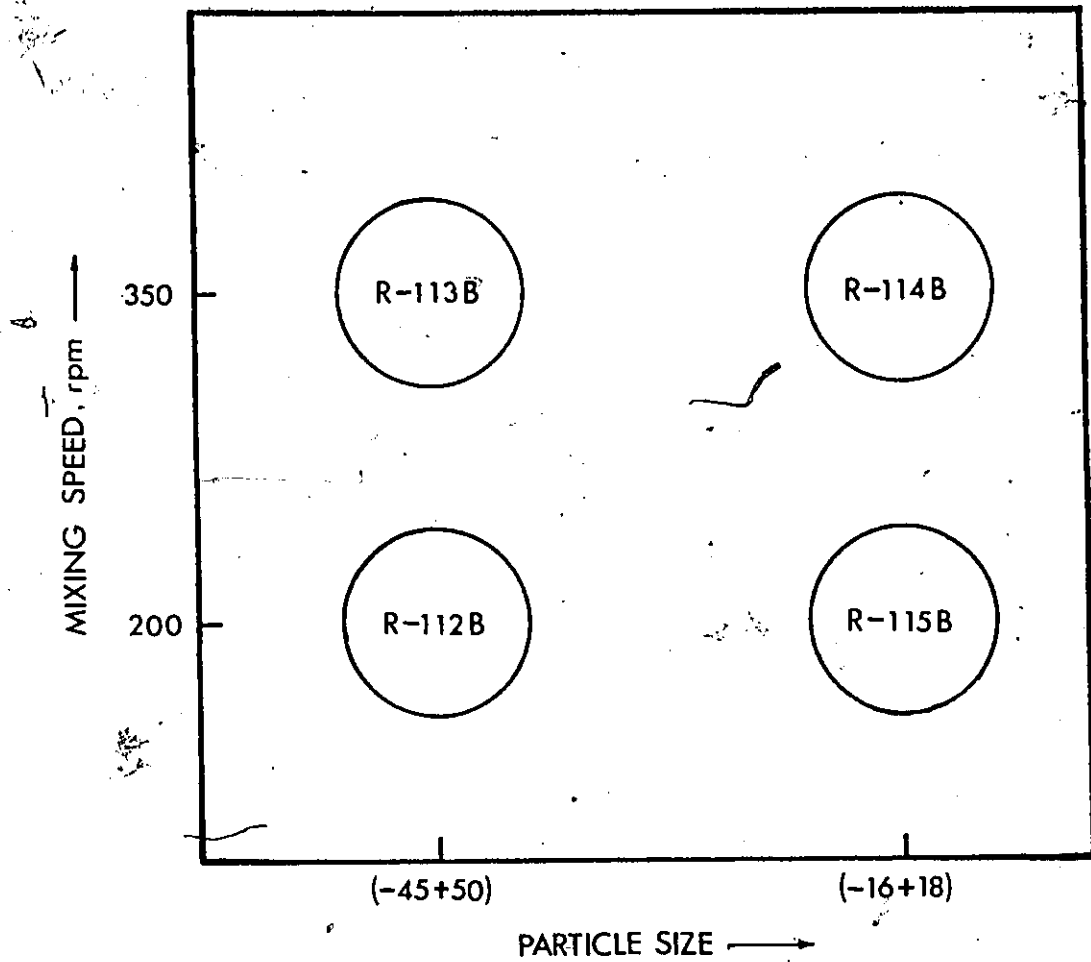


Fig. VI.2 Two-level Factorial Experiment

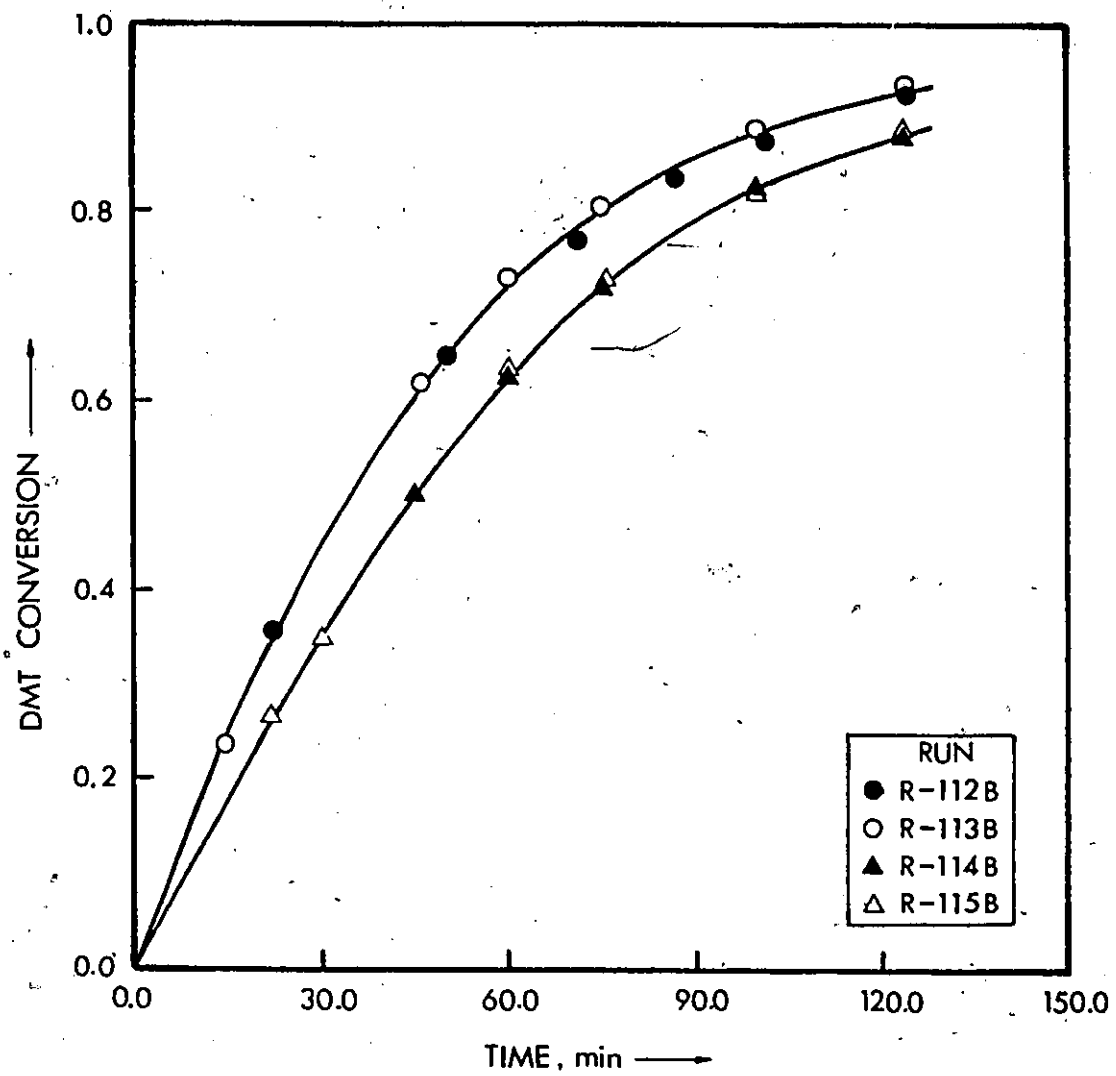


Fig. VI.3 Results of Two-level Factorial Experiment

the conversion data for the same particle size fraction are, within experimental error, the same for the two mixing levels investigated. The increase in the mixing speed did not have any significant effect, and since the low level at 200 rpm was already high, these data indicate that external mass transfer effects were negligible in the range of mixing speed studied. Nevertheless, subsequent experiments were run at high mixing speed. The plots in Fig. VI.3 also clearly show that the smaller particle size fraction resulted in higher DMT conversions than those obtained with the fraction of larger particle. It may, therefore, be concluded that intraparticle diffusion effects are significant in the particle size range used in the experiment. This evidence was later reinforced by the data (Table C.12 of Appendix C) of two other experiments carried out at the same reaction temperature as the factorial experiment but at a molar ratio of 16.0 and for particle size cuts of -35 + 40 (R-117B) and -140 + 325 (R-118). The results of these experiments are shown in Fig. VI.4, in which the ordinate is given in terms of moles DMT converted /g resin in order to account for the difference in catalyst mass used in the two experiments.

The above data strongly indicate that intraparticle diffusion effects are significant for the particle sizes of Amberlyst 15 commercially available at the transesterification temperature of 146°C. This despite the relatively large pore diameter on account of which this macroreticular resin was chosen for investigation.

2. Distribution of Terephthalate Esters

The batch reactor experiments for the factorial design achieved a DMT conversion of about 90% in two hours while the gas chromatographic

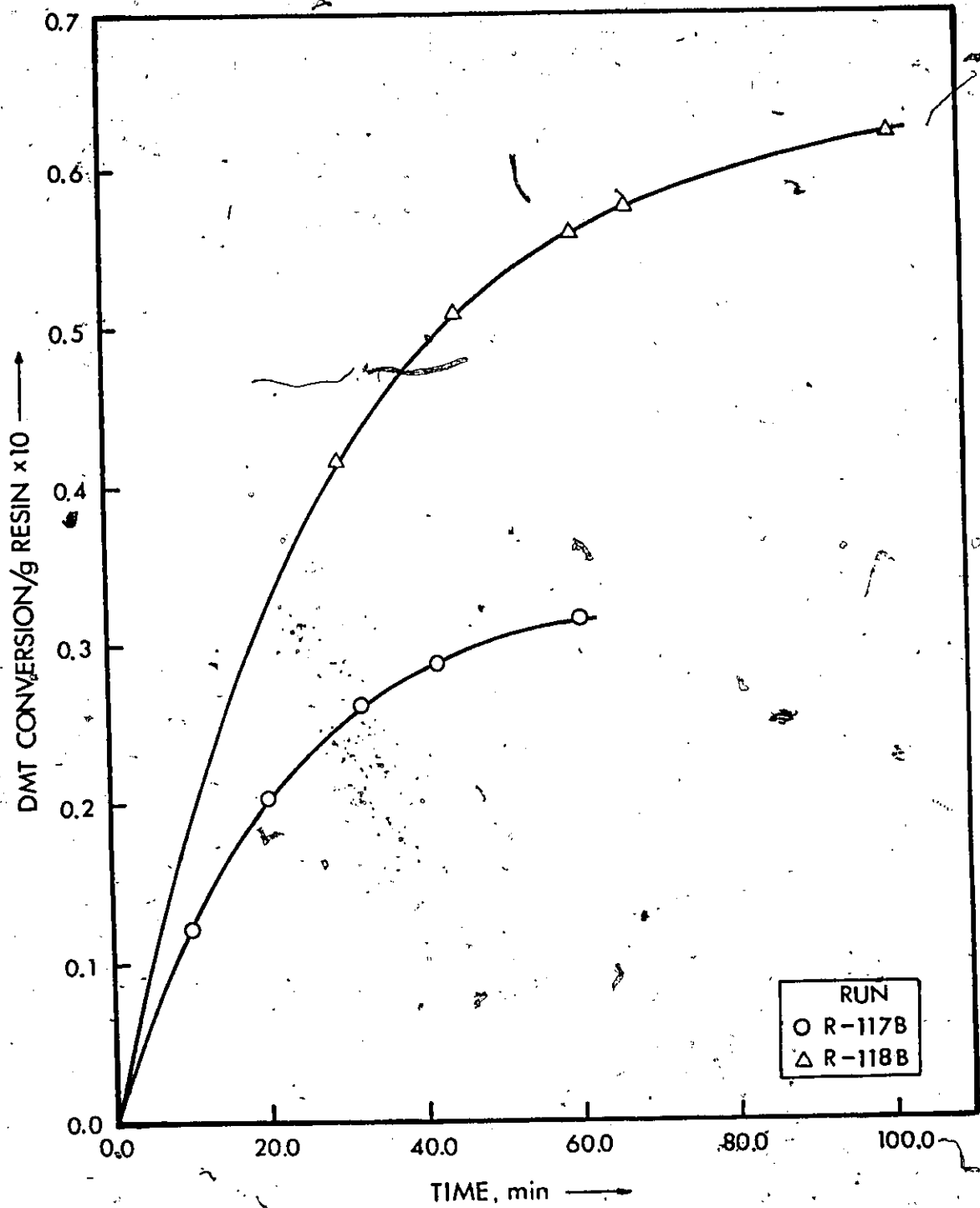
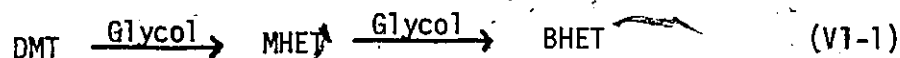


Fig. VI.4 Effects of Resin Particle Size

analysis of the liquid product samples provided experimental qualitative and quantitative information about product formation in each run.

The qualitative information was obtained by visually comparing a chromatogram of a liquid sample of higher DMT conversion (Fig. VI.5) with that of a calibration sample (Fig. IV.2). The extra peaks in the chromatogram of Fig. VI.5 clearly show that formation of products other than ethylene glycol esters of terephthalic acid did take place. The number of additional peaks, of course, indicate that at least that many different compounds were formed.

The seriousness of the extent of by-product formation was ascertained when the chromatograms of the samples for the four factorial runs were quantitatively analyzed. Typical time profiles for the terephthalate esters which could be determined by the gas chromatographic analysis (Ch. IV) are shown in Fig. VI.6. These profiles show a striking and overwhelming departure from the profiles expected on the assumption that the following series-parallel reactions



are the main reactions occurring in the transesterification of DMT with ethylene glycol. Under the above assumption the sum of the instantaneous molar amounts of MHET and BHET should be approximately equal to the moles of DMT converted. However, the profiles show that at all times the former is less than half the latter. This extremely significant difference is shown better in Fig. VI.7 in which the ordinate is the partial yield, ϕ_x , defined in Eq. (VI-2)

$$\phi_x = \frac{N_x - N_{x_0}}{-(N_A - N_{A_0})} \quad (\text{VI-2})$$

- A: Solvent @
- Reagents
- B: EG-TMS
- C: DEG-TMS
- D: ~~BMT~~
- E: Bibenzyl
- F: MHET-TMS
- G: BHET-TMS

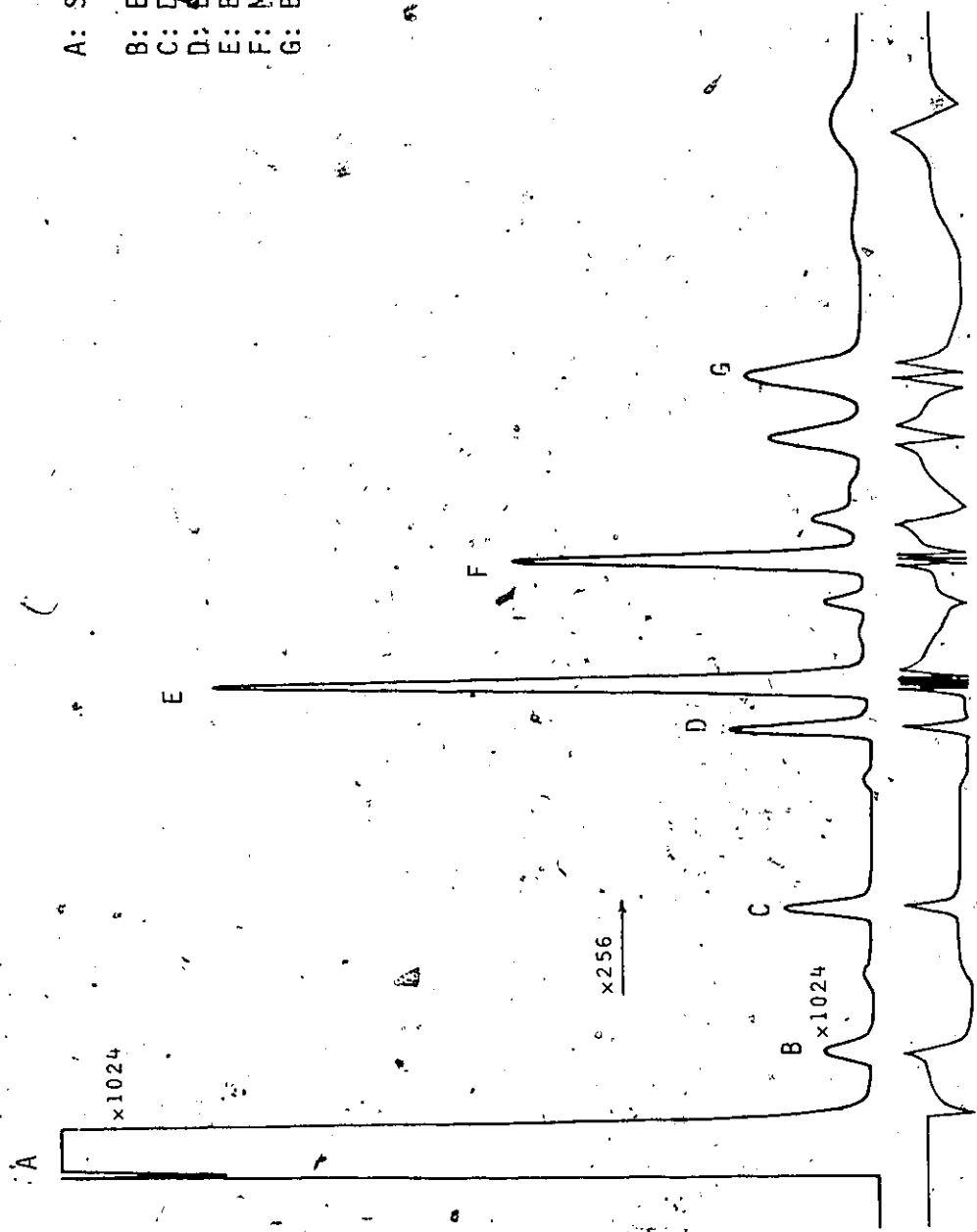


Fig. VI.5 Chromatogram of a Transesterification Sample (Run R-113B)

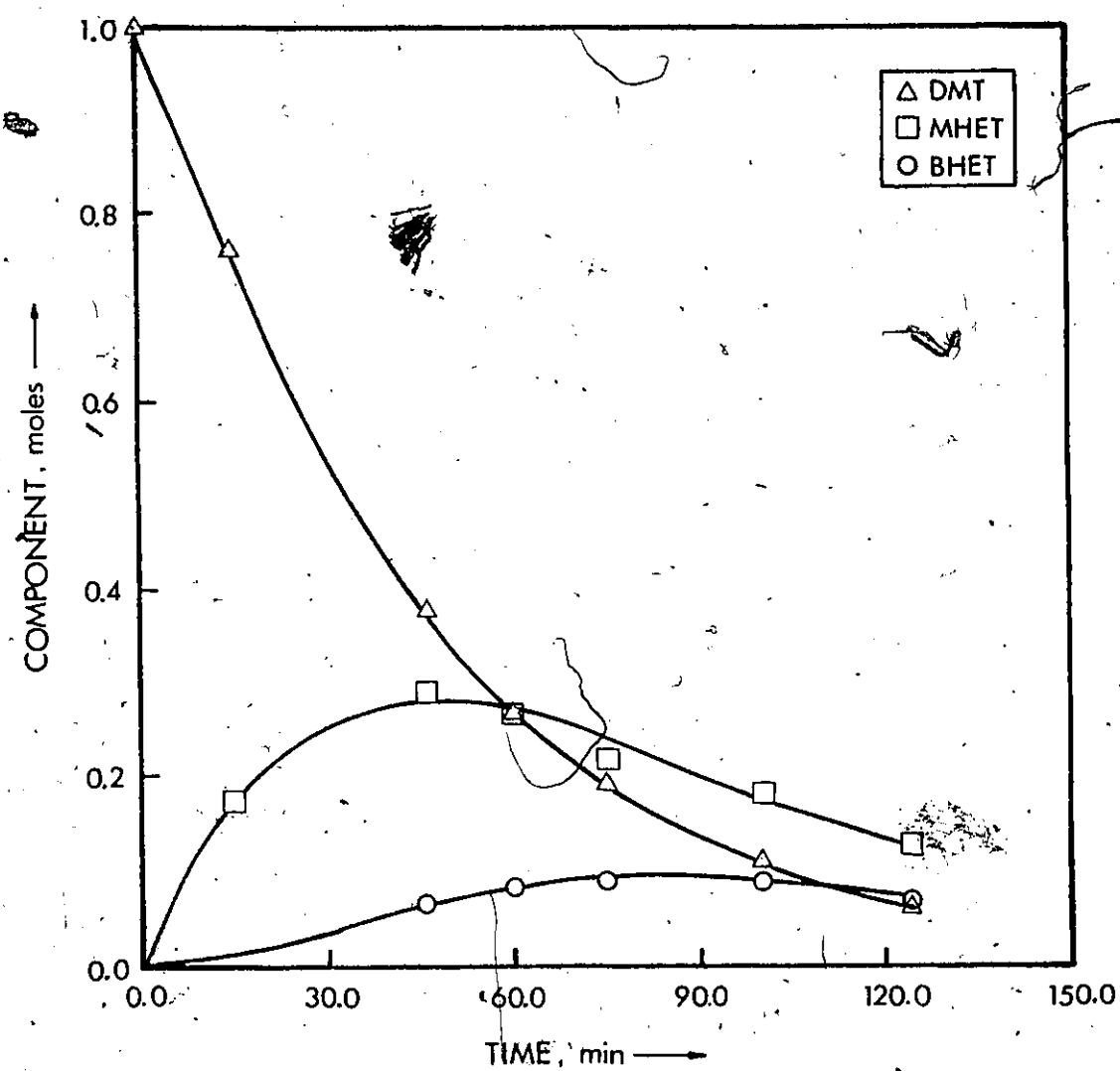


Fig. VI.6 Terephthalate Ester Profiles of Run R-113B

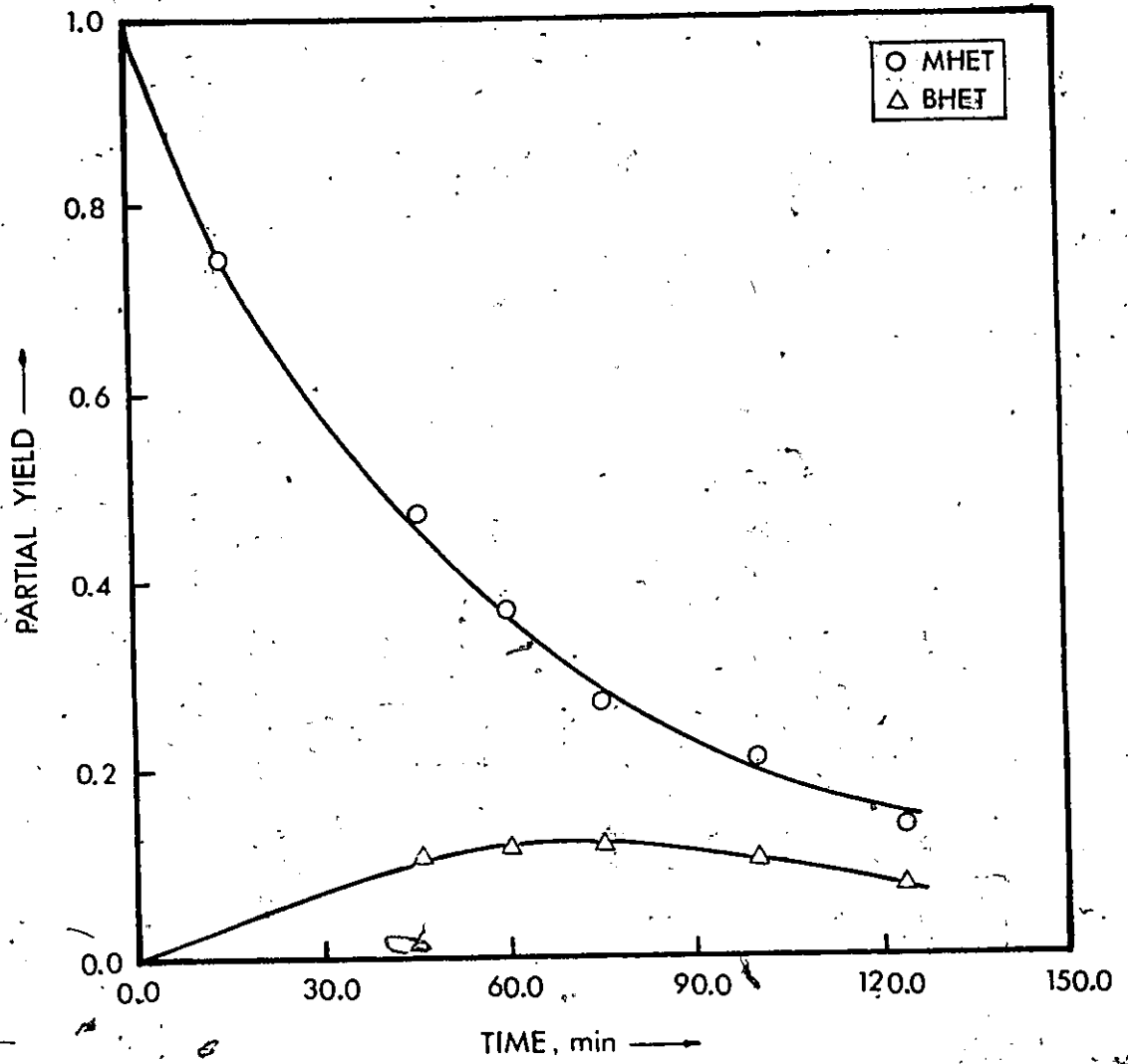


Fig. VI.7 Partial Yields vs. Time for Run R-113B

where N_x and N_A represent number of moles of components x and A at time t, respectively, x is either MHET or BHET, A is DMT and the subscript 0 denotes respective quantities initially present in the reactor. Then if the aforementioned assumption were true the two partial yields should add up to one, approximately.

Further experiments were carried out in which the initial molar ratio of reactants was widely varied in order to elucidate the effect of molar ratio on product distribution. The data of two runs, R-116B and R-117B, with molar ratios of four and sixteen, respectively, are given in Tables C.11 and C.12 of Appendix C, while the partial yields of intermediate and monomer are plotted against time in Figs. VI.8 and VI.9. These figures indicate some improvement in selectivity with higher molar ratios but the improvement is not dramatic. At the end of the run with molar ratio of EG:DMT of 16 about 47% of the converted DMT had gone to products other than MHET or BHET. Another experiment, run R-118B, was carried out at molar ratio of sixteen and the catalyst, Amberlyst 15, of -140 + 325 mesh, obtained by grinding in a pulverizer. The data of this run, given in Table C.12 of Appendix C, show larger experimental error for the glycol esters but, nevertheless, do not indicate any significant improvement in selectivity.

3. Discussion

The conversion of ethylene glycol in the batch reactor runs was much larger than what should have been consumed in the transesterification reactions. This indicated that ethylene glycol in the presence of Amberlyst 15 underwent other reactions to a significant extent. An experiment was carried out in which ethylene glycol alone was heated

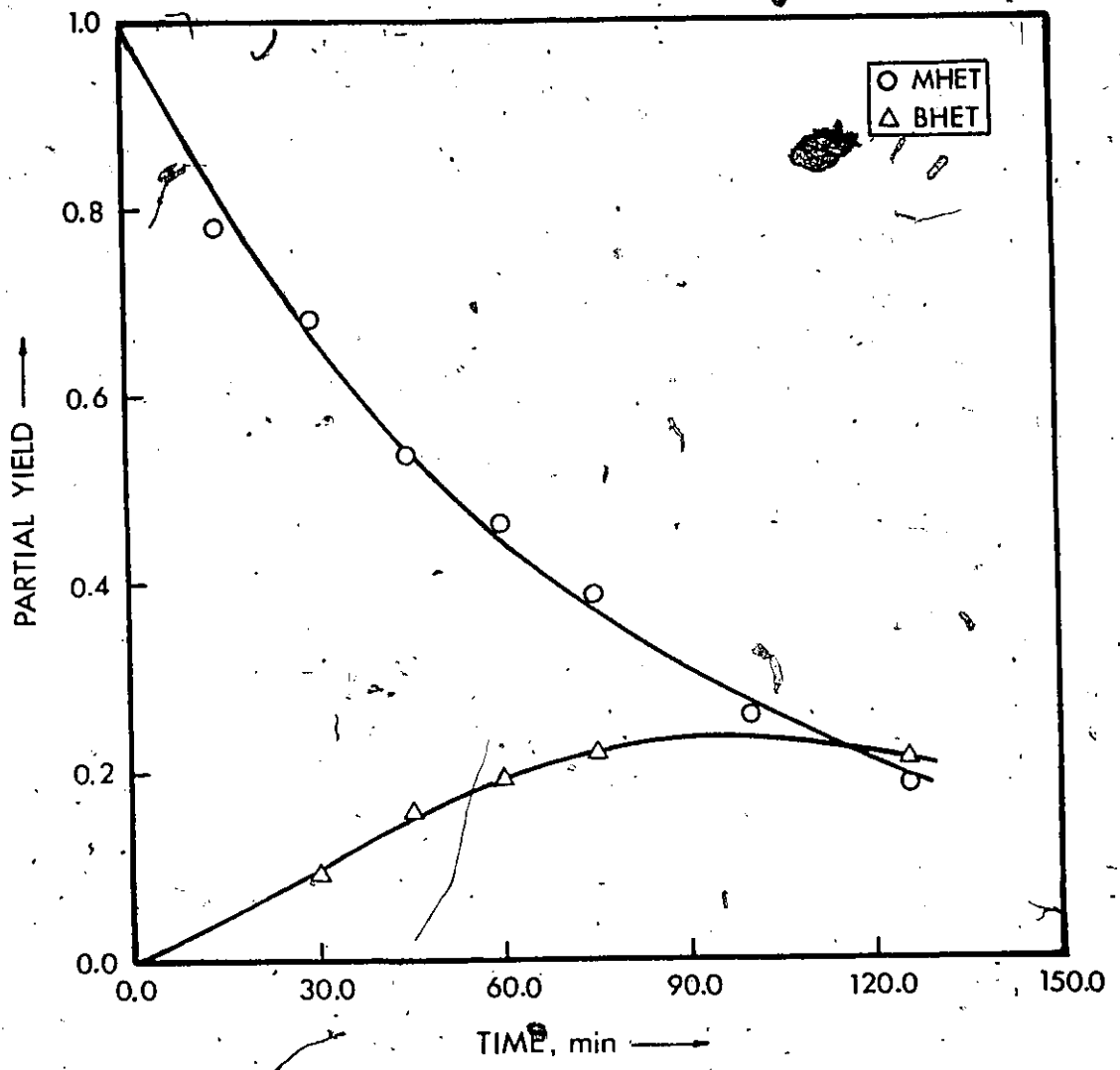


Fig. VI.8 Partial Yields vs. Time for Run R-116B.

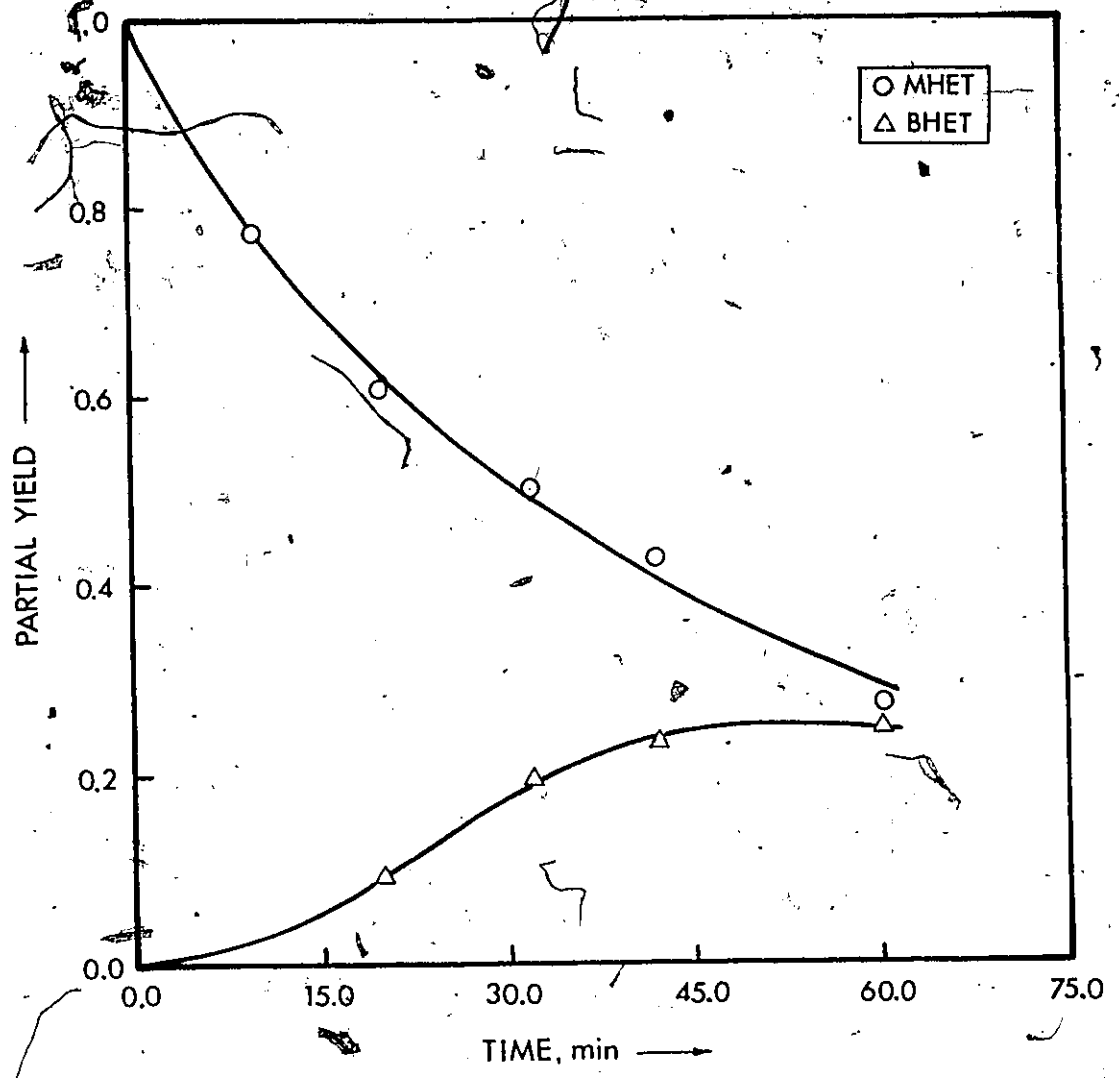


Fig. VI.9 Partial Yields vs. Time for Run R-117B.

in the presence of the cation exchange resin, and GLC analysis of the product showed diethylene glycol and other peaks some of which presumably were low molecular weight polyglycols.

Gas chromatographic analysis of the transesterification distillate showed that 1,4-dioxane and 2-methoxyethanol were formed, which, of course, were products of ethylene glycol. The distillate was quantitatively analyzed by GLC only for methanol, and the methanol profile for run R-116B is given in Table C.17 of Appendix C. In addition, water, presumably the product of ethylene glycol dehydration, was identified in the distillate.

The aforementioned qualitative and quantitative information implied that the reaction system under investigation was very complex. In fact, it was so complex that the quantitative information based on the determination of six components, though available in unprecedented quantity for the same process, was not sufficient to allow establishment of meaningful mass balances. There was need for more experimental information and further analyses were directed at a broad characterization of the transesterification product of one experimental run (R-113B). Experimental procedures are given in Chapter IV.

In order to obtain information about the extent to which esters of glycols and of 2-methoxyethanol formed during transesterification, a sample of left-over mass was saponified and prepared for GLC analysis. Chromatograms of the unsaponified sample were also taken, and the analytical procedures for the analysis of liquid product established the amounts of ethylene and diethylene glycol before and after saponification (Table C.13 of Appendix C). Triethylene glycol esters were

also formed to significant extent, as judged by the increase in the peak area ratio of a peak presumed to be due to the trimethyl-silyl derivative of this glycol. These determinations showed that diethylene glycol, the product of ethylene glycol polymerization, further reacted to form esters and that the corresponding amounts of esterified to free glycol were in the approximate ratio of 4:1. The saponification product was also analyzed to determine the amount of 2-methoxy-ethanol. This analysis was carried out at the conditions established for the GLC analysis of the distillate and quantitation was based on the bracketing technique (Table C.14 of Appendix C). Determination of 2-methoxy-ethanol in the unsaponified sample showed that about half of the amount of this compound as determined above was free while the other half was esterified. The distillate was also analyzed for 2-methoxy-ethanol (Table C.14).

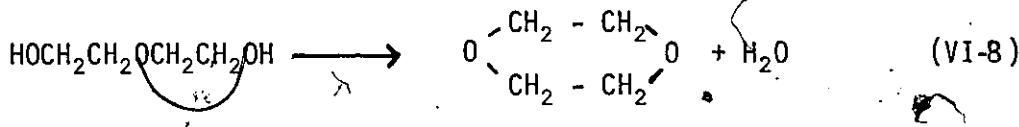
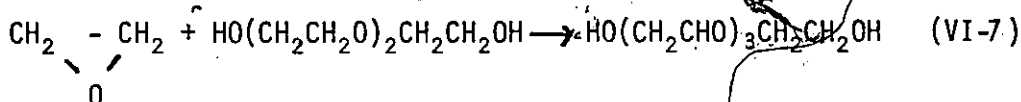
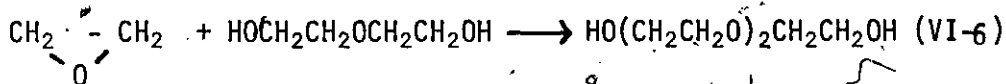
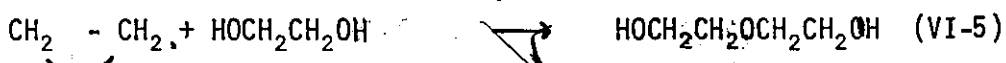
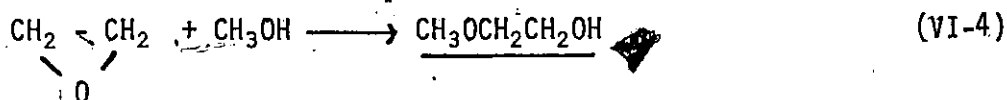
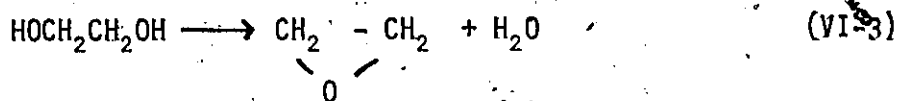
The above analyses resulted in the following quantitative data (Table VI.1) for conversion of

Table VI.1
Ethylene Glycol Products

Compound	% Initial Glycol
Diethylene Glycol	25.9
2-Methoxy-Ethanol	6.3

ethylene glycol. 1,4-Dioxane and triethylene glycol were also formed in significant amounts. It is, therefore, clear that over one third of ethylene glycol was converted to products other than transesterification compounds. These products are the result of the following reactions

which apparently are effectively catalyzed by Amberlyst 15:



where the underlined compounds have been positively identified while triethylene glycol has been tentatively identified. The occurrence of reactions (VI-5) to (VI-7) and of higher degree of polymerization in the presence of other catalysts is well established [38] while reaction (VI-8) is based on the evidence that dioxane formation from diethylene glycol is much faster than same from ethylene glycol, under the same experimental conditions. The above reactions clearly indicate that the dehydration of ethylene glycol to ethylene oxide is the basic stepping stone in the above reaction scheme.

The determination of ethylene and diethylene glycol and of

2-methoxy-ethanol in the transesterification product, before and after saponification, showed that a significant fraction of dimethyl terephthalate was converted to esters other than those with ethylene glycol, the latter being the desirable products.

Determination of total carboxylic groups in the liquid product by means of a saponification experiment showed that the number of carboxylic groups before transesterification, which is equal to the number of methyl-ester groups (Table C.3), and after reaction (Table C.15) are equal within experimental error. It was, therefore, concluded that decarboxylation did not occur. Determination of free carboxylic groups in the transesterification product (Table C.16) showed that ester groups were hydrolyzed to free acid groups to a significant extent (8.5%).

To test whether terephthalic acid was present in the transesterification product, a chromatogram of silylated pure terephthalic acid was obtained, under the conditions for the liquid product analysis. The retention time of silylated terephthalic acid was found to be significantly different from that of neighbouring peaks on the liquid product chromatogram, and it was concluded that ester hydrolysis was restricted to one ester group per DMT residue. This conclusion implied that some 17% of the initial DMT had been hydrolyzed to monoacid esters.

The liquid product characterization analyses led to the following quantitative results (Table VI.2)

Table VI.2

Undesirable Transesterification Products

Group	% Initial Methyl-Ester
Diethylene Glycol Ester ^a	10.14
2-Methoxy-Ethanol Ester	1.5
Free Carboxylic Groups	8.5

a. Assuming only one -OH group esterified.

for some undesirable transesterification products. The above table, which is not complete, clearly indicates that the products of ethylene glycol dehydration (water), polymerization (di- and tri- ethylene glycols), and etherification (2-methoxy-ethanol) reactions effectively participate in transesterification reactions and convert significant quantities of dimethyl terephthalate to unwanted products. The latter are undesirable because the ether 2-methoxy-ethanol would terminate polymer chain growth while the polyglycols would impair the properties of the final polyester product.

The batch reactor experiments showed that in the presence of Amberlyst 15 DMT is significantly converted to undesirable products irrespective of resin particle size and initial EG to DMT molar ratios. The undesirable products arise from transesterification reactions with compounds produced by the ethylene glycol dehydration and subsequent etherification and polymerization reactions. The latter reactions were

found to be effectively catalyzed by Amberlyst 15 at the temperature of 146°C.

The effect of temperature on product distribution was not investigated because the lower limit at which a clear melt of reactants may form is only 130°C and the resulting possible temperature range of 15°C was considered too small to effect the required changes in product distribution.

It was, therefore, concluded that the transesterification of dimethyl terephthalate with ethylene glycol in the presence of Amberlyst 15 was an unselective and inefficient process.

VII MATHEMATICAL ANALYSIS OF THE DIFFERENTIAL RECYCLE REACTOR

As was mentioned in Ch. V the inclusion of the methanol stripper in the recycle loop of the continuous reactor necessitated control of the outlet stream and the controller actually used, an on-off liquid level controller, made the reactor liquid volume variable with distinct accumulation and discharge intervals. This volume variability raised the question of this system coming to steady state, a necessary requirement for obtaining reaction rate data.

The author [38] obtained an answer to the above question by carrying out a mathematical analysis of the differential recirculation reactor subject to linear variations of volume. The analysis dealt with the unsteady state of the reactor, and is given below.

A. Volume Mathematical Functions

A simplified schematic of a differential recirculation reactor for a liquid phase reaction with on-off control of the output stream, is shown in Fig. VII.1. The volume of reacting material increases until the liquid reaches the "high" probe which activates the controller and discharge begins. The volume of reactant-product mixture then decreases until the liquid level drops to just below the "low" probe when the controller is deactivated and the cycle is repeated.

Assuming that the density of the reaction mixture is constant throughout the system, the volume of the reaction system as a function of time is as shown in Fig. VII.2. t_a is the accumulation time interval while the controller is activated and $t_c = t_a + t_d$ is the period for the cycle of the volume variation. The output stream flow rate during

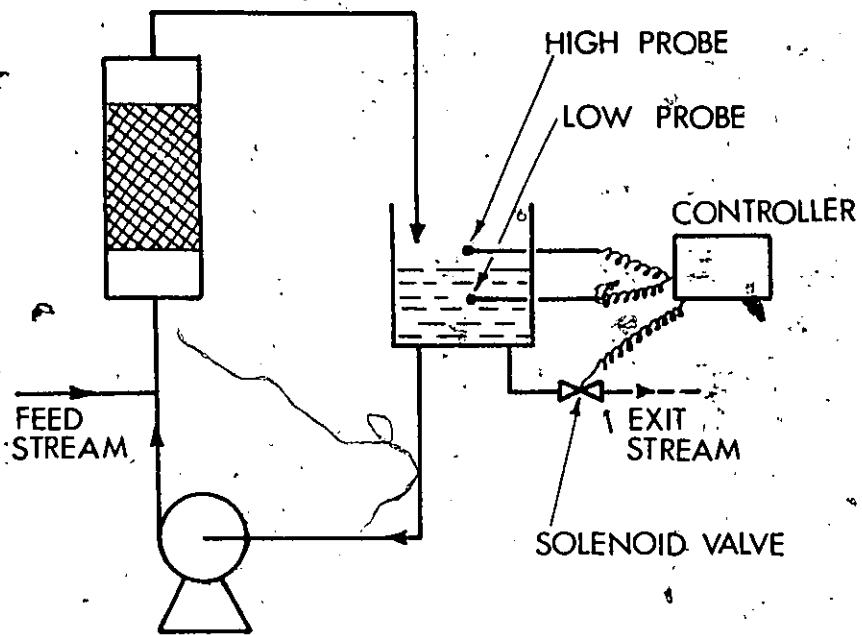


Fig. VII.1 Schematic of Recycle Reactor with On-Off Control of Outlet Stream

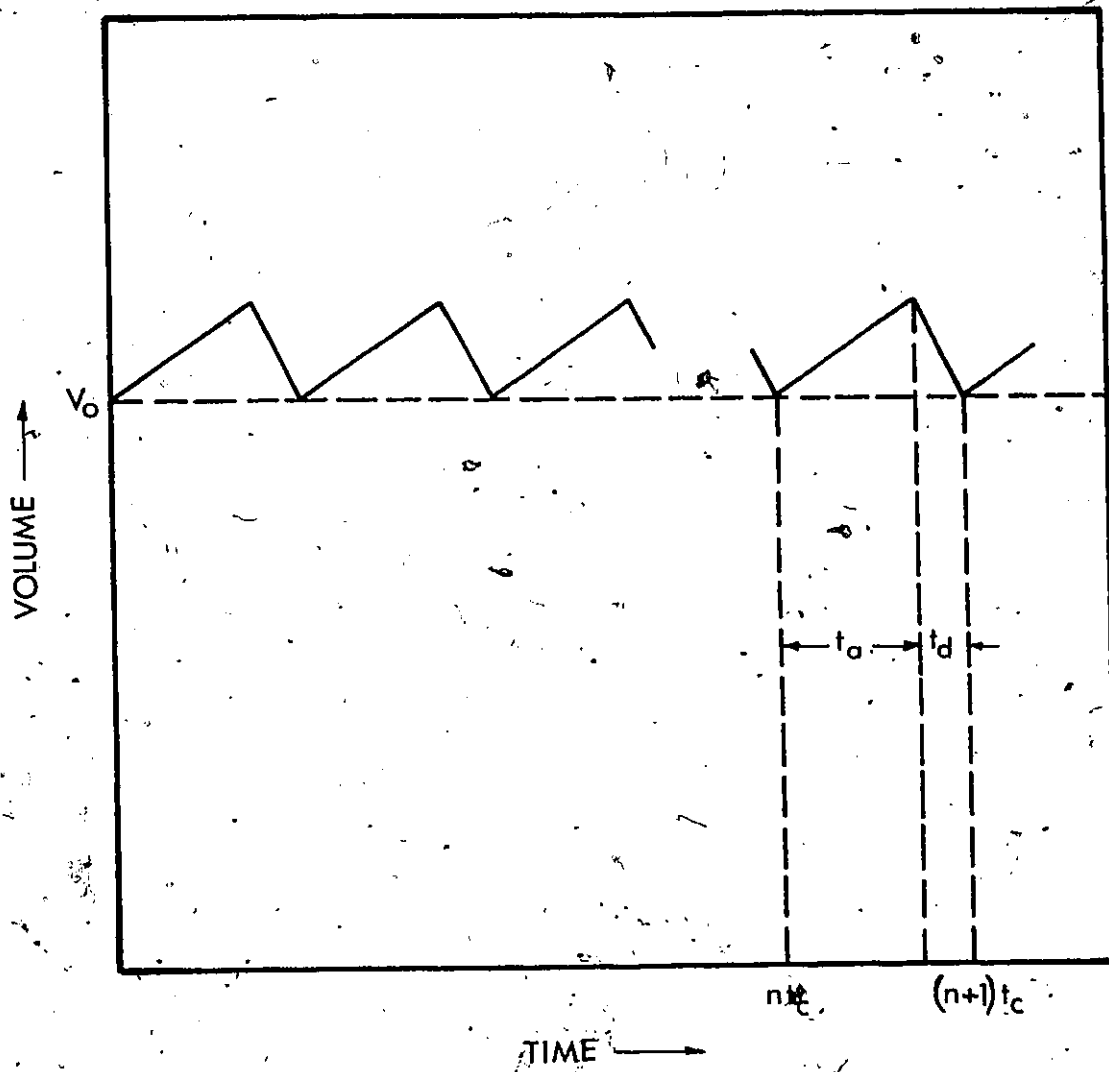


Fig. VII.2. Graph of Reactor Liquid Volume.

discharge is

$$V = \frac{t_a}{t_d} V_0 = \beta V_0$$

where $\beta = t_a/t_d$ and v_0 is feed stream flow rate.

The time function for volume during the accumulation interval in the (n+1)st cycle is given by:

$$V = V_0 + v_0(t + nt_c) \quad (\text{VII-2})$$

and during the discharge interval is given by:

$$V = V_0 + v_0 \beta [(n-1)t_c - t] \quad (\text{VII-3})$$

where n is the number of completed cycles and V_0 is base reactor volume.

B. Differential Equations

In deriving the differential equation which describes the present differential recirculation reactor, it was assumed that the reaction rate is expressed in terms of catalyst mass, as is usually the case in heterogeneously catalyzed reactions, and that the recycle rate is much greater than the feed flow rate so that the concentration throughout the reactor is uniform. The usefulness of the recirculation reactor is indeed based on the latter assumption, which may easily be fulfilled. Under these conditions the exit stream concentration is equal to that in the reactor.

The governing differential equation was obtained from the following material balance in terms of reactant A:

$$\left[\begin{array}{c} \text{moles of A} \\ \text{in} \end{array} \right] = \left[\begin{array}{c} \text{moles of A} \\ \text{out} \end{array} \right] + \left[\begin{array}{c} \text{moles of A} \\ \text{converted} \\ \text{by reaction} \end{array} \right] + \left[\begin{array}{c} \text{moles of A} \\ \text{accumulated} \end{array} \right]$$

The accumulation term in this case is

$$\left[\begin{array}{l} \text{moles of A} \\ \text{accumulated} \end{array} \right] = \frac{d(V C_A)}{dt} = C_A \frac{dv}{dt} + v \frac{dC_A}{dt}$$

and it can be seen from Fig. VII.2 or Eqs. (VII-2) and (VII-3) that though the function V is discontinuous its derivative has finite discontinuous jumps when the time variable is considered in its entire range. Also the output term is discontinuous with finite jumps. Therefore, the equation obtainable from the material balance would be nonlinear, which would be very difficult, if at all possible, to solve analytically. However, the material balance yields linear equations in the restricted intervals of accumulation and discharge, and viewed as such the problem becomes piecewise linear which may be solved by fitting together the solutions of the linear equations [39].

For the accumulation interval in the $(n+1)$ st cycle the material balance gives

$$v_o C_{A_o} = 0 + (-r_A)W + C_A \frac{dV}{dt} + V \frac{dC_A}{dt} \quad (\text{VII-4})$$

Substituting V from Eq. (VII-2) and differentiating there is obtained:

$$v_o C_{A_o} = (-r_A)W + C_A v_o + [V_o + v_o(t - nt_c)] \frac{dC_A}{dt} \quad (\text{VII-5})$$

which, upon dividing through by v_o , becomes

$$C_{A_o} = C_A + \alpha(-r_A) + (\tau_o - nt_c + t) \frac{dC_A}{dt} \quad (\text{VII-6})$$

where $\alpha = W/v_o$ and $\tau_o = V_o/v_o$. Equation (VII-6) is the differential equation describing the reactor in the time interval $nt_c < t < nt_c + t_a$.

For the discharge interval the material balance gives

$$v_0 C_{A_0} = v C_A + (-r_A)W + C_A \frac{dV}{dt} + v \frac{dC_A}{dt} \quad (\text{VII-7})$$

Substituting v from Eq. (VII-1) and V from Eq. (VII-3), differentiating etc., there is obtained Eq. (VII-8)

$$C_{A_0} = C_A + \alpha(-r_A) + [\tau_0 + \beta(n+1)t_c - \beta t] \frac{dC_A}{dt} \quad (\text{VII-8})$$

which describes the reactor in the interval $n t_c + t_a < t < (n+1)t_c$.

When parameter n is allowed to take on its values of 0, 1, 2, 3, ..., Eqs. (VII-6) and (VII-8) yield two sets of differential equations in which the time variable, t , is considered in its entire range. Therefore, fitting together the solutions of these sets, for a specified form of the function $(-r_A)$, gives the transient response of the recirculation reactor.

It may be seen from Eq. (VII-6) that the form of the general solutions of the set resulting from it would be the same for different values of n , and the only differences between segmental solutions would be in the values of n and the integration constant. The same holds true for the set resulting from Eq. (VII-8). The general solution was, therefore, obtained by finding the forms of solutions for unspecified n and then fitting together the segmental solutions by specifying n and calculating integration constants from appropriate initial or boundary conditions.

C. Transient Response

Since the objective of the work was to investigate the behaviour of the transient response, analytic solutions were considered very desirable and, therefore, further analysis was restricted to simple forms of rate expressions.

1. Irreversible First Order Reaction

The assumed rate expression for the reaction $A \rightarrow R$ is

$$-r_A = \frac{1}{V} \frac{dN_A}{dt} = k C_A \quad (\text{VII-9})$$

Substitution of Eq. (VII-9) into Eq. (VII-6) yields

$$C_{A_0} = (\alpha k + 1) C_A + (\tau_0 - n t_c + t) \quad (\text{VII-10})$$

the solution of which is

$$C_A = \frac{C_{A_0}}{\theta} \frac{A_n}{(\tau_0 - n t_c + t)^\theta} \quad (\text{VII-11})$$

where $\theta = \alpha k + 1$ and A_n is the integration constant the value of which varies with n .

Substitution of Eq. (VII-9) into Eq. (VII-8) yields

$$C_{A_0} = (\alpha k + 1) C_A + [\tau_0 + \beta(n+1)t_c - \beta t] \frac{dC_A}{dt} \quad (\text{VII-12})$$

the solution of which is

$$C_A = \frac{C_{A_0}}{\theta} + D [\tau_0 + \beta(n+1)t_c - t]^{\theta/\beta} \quad (\text{VII-13})$$

where D_n is the integration constant the value of which changes with n .

Eqs. (VII-11) and (VII-13) are the forms of solutions of the aforementioned sets of differential equations from which the general solution was built by alternatively using these equations and successively specifying n and calculating the integration constants. For example, in the time interval $0 < t < t_a$ we have $n = 0$ and from Eq. (VII-11)

$$C_A = \frac{C_{A_0}}{\theta} \frac{A_0}{(\tau_0 + t)^\theta} \quad (\text{VII-14})$$

and at $t = 0^+$, $C_A = C_{A_0}$

from which

$$A_0 = \frac{\alpha k C_{A_0}}{\theta} \tau_0^\theta \quad (\text{VII-15})$$

and upon substituting of A_0 in Eq. (VII-14) there is obtained

$$C_A = \frac{C_{A_0}}{\theta} \left[1 + \alpha k \left(\frac{\tau_0}{\tau_0 + t} \right)^\theta \right] \quad (\text{VII-16})$$

At $t = t_a^-$, we have

$$C_A^{(o)} = \frac{C_{A_0}}{\theta} \left[1 + \alpha k \left(\frac{\tau_0}{\tau_0 + t_a} \right)^\theta \right] \quad (\text{VII-17})$$

which becomes the boundary condition for the next segment.

In the interval $t_a < t < t_c$, we have $n = 0$ and from Eq. (VII-13)

$$C_A = \frac{C_{A_0}}{\theta} + D_0 (\tau_0 + \beta t_c - \beta t)^{\theta/\beta} \quad (\text{VII-18})$$

and at $t = t_a^+$, $C_A = C_A^{(o)}$ yielding

$$D_0 = \frac{\alpha k C_{A_0}}{\theta} \left(\frac{\tau_0}{\tau_0 + t_a} \right)^\theta \frac{1}{(\tau_0 + t_a)^{\theta/\beta}} \quad (\text{VII-19})$$

which upon substitution into Eq. (VII-18) gives

$$C_A = \frac{C_{A_0}}{\theta} \left[1 + \alpha k \left(\frac{\tau_0 + \beta t_c - \beta t}{\tau_0 + t_a} \right)^{\theta/\beta} \right] \quad (\text{VII-20})$$

where $T = \tau_o / (\tau_o + t_a)$.

The value of C_A obtained from Eq. (VII-20) at $t = t_c^*$ is the boundary condition for the next interval when $n = 1$ and Eq. (VII-11) holds. The process is repeated in the same manner and the general solution is obtained by mathematical induction. This is

$$C_A = \frac{C_{A_0}}{\theta} \left[1 + \alpha k T^{n\gamma\theta} \left(\frac{\tau_o}{\tau_o - nt_c + t} \right)^\theta \right] \quad (\text{VII-21})$$

in the interval $nt_c < t < nt_c + t_a$ and

$$C_A = \frac{C_{A_0}}{\theta} \left\{ 1 + \alpha k T^{n\gamma\theta/\beta} \frac{\tau_o^\theta [\tau_o + \beta(n+1)t_c - \beta t]^{\theta/\beta}}{(\tau_o + t_a)^{\gamma\theta/\beta}} \right\} \quad (\text{VII-22})$$

in the interval $nt_c + t_a < t < (n+1)t_c$, where $\gamma = \beta + 1$.

Since $T = \tau_o / (\tau_o + t_a)$ is less than unity, $T^{\gamma\theta/\beta}$ is also less than unity and the term $(T^{\gamma\theta/\beta})^n$ tends to zero as n increases. As a matter of fact

$$\lim_{n \rightarrow \infty} (T^{\gamma\theta/\beta})^n = 0 \quad (\text{VII-23})$$

and consequently the time terms in the brackets in Eqs. (VII-21) and (VII-22) vanish. Therefore, the system comes to steady state after sufficiently long time and the steady state concentration is

$$C_A = \frac{C_{A_0}}{\theta} = \frac{C_{A_0}}{\alpha k + 1} \quad (\text{VII-24})$$

which is exactly the same as that for the continuously operated reactor, under the same conditions, of course.

2. Irreversible Second Order Reaction

The assumed rate expression for the reaction $A + B \rightarrow R + S$ is

$$-r_A = -\frac{1}{W} \frac{dN_A}{dt} = kC_A C_B = kC_{A_0} (M - 1)C_A + kC_A^2 \quad (\text{VII-25})$$

where M is the initial molar ratio of reactants assumed different from one.

Substitution of $(-r_A)$ in Eq. (VII-6) by its equal results in

$$C_{A_0} = gC_A + \alpha k C_A^2 + (\tau_0 - nt_c + t) \frac{dC_A}{dt} \quad (\text{VII-26})$$

which is the differential equation for the accumulation interval in the $(n + 1)$ st cycle, where $g = 1 + \alpha k C_{A_0} (M - 1)$. Equation (VII-26) was solved by separation of variables, and the solution is

$$\frac{C_A + a}{C_A + b} = \frac{A_n}{(\tau_0 - nt_c + t)^e} \quad (\text{VII-27})$$

where

$$e = \sqrt{g^2 + 4\alpha k C_{A_0}}$$

$$a = \frac{g - e}{2\alpha k}$$

and

$$b = \frac{g + e}{2\alpha k}$$

Substitution of $(-r_A)$ in Eq. (VII-8) by its equal in Eq. (VII-25)

yields

$$C_{A_0} = g C_A + \alpha k C_A^2 + [\tau_0 + \beta(n + 1)t_c - \beta t] \frac{dC_A}{dt} \quad (\text{VII-28})$$

whose solution is

$$\frac{C_A + a}{C_A} = D_n [\tau_0 + \beta(n+1)t_c + \beta t]^{e/\beta} \quad (\text{VII-29})$$

where a , b , e , and g are the quantities defined previously.

Equations (VII-27) and (VII-29) are the forms of solutions of the two sets of differential equations obtained from Eqs. (VII-6) and (VII-8) which the general solution was built in a manner similar to that used for the first order reaction. The general solution is

$$\left(\frac{C_A + a}{C_A} \right) = \left(\frac{C_{A_0} + a}{C_{A_0} + b} \right) T^{ne\gamma/\beta} \left(\frac{\tau_0}{\tau_0 - nt_c + t} \right)^e \quad (\text{VII-30})$$

in the interval $nt_c < t < nt_c + t_a$ and

$$\left(\frac{C_A + a}{C_A} \right) = \left(\frac{C_{A_0} + a}{C_{A_0} + b} \right) T^{ne\gamma/\beta} \frac{\tau_0^e [\tau_0 + \beta(n+1)t_c - \beta t]^{e/\beta}}{(\tau_0 + t_a)^{e\gamma/\beta}} \quad (\text{VII-31})$$

in the interval $nt_c + t_a < t < (n+1)t_c$, where $T = \tau_0 / (\tau_0 + t_a)$.

Since T is smaller than unity we have that

$$(T^{e\gamma/\beta}) < 1 \text{ and } \lim_{n \rightarrow \infty} (T^{e\gamma/\beta})^n = 0 \quad (\text{VII-32})$$

and, consequently, the time terms in Eqs. (VII-30) and (VII-31) vanish after sufficiently long time. Hence the reactor system comes to steady state and the steady state concentration is given by

$$C_A = -a + \frac{-g + \sqrt{g^2 + 4\alpha k C_{A_0}}}{2\alpha k} \quad (\text{VII-33})$$

which is exactly the same as that of the continuously operated reactor under the same conditions.

D. Discussion

A number of numerical case studies were undertaken on a computer, by assuming values for the variables involved in the solutions, in order to visualize the transient response of a differential recirculation reactor subject to cyclic linear variations of volume. Figures VII.3 and VII.4 show typical responses for first and second order reactions, respectively.

From the cases examined it was found that the transient response of the type of the semibatch reactor considered here always lies between the response of the continuously operated reactors with residence times in the reactor system of τ_0 and $(\tau_0 + t_a)$, all other variables being equal. This should be attributed to the fact that the mass of the semibatch reactor lies in between that of the continuously operated reactors. In the long run, however, all three reactors reach the same steady state which is a function of the initial concentration, the rate constant and the ratio of catalyst mass to feed flow rate.

Though the mathematical analysis showed that, for the kinetics considered, the semibatch reactor comes to steady state and in this regime the discontinuous operation of the reactor does not cause the reactor concentration to fluctuate, it would be expected that concentration fluctuations, due to the accumulation and discharge intervals, would occur during the transient period. Since such fluctuations were not obvious in the computer plots of the transient response, due to scale limitations, and not easily discernible from the numerical output, it

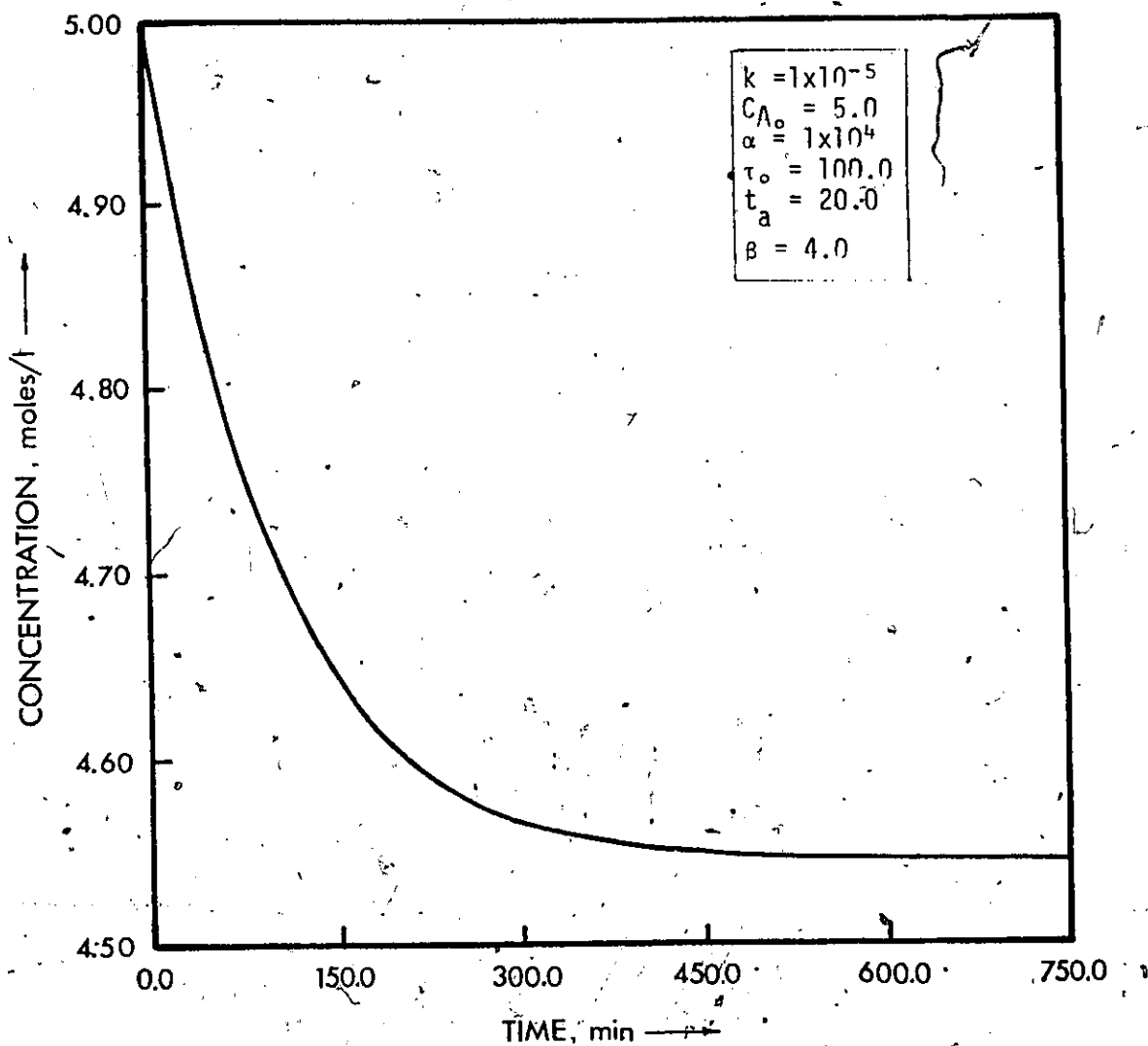


Fig. VII.3 Transient Response for First Order Kinetics

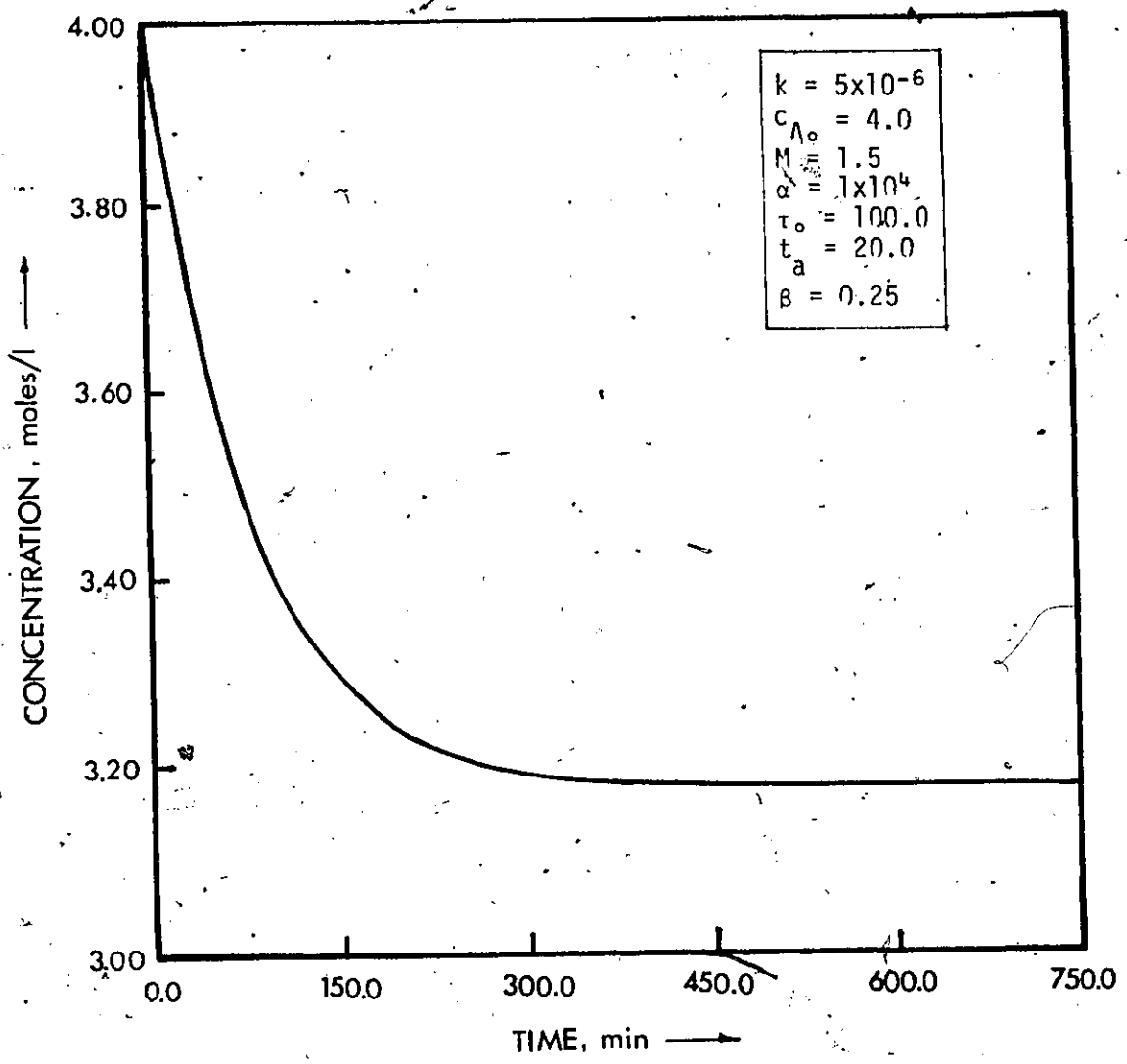


Fig. VII.4 Transient Response for Second Order Kinetics

was decided to examine the difference between the concentration of a continuously operated reactor, whose response is a smooth decreasing function of time, and that of the semibatch reactor. The cases studied showed that concentration fluctuations do occur, and Fig. VII.5 and VII.6 illustrate the fluctuations in the response of first and second order kinetics, respectively, corresponding to the cases shown in Fig. VII.3 and VII.4. For these illustrations the residence time in the system for the continuously operated reactor was taken equal to $(\tau_0 + 0.5 t_a)$, the average residence time in the semibatch reactor. The fluctuations depend on β , the ratio of accumulation to discharge time intervals, all other variables considered constant. Figures VII.5 and VII.6 have actually been plotted for different β 's in order to show the effect of this parameter on the magnitude and frequency of these fluctuations during the transient period.

The attainment of steady state and the lack of concentration fluctuations in that regime imply that the determining factor in the behaviour of the semibatch reactor considered is the invariant quantity of catalyst. Hence the indications are that differential recirculation reactors operated with on-off control of the exit stream will come to steady state for other rate expressions as well.

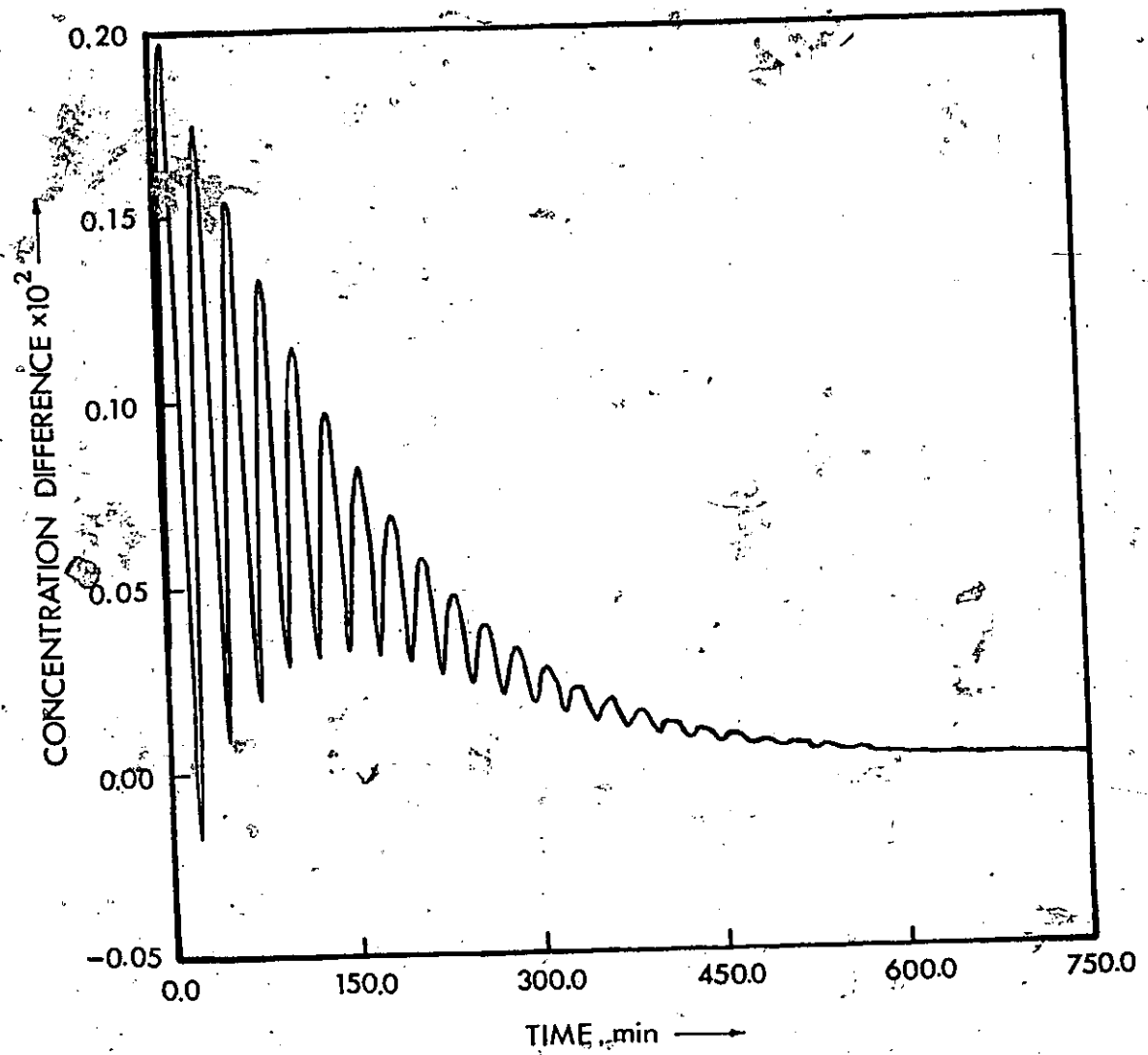


Fig. VII.5 Concentration Fluctuations during Transient Period for First Order Kinetics

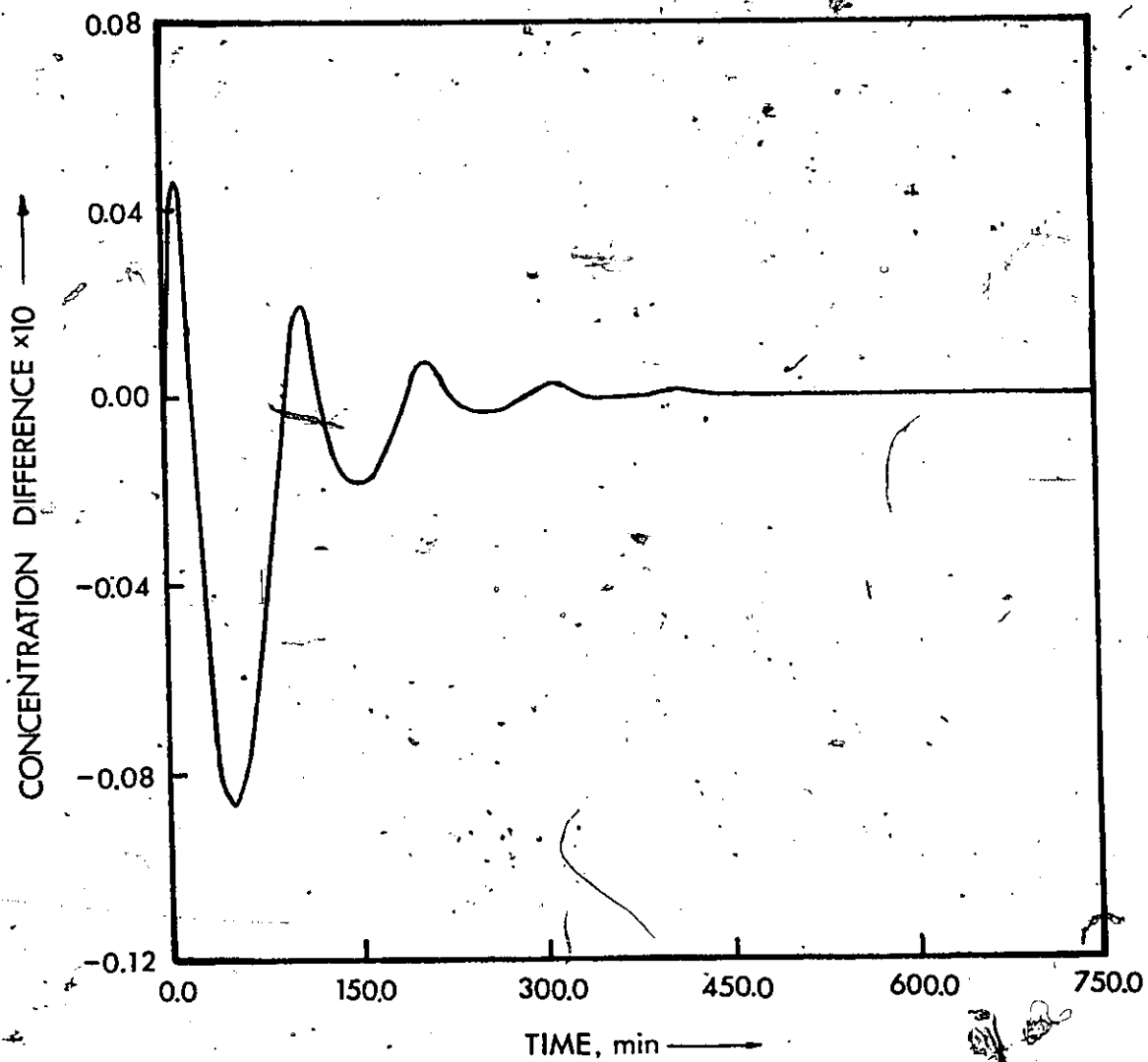
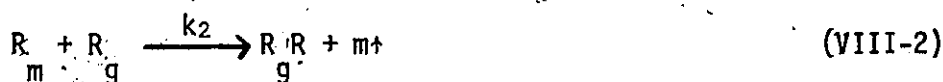


Fig. VII.6 Concentration Fluctuations during Transient Period for Second Order Kinetics

VIII OLIGOMERIZATION REACTIONS

The reaction model considered by Fontana for the precondensation stage reactions would be applicable if polymerization reactions do not occur during this stage to any significant extent. Under this assumption, the reaction model given by reactions (VIII-1) and (VIII-2)



could be used as a basis for developing adequate kinetic models for this stage. For this model to be of any value, however, the additional assumption of Flory's principle of equal reactivities [41] must be made. But the principle acknowledges the possibility of deviations when the functional groups are attached to low molecular weight species so that its application to the above system without supporting experimental evidence is not warranted.

Nevertheless, since Challa's data [8] led him to conclude that the two methyl-ester groups on DMT are equally reactive, it may be safe to assume that the reactivity of methyl-ester end groups on dimethyl terephthalate and on oligomers is the same. There is no evidence with regard to the reactivity of the hydroxyl group of the 2-hydroxyethyl-ester end group attached to monomers and oligomers, and the assumption must be made that this reactivity is independent of oligomer size. In other words, it is assumed that the reactivity of -OH groups on MHET, BHET and oligomers is the same but different from that of -OH groups on glycol.

With the above assumptions we may proceed to analyze the kinetics of the reactions (VIII-1) and (VIII-2) by using only two rate constants, one (k_1) for ester interchange reactions and one (k_2) for the transesterification reactions. In other words, the assumptions have reduced the complex system of reactions in terms of molecular species to the above fairly simple system in terms of functional groups. This is a competitive, consecutive model for which rate expressions could be established by determining the profiles of ethylene glycol and methanol. The profiles of the other components would be estimated from the following material balances:

$$R_m = R_{m_0} - m \quad \text{(VIII-3)}$$

$$R_g = 2(g_0 - g) - m \quad \text{(VIII-4)}$$

$$R_g R = m + g - g_0 \quad \text{(VIII-5)}$$

where it is assumed that only DMT and glycol are used at the beginning of the reaction, and ethylene glycol is expressed in moles while the other quantities in equivalent's. An alternative approach in elucidating the kinetics of the above system is to determine experimentally only one component [42]. Because the available transesterification data are one component data a variant of the latter approach was followed in establishing an adequate kinetic model.

A. Oligomerization Model

The various published kinetic studies though inconclusive indicate that the reaction rates in the precondensation stage have an overall order of three, with one order each for methylester end-groups, hydroxyl or 2-hydroxyethyl ester end-groups, and catalyst concentration. The following

analysis is, therefore, developed for third order kinetics. Also, following the generally accepted practice [43], reaction rates are defined in terms of equivalents.

The rate expressions for hydroxyl and R_g groups are:

$$\frac{1}{V} \frac{dg_e}{dt} = -2 k_1 [R_m] [g_e] [N_C] \quad (\text{VIII-6})$$

and

$$\frac{1}{V} \frac{dR_g}{dt} = k_1 [R_m] [g_e] [N_C] - k_2 [R_m] [R_g] [N_C] \quad (\text{VIII-7})$$

respectively. The rate constants k_1 and k_2 are defined in terms of equivalents with respect to R_m , g_e is ethylene glycol in equivalents and the brackets denote concentrations.

Equations (VIII-6) and (VIII-7), expressed in terms of moles for glycol, become

$$\frac{1}{V} \frac{dg}{dt} = -2 k_1 [R_m] [g] [N_C] \quad (\text{VIII-8})$$

$$\frac{1}{V} \frac{dR_g}{dt} = 2 k_1 [R_m] [g] [N_C] - k_2 [R_m] [R_g] [N_C] \quad (\text{VIII-9})$$

and, upon dividing Eq. (VIII-9) by Eq. (VIII-8), the following differential equation is obtained

$$\frac{dR_g}{dg} - \left(\frac{\kappa}{g}\right) R_g = -1 \quad (\text{VIII-10})$$

where $\kappa = k_2/2 k_1$. Since κ is unknown, the solution of Eq. (VIII-10) are

$$R_g = \frac{1}{(1-\kappa)} \left[g_0^{(1-\kappa)} - g^{\kappa} - g \right] \quad \text{for } \kappa \neq 1 \quad (\text{VIII-11})$$

and

$$R_g = g [\ln g_0 - \ln g] \quad \text{for } \kappa = 1 \quad (\text{VIII-12})$$

which, for a particular value of κ , establish a product distribution relationship.

The rate of production of methanol, or of methylester end group conversion, for the oligomerization reaction model is:

$$\frac{dm}{dt} = 2 k_1 R_m (g + \kappa R_g) N_c / V^2 \quad (\text{VIII-13})$$

where V , the reaction volume, is estimated by means of the volume functions given by Fontana [13] (see Appendix D).

Fitting of the model given by Eq. (VIII-13) to methanol data of unplanned experiments requires knowledge of κ , so that the model as well as the product distribution function between R_g end-groups and ethylene glycol are completely defined. In the absence of such knowledge, one might follow a trial-and-error procedure in which arbitrary values are assigned to κ and the resultant models are examined for adequacy of fit.

The determination of product distributions from the methanol data is carried out as follows. For κ different from one, Eqs. (VIII-4) and (VIII-11) yield:

$$G_1(g, \kappa) = \frac{1}{(1-\kappa)} [g_0^{1-\kappa} g^\kappa - g] - 2(g_0 - g) + m = 0, \quad \kappa \neq 1 \quad (\text{VIII-14})$$

while for κ equal to one, Eqs. (VIII-4) and (VIII-12) give:

$$G_2(g, \kappa) = g [\ln g_0 - \ln g] - 2(g_0 - g) + m = 0, \quad \kappa = 1 \quad (\text{VIII-15})$$

so that either Eq. (VIII-14) or Eq. (VIII-15) may be used to estimate

the amount of ethylene glycol remaining unreacted when m moles of methanol have been produced. Equations (VIII-14) and (VIII-15) cannot be solved analytically but the functions $G_1(g, \kappa)$ and $G_2(g, \kappa)$ are well behaved, as the typical graphs in Figs. VIII.1 and VIII.2 show, and the root may be located by Newton's algorithm [44] in just a few iterations. Subsequent to estimating ethylene glycol by the above procedure, the equivalents of 2-hydroxyethylester end groups (R_g) and of the methyl-ester end groups (R_m) are calculated from Eqs. (VIII-4) and (VIII-3), respectively.

The rate expression given by Eq. (VIII-13) will be called the oligomerization model. The procedure of fitting this model to actual data depends on whether the data are isothermal or not.

B. Oligomerization Model. Non-isothermal Data

As it was mentioned earlier, it is generally accepted that it is very hazardous to try to fit kinetic models to non-isothermal kinetic data. However Fontana used such data to establish kinetic models, and for the sake of comparison and examination of the consequences, non-isothermal data have been analyzed by the author as well.

The model was fitted to the non-isothermal data reported by Fontana (see Appendix D) by using the differential method and assumed values of κ and both of the following approaches. In the first approach, which is the same as that followed by Fontana, Eq. (VIII-13) was used to calculate k_1 values. For each value assumed for the parameter κ the data yielded one set of k_1 values which were subsequently tested for significance of correlation with reciprocal absolute temperature according to the equation:

$$\ln k_1 = \beta_0 + \beta_1/T$$

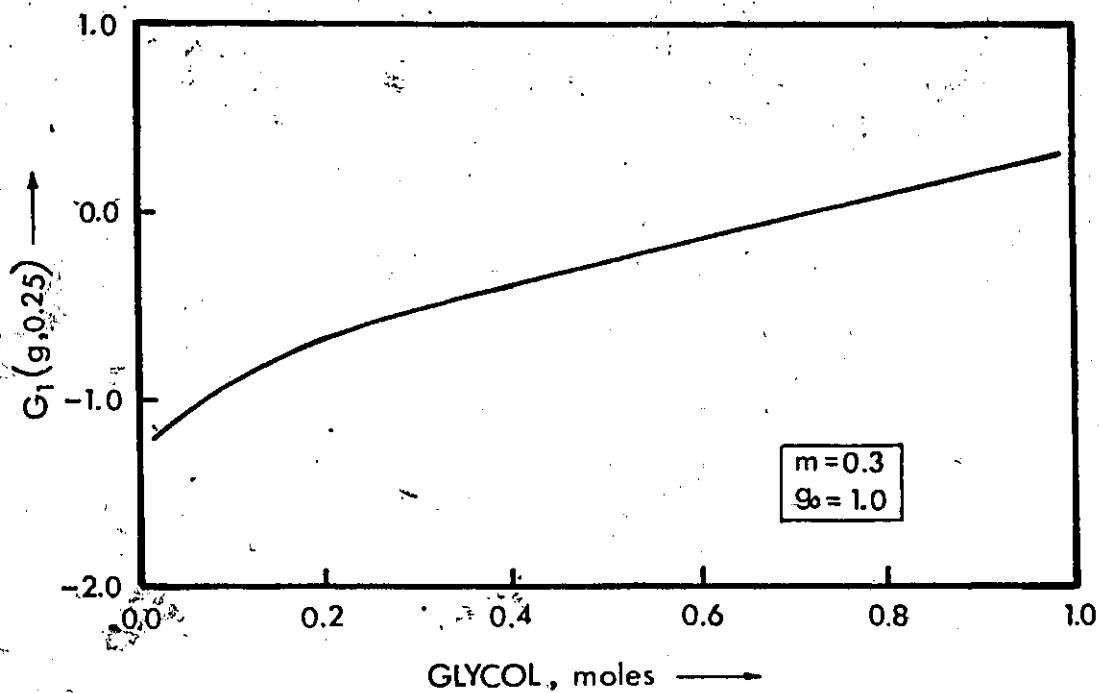


Fig. VIII.1 Graph of First Glycol Function

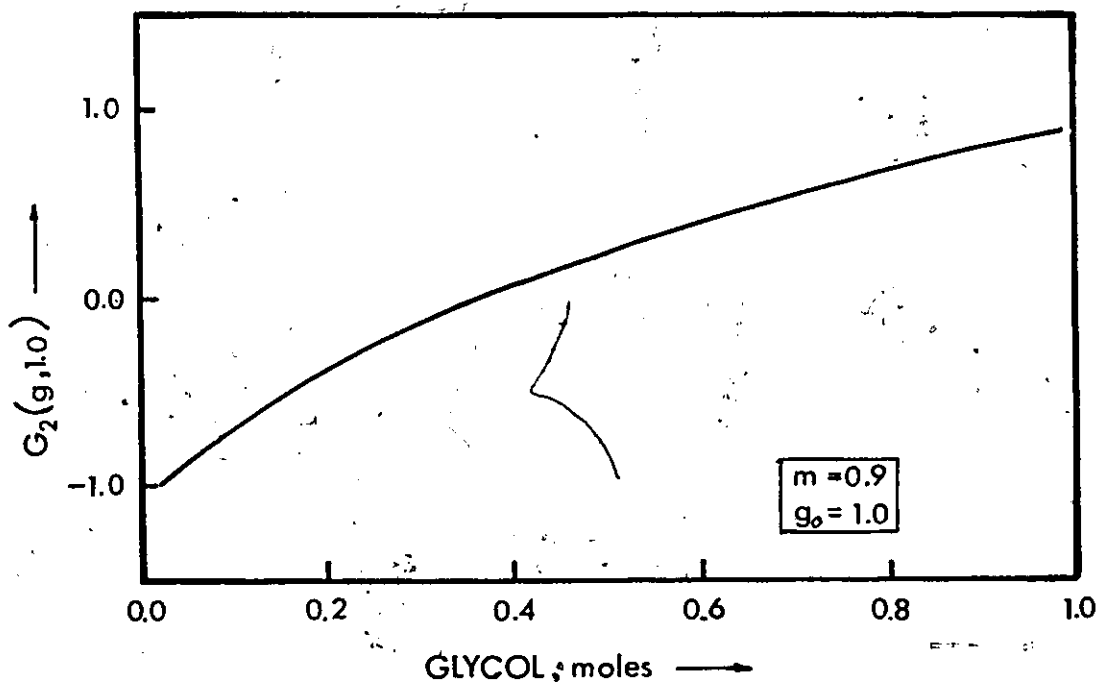


Fig. VIII.2 Graph of Second Glycol Function

and it was found that the correlation for each set was significant at the 0.001 probability level. Table VIII.1 gives the results of fitting Eq. (VIII-16) to the calculated values of the rate constant for some values of κ , while Fig. VIII.3 shows some plots of k_1 versus $1/T$.

In the second approach, Eq. (VIII-13) was transformed to:

$$\frac{dm}{dt} = 2A \exp(\beta/T) R_m (g + \kappa R_g) C/V^2 \quad (\text{VIII-17})$$

which is a non-linear model. Eq. (VIII-17) was fitted to the experimental rates for different values of κ using a non-linear least squares routine [45]. The results of fitting, given in Table VIII.2 show the error sum of squares to be of the same order of magnitude for each and every preassigned value of κ . In addition, plots of residuals against the estimated rates showed no abnormality, and the error sum of squares is very low indeed.

Based on the above analysis it must be concluded that the model, Eq. (VIII-13) fits the non-isothermal data for every value assigned to the parameter κ . Fontana assigned to κ the value of 0.25 by a so-called interpretation of the value of the polycondensation equilibrium constant, obtained by averaging the observed values over temperature and degree of polymerization. This averaging process, however, could be nothing more than a crude approximation because Challa's data [46] have shown that the polycondensation equilibrium constant (K) varies with degree of polymerization and the following analysis demonstrates that K varies significantly with temperature as well.

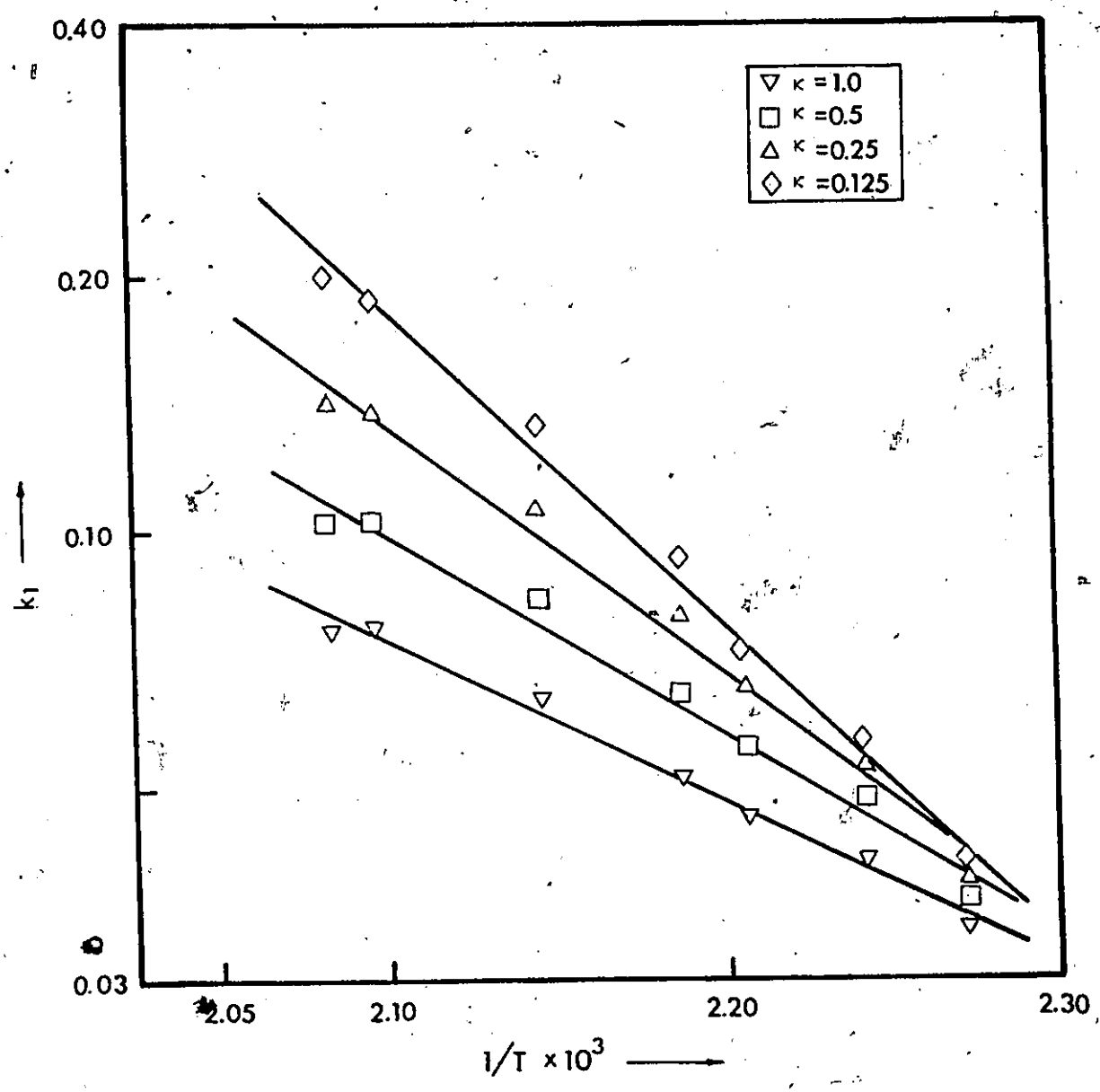


Fig. VIII.3 Rate Constant vs. Reciprocal Absolute Temperature

TABLE VIII.1

Results of Rate Constant Regression

k_2/k_1	κ	β_0	β_1	E(Kcal/mole)
2	1.0	6.5165	-4340.6	8.6
1	0.5	8.8948	-5337.4	10.6
2/3	0.333	10.732	-6126.9	12.2
1/2	0.25	12.174	-6752.3	13.4
1/3	0.6666	14.325	-7691.5	15.3
1/4	0.125	15.873	-8371.6	16.6

TABLE VIII.2

Non-Linear L.S. Analysis of Rate Model

k_2/k_1	κ	Error sum of Squares ($\times 10^6$)	A	β	E(Kcal/mole)
2	1.0	0.520	1157.2	-4583.4	9.1
1	0.5	1.06	18772.0	-5764.9	11.5
2/3	0.3333	1.40	138450.0	-6627.0	13.2
1/2	0.25	1.55	619400.0	-7278.3	14.4
1/3	0.1666	1.58	5251500.0	-8211.9	16.3
1/4	0.125	1.48	22916000.0	-8858.0	17.6

C. Polycondensation Equilibrium Constant and its Implications

Values of the polycondensation equilibrium constant (K), experimentally determined by Fontana [13] and Challa [46] for about the same degree of polymerization, are plotted against absolute temperature in Fig. VIII.4. Least square analysis of these data showed that a significant correlation (correlation coefficient $r = 0.8935$) exists between K and $1/T$ at the 0.001 probability level.

The least-squares line is given by Eq. (VIII-18)

$$\ln K = 1049./T - 2.775 \quad (\text{VIII-18})$$

where point $(0.43, 2.21 \times 10^{-3})$ was not taken into account in the correlation, having been discarded as an outlier by the extreme deviate test [47] at the 0.01 probability level.

The standard heat of reaction estimated from Eq. (VIII-18) is equal to -2.08 Kcal/mole, and this value is in very good agreement with the value reported by Challa [46]. Equation (VIII-18) shows that the polycondensation equilibrium constant is not very sensitive to temperature. However, the constant does vary, and as a matter of fact its value should have varied from 0.5 to 0.75 for the temperature range of Fontana's transesterification data.

The temperature dependence of the equilibrium constant substantially undermines Fontana's claim that the value of K determines the ratio of k_2/k_1 for, if the claim were true, it should not have been possible to correlate the kinetic data by assuming a constant value of k when its actual value should have changed by 50%. Also, if the claim were true it should not have been possible to correlate the data by the numerous and widely different values assumed for k in the present analysis. It

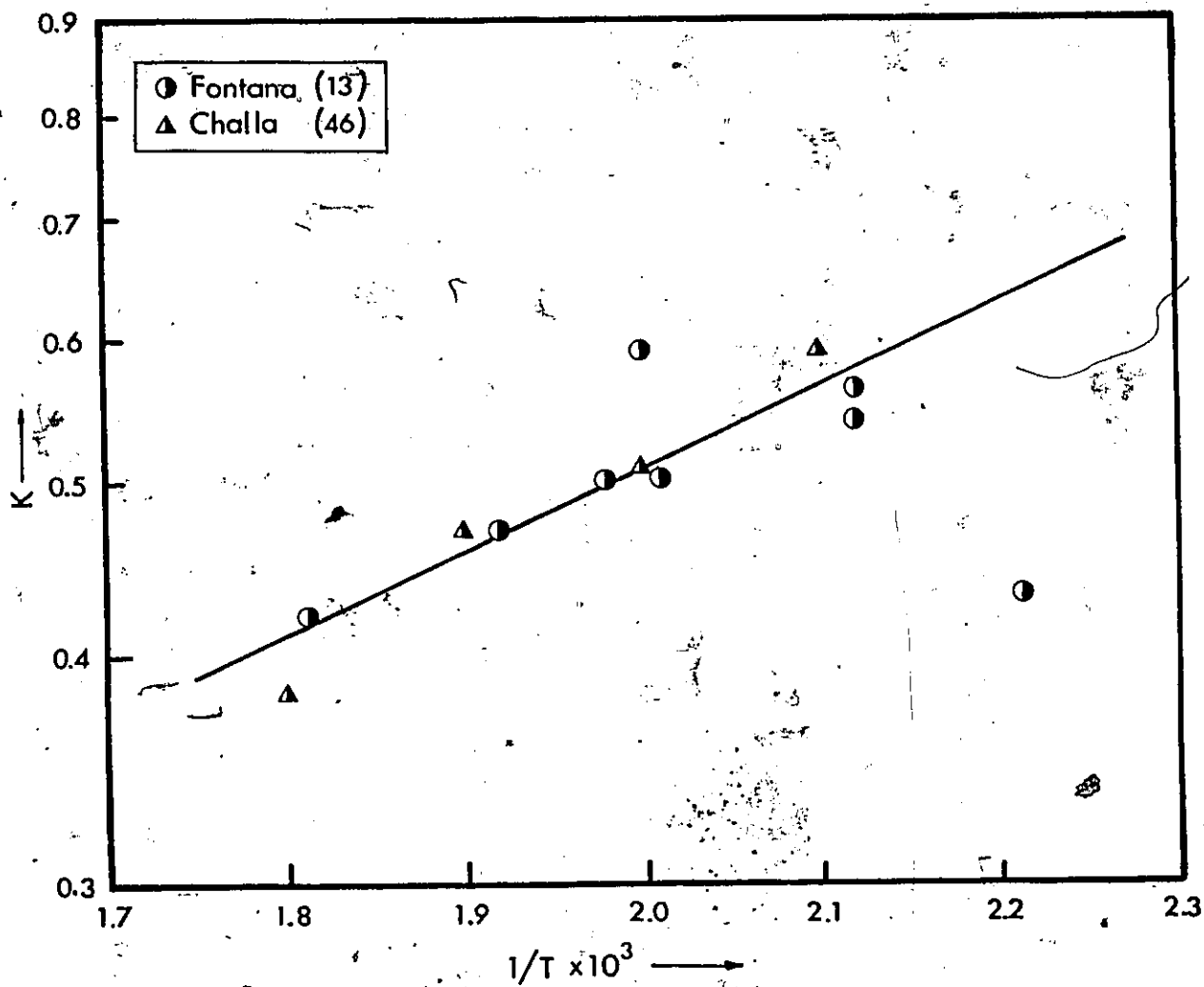


Fig. VIII.4 Polycondensation Equilibrium Constant vs. Reciprocal Absolute Temperature

may be, however, that the use of non-isothermal data does not afford any discriminating power to the model, and this possibility made further testing of the kinetic model with isothermal data necessary.

D. Oligomerization Model. Isothermal Data

Most of the kinetic data obtained and used by Fontana were non-isothermal, but he did report the data of a run which, he claimed, had a constant temperature portion [Table II of 13]. The temperature does vary a little (see Appendix D) but these near-isothermal data might safely be assumed isothermal. However, because the aim was to establish adequate and conclusive kinetic models, model testing was not restricted to these data but was extended to include the isothermal data, given in Appendix D, which were read off from the graphs reported by Peebles and Wagner [12] and Tomita and Ida [Fig. 2 of 18].

Fontana analyzed his near-isothermal data but his differential analysis was limited to calculating k_1 values according to Eq. (VIII-13) with $\kappa = 0.25$ and averaging the values thus obtained. The coefficient of variation of these k_1 values from the mean are not random and further analysis using standard kinetic analysis techniques was undertaken. To this end, Eq. (VIII-13) was modified to

$$\frac{dm}{dt} = 2k_1 N_C f(m, \kappa) \quad (\text{VIII-19})$$

where

$$f(m, \kappa) = R_m (g + \kappa R_g) / Y^2 \quad (\text{VIII-20})$$

Equation (VIII-19) shows that, if the assumed model is valid, the graph of methanol production rates versus $f(m, \kappa)$ should be a straight line passing through the origin. Figure VIII.5 is the plot of the numerically computed rates against the abscissa with κ equal to 0.25, the value assumed.

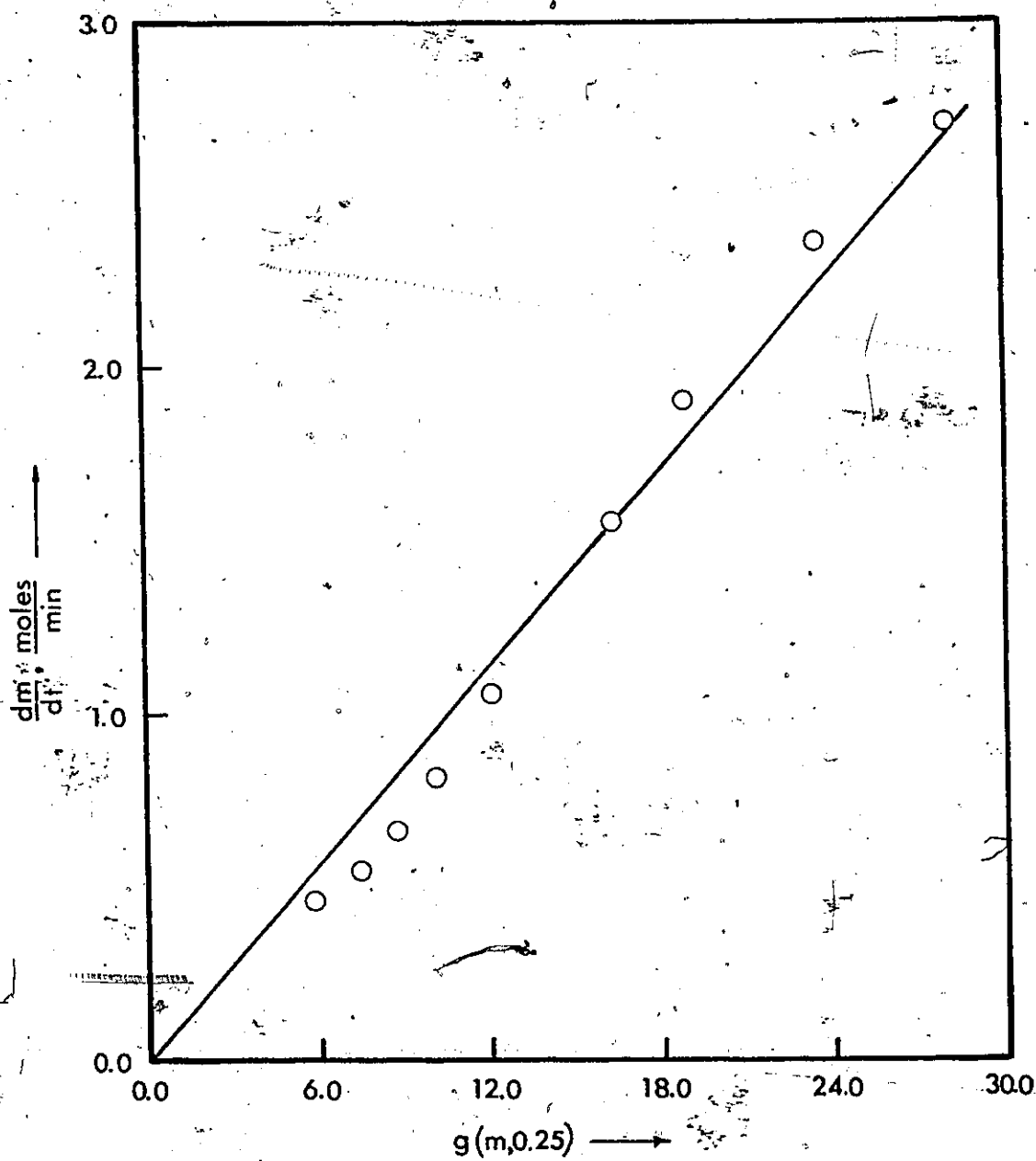


Fig. VIII.5 Differential Analysis of Oligomerization Model

by Fontana. The solid line is the zero intercept least squares line supported by the data, which clearly show a substantial trend. The deviations are not random, and this lack of randomness renders both the least squares analysis and the model invalid. It must, therefore, be concluded that Fontana's near-isothermal integral data, analyzed by the differential method, do not support his model. However, because the analysis of integral data by the differential method is subject to potentially large errors, it was decided to use the integral method in testing the oligomerization kinetic model before drawing final conclusions about its adequacy.

To this end, Eq. (VIII-19) is rewritten as:

$$\frac{dm}{f(m,\kappa)} = 2 k_1 N_C dt \quad (\text{VIII-21})$$

The left hand side of Eq. (VIII-21) cannot be integrated analytically because of the complexity of the function $f(m,\kappa)$, but the integral in Eq. (VIII-22).

$$H(m,\kappa) = \int_0^m \frac{dm}{f(m,\kappa)} = 2k_1 N_C t \quad (\text{VIII-22})$$

may be evaluated numerically, and numerical integration make application of the integral method possible. This approach is essentially the same as the approach in the case when the integral in Eq. (VIII-22) may be obtained analytically, the only difference between the two being the way the integral values are calculated. The numerical integration may be carried out using any numerical quadrature routine. Since the function $1/f(m,\kappa)$ is a smooth increasing function of m , as Fig. VIII.6 shows, Simpson's rule [48] was used to evaluate the integral using a suitable step size and double precision arithmetic.

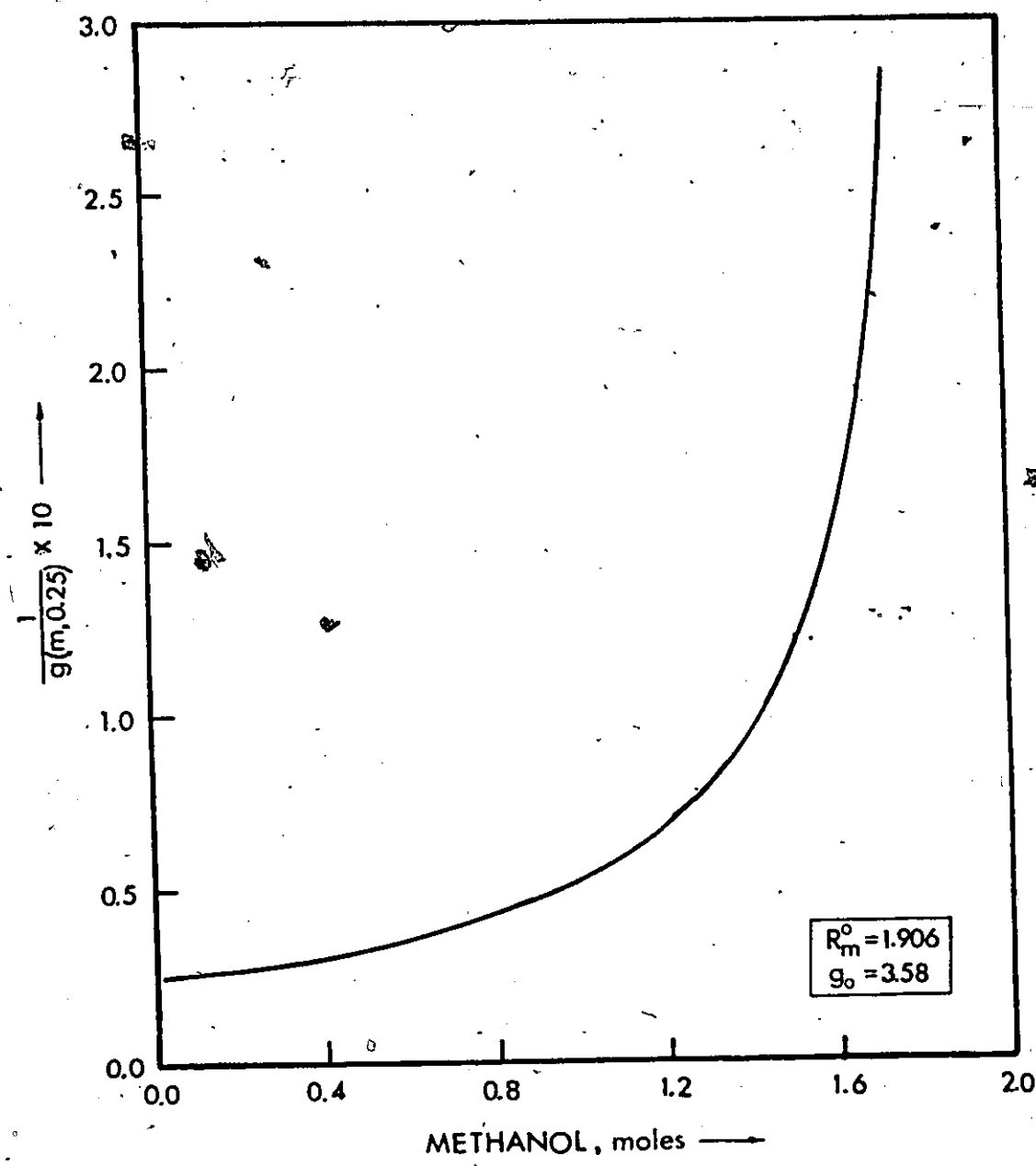


Fig. VIII.6 Graph of Integrand

Analysis of the available transesterification data using the integral method was carried out by assuming values for the parameter κ , that is, assuming the ratio of reactivities of hydroxyl groups on free glycol and half-esterified glycol, and testing the corresponding model for adequacy of fit. First the value assumed by Fontana, i.e. $\kappa = 0.25$, was tested and significant trends in the residuals showed that the model was inadequate. Other values for κ were also assumed and some typical results of the analysis are shown in Figs. VIII.7, VIII.8, and VIII.9. These Figures make it quite clear that the various models are inadequate. Only very low values of κ give a reasonable fit, but only in the case of Tomita's data an entirely adequate fit is obtained. However, at these low values of κ the importance of the transesterification reaction, Eq. (VIII-2), becomes negligible. It must, therefore, be concluded that oligomerization reactions do not proceed to any significant extent during the precondensation stage. This conclusion is validated by the available one-component data for methyl-ester end group conversion up to 90% and initial molar ratios of ethylene glycol to DMT greater or equal to two, and seems to be confirmed by the work of Sorokin and Chebotareva [17] who reported the identification of MHET and BHET only.

The implication of the aforementioned conclusion is that the reactivity of hydroxyl groups on half-esterified glycol is, in the experimental temperature range of 175°C to 197°C, negligibly small when compared with the reactivity of hydroxyl groups on free ethylene glycol.

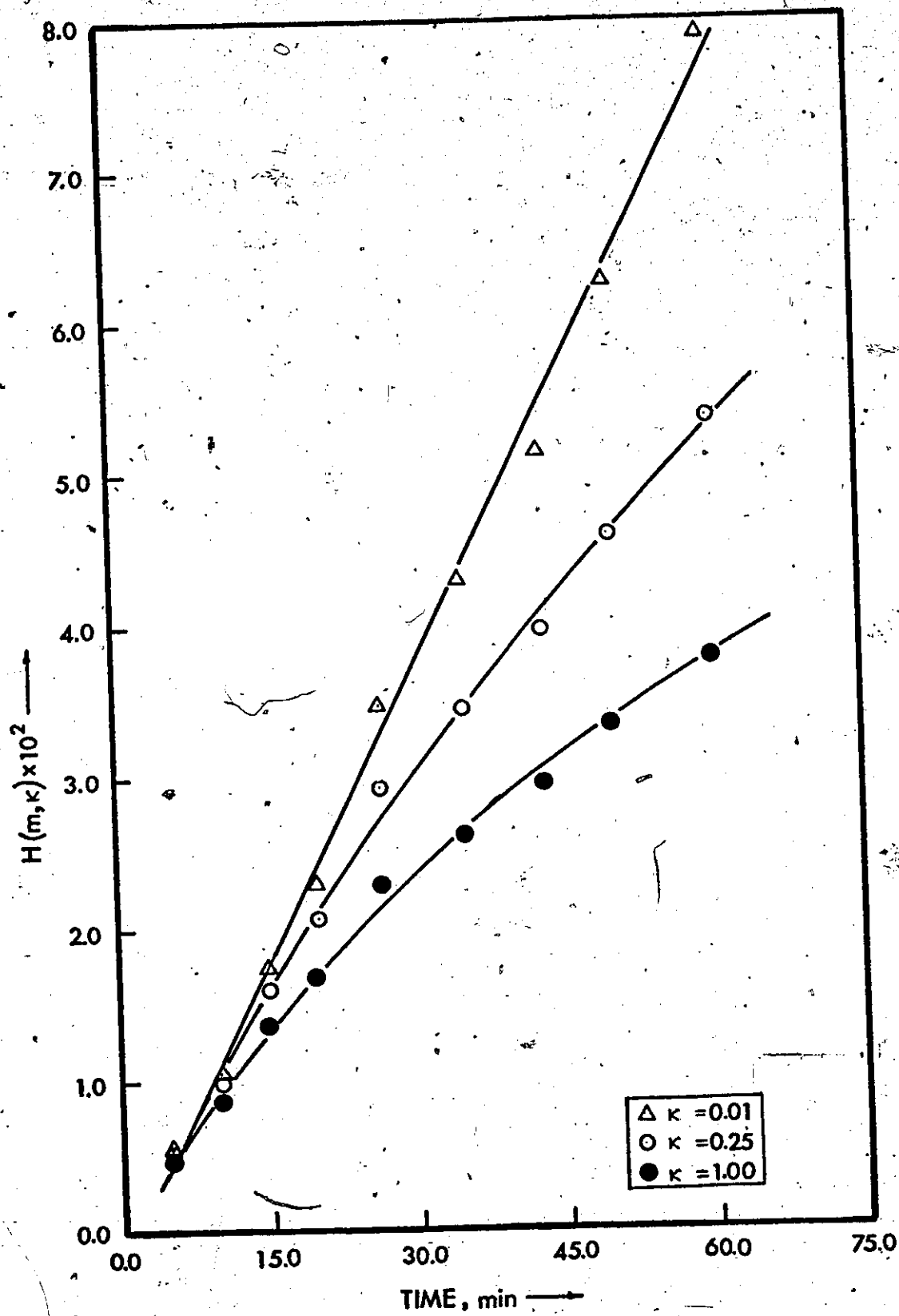


Fig. VIII.7 Oligomerization Model Applied to Fontana's Data

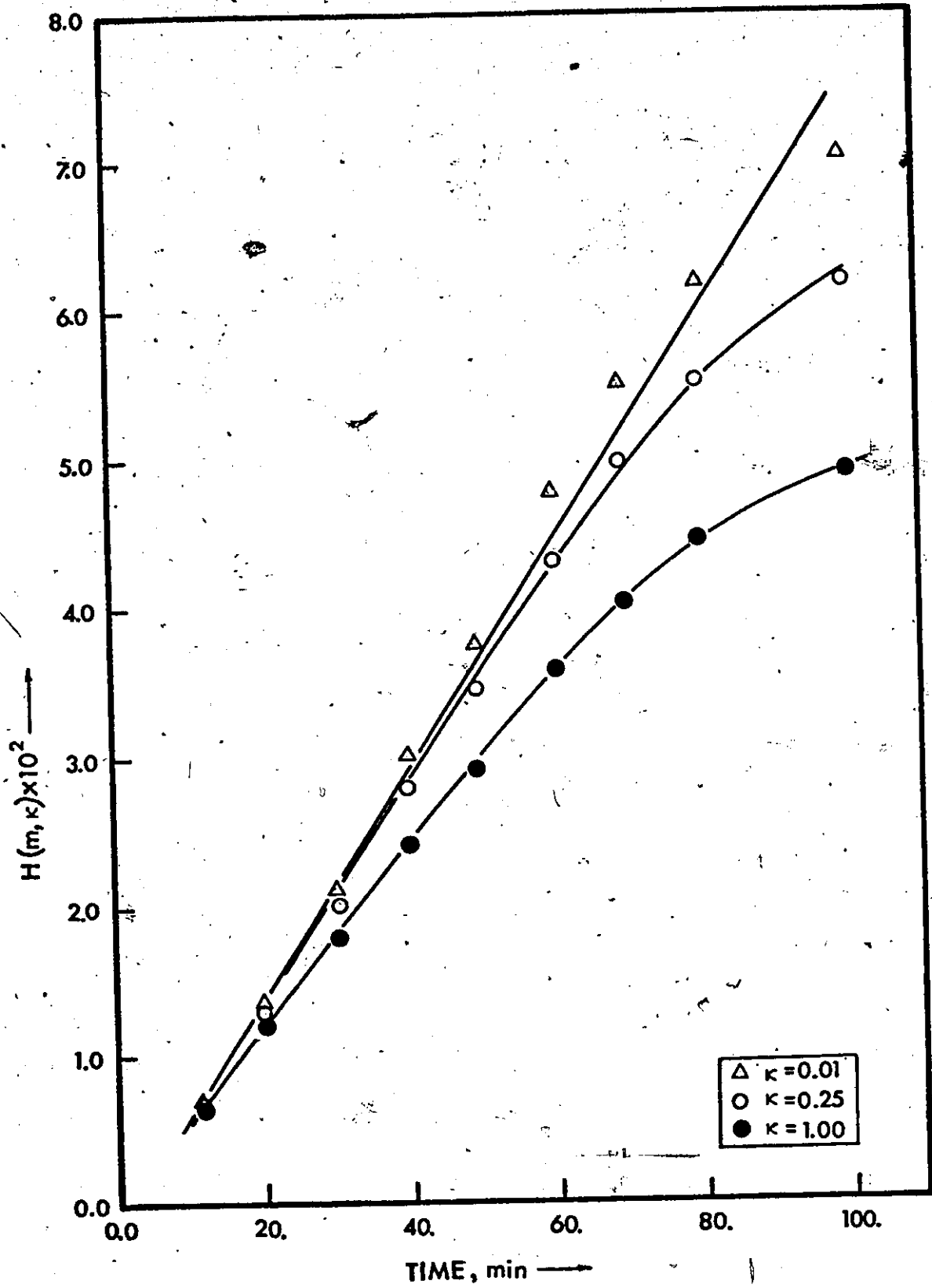


Fig. VIII.8 Oligomerization Model Applied to Peebles and Wagner's Data

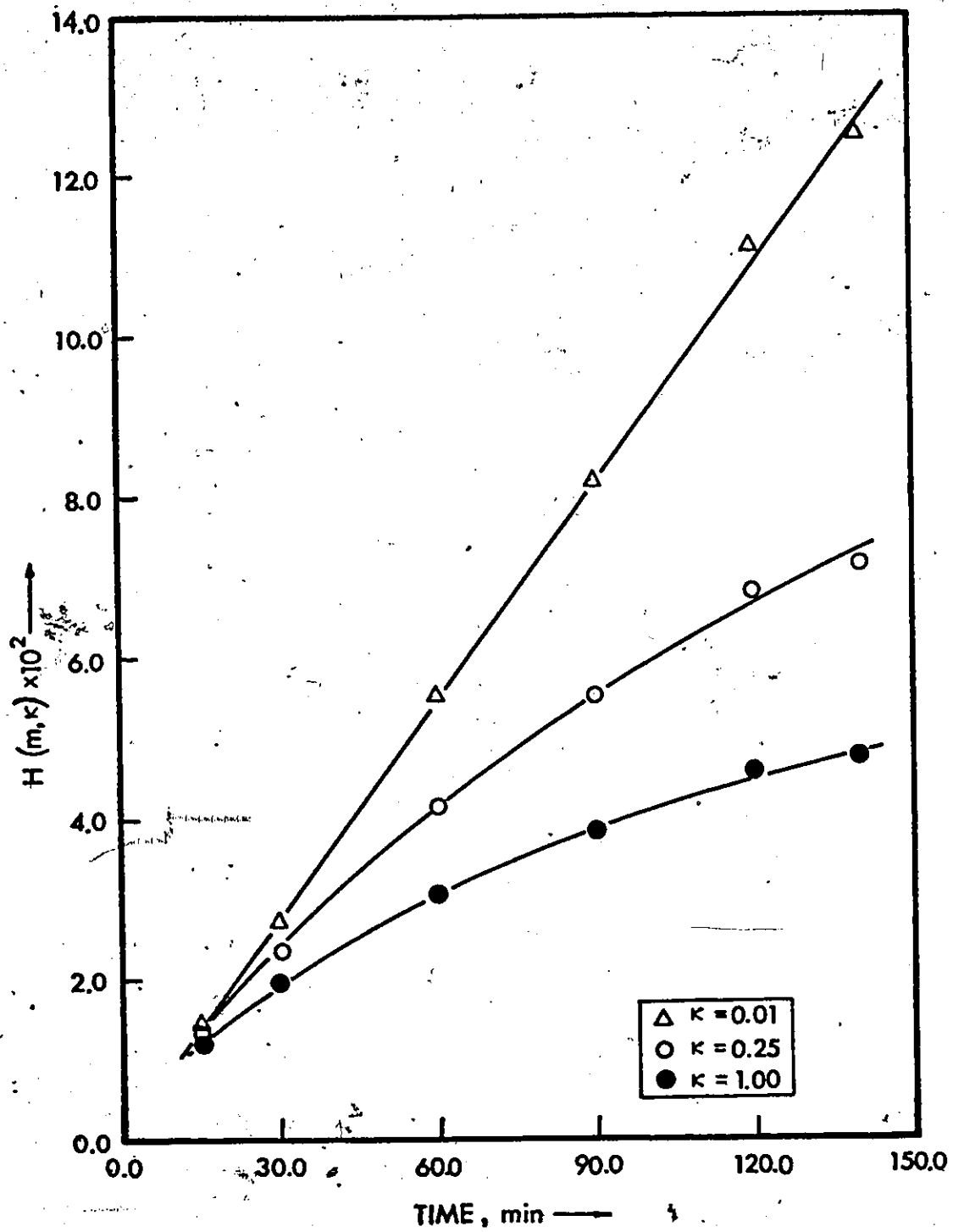
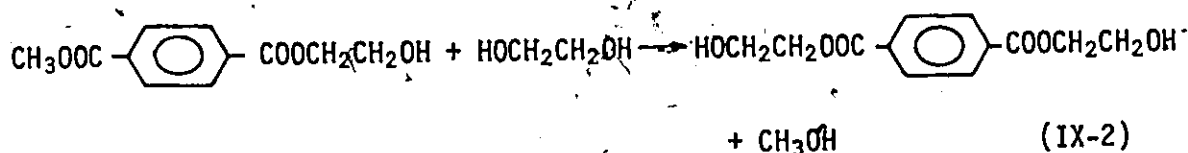
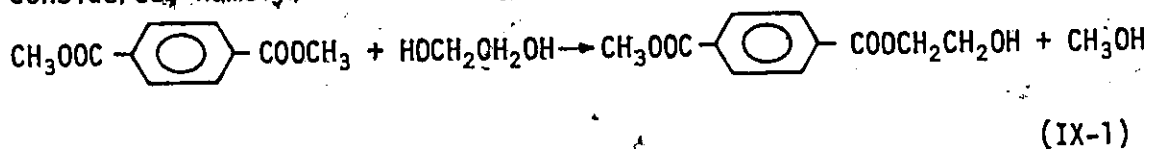


Fig. VIII.9 Oligomerization Model Applied to Tomita and Ida's Data

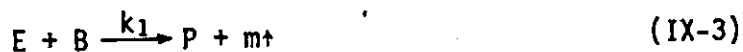
IX METHYL-ESTER GROUP REACTION

The conclusion drawn in the analysis of the oligomerization model clearly implies that only monomer ester interchange reactions should be considered, namely:



These reactions were hypothesized by Peebles and Wagner [12] and proposed by Sorokin and Chebotareva [15] on account of experimental evidence.

Now, in view of Challa's finding [8] that methylester groups on dimethyl terephthalate and MHET are equally reactive, the above reaction system may be compacted to the reaction of a methylester group and ethylene glycol, i.e., Eq. (II-13) or



where E and B are methyl-ester and 2-hydroxyethyl-ester groups, respectively while P and m are defined as before.

A. Methyl-Ester Group Model

The kinetic model for the rate of reaction of methyl-ester groups is assumed to be:

$$-\frac{1}{V} \frac{dN_E}{dt} = 2k_1 \frac{N_C}{V} \frac{N_E}{V} \frac{N_B}{V} \quad (\text{IX-4})$$

where N_C is the amount of catalyst in moles, N_E is methyl-ester groups in equivalents, N_B is ethylene glycol in moles, and k_1 is defined in terms of equivalents of methyl-ester and hydroxyl groups.

The material balances from Eq. (IX-3) are:

$$N_E = N_{E_0}(1-x) \quad (IX-5)$$

$$N_B = N_{E_0}(M-x) \quad (IX-6)$$

and

$$N_m = N_{E_0} X \quad (IX-7)$$

where x is the conversion of methyl-ester groups, M is the initial ratio of ethylene glycol to methyl-ester groups i.e., $M = N_{B_0}/N_{E_0}$, and m the amount of methanol produced in moles. Now the reaction volume V is defined as:

$$V = V_0(1-\epsilon x) \quad (IX-8)$$

where ϵ , the fractional change in volume, is defined, in terms of the reaction volume at zero, V_0 , and complete, V_f , conversion of methyl-ester groups, by:

$$\epsilon = (V_0 - V_f)/V_0 \quad (IX-9)$$

The zero and complete conversion volumes are given [13] in litres by:

$$V_0 = (0.1915N_{E_0}/2 + 0.0606N_{B_0})[1 + 0.0014(\theta - 140)] \quad (IX-10)$$

and

$$V_f = V_0 - 0.0439N_{E_0}[1 + 0.0014(\theta - 140)]. \quad (IX-11)$$

where θ is reaction temperature in degrees Centigrade.

By use of Eqs. (IX-5) and (IX-6) and (IX-8) and manipulations, the model, Eq. (IX-4), is transformed to:

$$\frac{dx}{dt} = k_a C_{E_0} \frac{(1-x)(M-x)}{(1-\epsilon x)^2} \quad (IX-12)$$

where $k_a = 2k_1 N_C/V$. Analytical integrals for Eq. (IX-12) are obtained

in Appendix E and are given by Eq. (IX-13), for M different from one

$$k_a t = \frac{V_o}{N_{E_o}} [\alpha x + \beta \ln \frac{(M-x)}{M(1-x)} + \gamma \ln \frac{(1-x)(M-x)}{M}] = F_1(x) \quad (\text{IX-13})$$

and Eq. (IX-14), for M equal to one

$$k_a t = \frac{V_o}{N_{E_o}} [\epsilon^2 x + (\epsilon-1)^2 \frac{x}{1-x} + 2\epsilon(\epsilon-1) \ln(1-x)] = F_2(x) \quad (\text{IX-14})$$

where

$$\alpha = \epsilon^2 \quad (\text{IX-15})$$

$$\beta = [2 - 2(M+1)\epsilon + (M-1)^2 \epsilon^2] / 2(M-1) \quad (\text{IX-16})$$

$$\gamma = \epsilon[\epsilon(M+1) - 2] / 2$$

B. Testing of the Methyl-Ester Group Model

Testing of the assumed methyl-ester group model is carried out by the integral method according to which plotting of the right hand side of Eqs. (IX-13) or (IX-14), depending on the value of M, should result in a straight line passing through the origin. Only isothermal data were used in testing this model.

In Figure IX.1 integral values for Fontana's near-isothermal data are plotted against time, and the adequacy of fit is clearly apparent. The line shown is the least squares line

$$F_1(x) = \hat{\beta}_0 + \hat{\beta}_1 t \quad (\text{IX-18})$$

where the subscript is equal to two. The residuals do not show any significant trend, and, since the intercept is not significantly different from zero at 0.001 probability level, it must be concluded that the model describes Fontana's data exceptionally well.

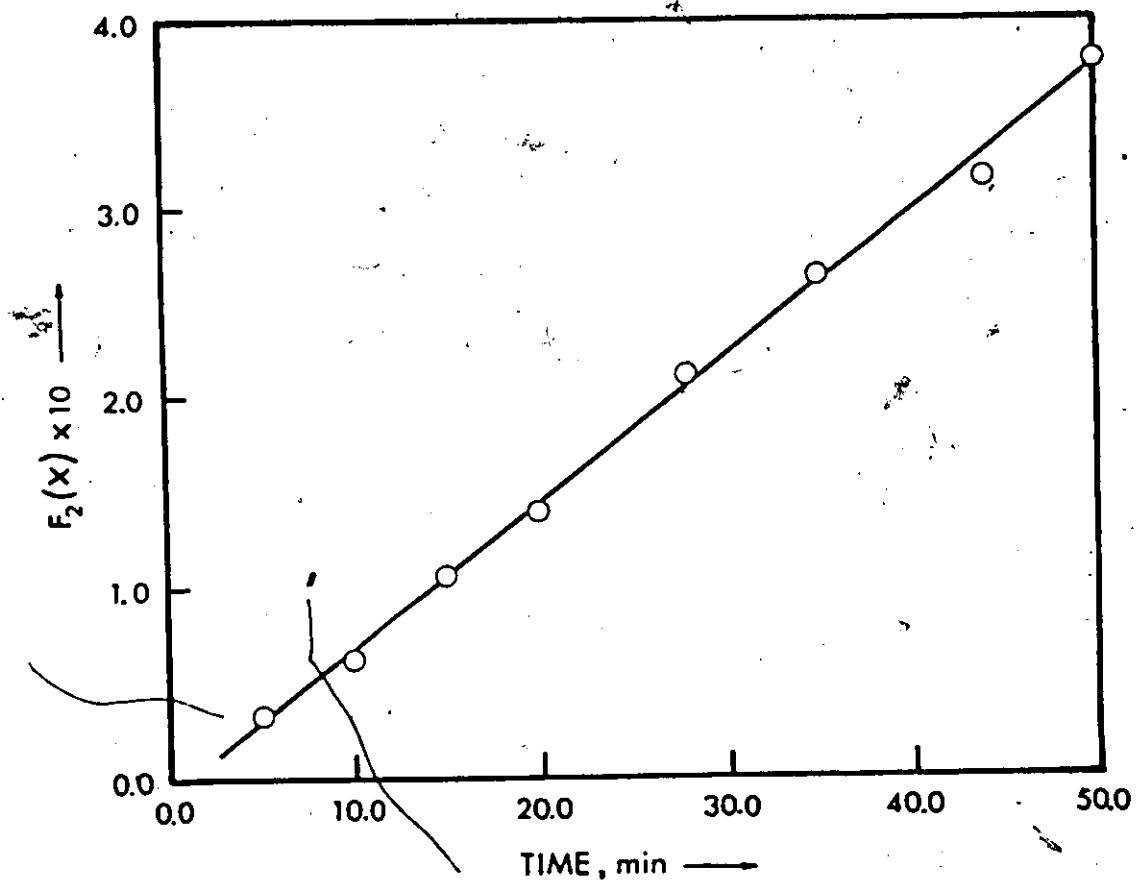


Fig. IX.1 Methyl-Ester Group Model Applied to Fontana's Data

The methyl-ester group model fits Tomita and Ida's data (the four sets given in Appendix D) quite well, and Fig. IX.2 shows the plot of the integral values for set No. 1 against time. The relatively large deviation of the point at 120 min may well be the result of error in reading the datum off the graph at high conversion. Of course, the correlation is very significant, and, since the intercept is not significantly different from zero, the model fits the data very well.

The application of the model to Peebles and Wagner's data is shown in Fig. IX.3. It is very clear that the integral values, $F_1(x)$, vary linearly with time. The intercept is significantly different from zero at 0.01 probability level but not so at 0.001 probability, and it would be quite difficult to argue that the model does not fit the data. This is a borderline situation, and it may be due to the way the data were collected (methanol pumped through reactor).

Some statistics of the least squares analysis of the model are given in Table IX.1. These statistics show that the model, tested up to 88% conversion with Tomita and Ida's and Peebles and Wagner's data, easily passes the test for adequacy of fit. Table IX.2 gives the apparent rate constants, k_a , which are the slopes of the least squares lines and the true rate constants, k_1 , for the data analyzed in the present work. The estimates for the true rate constants given in the last column are very good and the agreement between the values estimated from Fontana's and Tomita and Ida's data at 180°C is excellent.

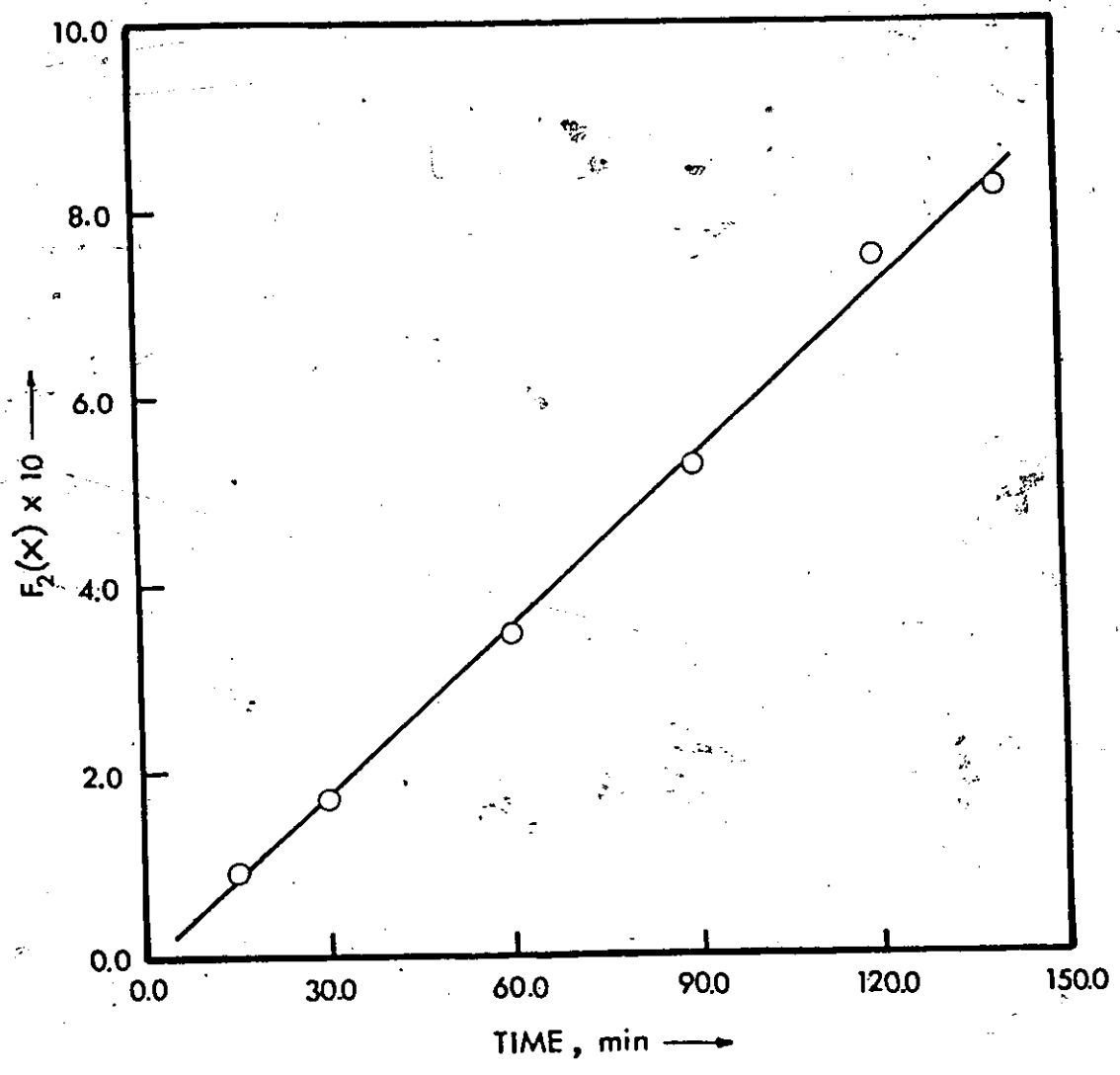


Fig. IX.2 Methyl-Ester Group Model Applied to Tomita and Ida's Data

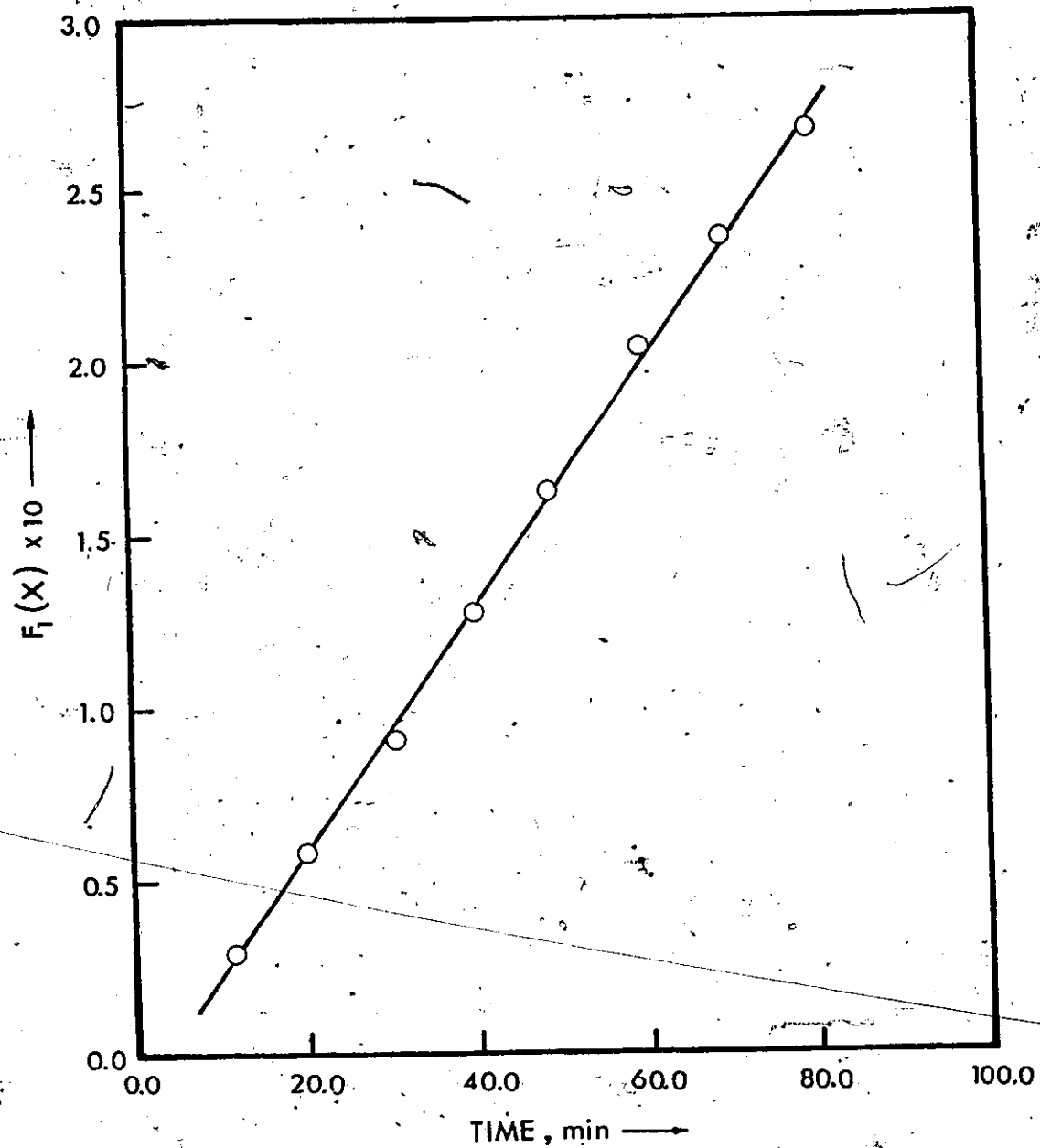


Fig. IX.3 Methyl Ester Group Model Applied to Peebles and Wagner's Data.

TABLE IX.1
Statistics for the
Methyl Ester Group Model

Data	Degrees of Freedom	F-Value	Student's t for β_0
Fontana	6	4327.4 ^a	-2.869
Tomita & Ida #1	4	1088.6 ^a	-0.410
Tomita & Ida #2	4	1387.7 ^a	-0.032
Tomita & Ida #3	5	1932.1 ^a	-0.346
Tomita & Ida #4	3	561.0 ^a	-0.380
Peebles & Wagner	6	5348.3 ^a	-5.416 ^b

a. Very highly significant

b. Not significant at 0.001 probability level

TABLE IX.2

Rate Constants for the
Methyl Ester Group Model

Data	Catalyst		Reaction Temperature (°C)	Apparent Rate Constant ($k_a \times 10^3$)	True Rate Constant (k_1), $l^2 \text{mole}^{-2} \text{min}^{-1}$
	Compound	Mass (moles $\times 10^4$)			
Fontana	Zinc Acetate	1.81	180	7.7373	3.527
Tomita & Ida #1	Zinc Acetate	1.00	197	6.0264	5.092
Tomita & Ida #2	Zinc Acetate	0.70	197	4.1646	5.027
Tomita & Ida #3	Zinc Acetate	0.50	197	2.9248	4.943
Tomita & Ida #4	Zinc Acetate	1.00	180	4.3551	3.593
Peebles & Wagner	Zinc Acetyl-acetonate	5.51	175	3.55	1.350

The activation energy for zinc acetate was estimated to be 8.6 Kcal/mol by fitting the Arrhenius equation to the average values of the true rate constant at 180°C and 197°C. The Arrhenius equation of k_1 for zinc acetate is given by:

$$\ln k_1 = - \frac{4306.8}{T} + 10.777 \quad (\text{IX-19})$$

The previous analysis clearly shows that the kinetic model for methyl-ester group conversion given by Eq. (IX-12) or Eq. IX-20)

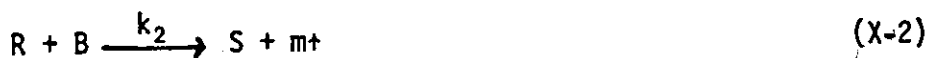
$$- \frac{dN_E}{dt} = 2k_1 N_C C_E C_B \quad (\text{IX-20})$$

is, in the light of the available experimental data, an adequate model for the ester interchange reactions occurring in the precondensation stage.

X MOLECULAR SPECIES REACTIONS

In the previous section it was shown that the proposed methyl-ester group model adequately described the rate of conversion of methyl-ester groups, or, for that matter, the rate of production of methanol. However, the model does not give information as to which molecular species the unreacted methyl-ester groups are attached. Since such information might be desirable and since the above model is a kinetically simplified description of the essentially competitive, consecutive reaction system given by Eqs. (IX-1) and (IX-2), it was considered advisable to set up a series-parallel kinetic model and test its adequacy of fit. Such an analysis should be enlightening in view of the conclusions drawn by Peebles and Wagner, who, as mentioned earlier, based their analysis on incorrect premises.

For the sake of brevity, the system of Eqs. (IX-1) and (IX-2) will be analyzed in terms of the kinetics of the reactions (II-13) and (II-14), that is



where A, B, R, S, and m are dimethyl terephthalate, ethylene glycol, methyl-2-hydroxyethyl terephthalate, bis-(2-hydroxyethyl) terephthalate and methanol respectively.

A. Molecular Species Model

From the mathematical point of view the system of reactions (X-1) and (X-2) is exactly the same as the oligomerization reaction model, and

the analysis of the former will follow the same steps as the analysis of the latter, which was given in detail in the appropriate section. It will be assumed that all the rate expressions have an overall order of three.

The rate of conversion of A, that is DMT, is assumed to be given by:

$$-\frac{1}{V} \frac{dN_A}{dt} = k_1 (2C_A)(2C_B) C_C \quad (X-3)$$

where k_1 is defined in terms of equivalents of methyl-ester groups on DMT and of hydroxyl groups on ethylene glycol. Similarly the reaction rate for R, that is MHET, is assumed to be given by:

$$-\frac{1}{V} \frac{dN_R}{dt} = -4k_1 C_A C_B C_C + 2k_2 C_R C_B C_C \quad (X-4)$$

where k_2 is also defined in terms of equivalents.

Further analysis of this system using experimental profiles of one component only requires knowledge of the rate constant ratio, namely, k_2/k_1 . This, of course, is available from Challa's work [8] in which it was concluded that the methyl-ester groups on DMT and MHET are of equal reactivity, which implies that k_2/k_1 is equal to one.

Dividing Eq. (X-4) by Eq. (X-3) results in

$$\frac{dN_R}{dN_A} = -1 + \frac{k_2 C_R}{2k_1 C_A} \quad (X-5)$$

or

$$\frac{dN_R}{dN_A} - \frac{N_R}{N_A} = -1 \quad (X-6)$$

where $\kappa = k_2/2k_1$. The solutions of the differential equation (X-6) are:

$$N_B = \left(\frac{N_A}{1-\kappa}\right) \left[\left(\frac{N_A}{N_{A_0}}\right)^{1-\kappa} - 1 \right] \quad (X-7)$$

for κ different from one and

$$N_R = N_A \ln(N_{A_0}/N_A) \quad (X-8)$$

for κ equal to one. Equation (X-7) or (X-8) establishes a product distribution relationship between MHET and DMT for a given value of κ , and it is these equations that make analysis of the series-parallel system possible with experimental data of only one component. Of course, since the value of κ is equal to 0.5 only Eq. (X-7) is applicable. However, disregarding the equivalence of methyl-ester groups the models are, for the sake of completeness, developed for any κ .

The material balances for reactions (X-1) and (X-2) are

$$N_B = N_{B_0} - N_m \quad (X-9)$$

$$N_R = 2(N_A - N_{A_0}) - N_m \quad (X-10)$$

$$N_S = (N_A - N_{A_0}) - N_m \quad (X-11)$$

and it is immediately apparent that Eqs. (X-7) and (X-10) or Eqs. (X-8) and (X-11) allow estimation of unreacted DMT, that is N_A , when N_m moles of methanol have been produced.

The rate of methyl ester group conversion is given by:

$$-\frac{1}{V} \frac{dN_E}{dt} = 4k_1 C_A C_B C_C + 2k_2 C_R C_B C_C \quad (X-12)$$

since the rate of methyl-ester conversion for equation (X-1) is equal to the rate of DMT conversion, and Eq. (X-12) simplifies to

$$-\frac{dN_E}{dt} = 4k_1 N_C C_A C_B + 2k_2 N_C C_R C_B \quad (X-13)$$

But the rate of methyl-ester conversion is equal to the rate of methanol production so that the latter from Eq. (X-13) is:

$$\frac{dN_m}{dt} = 4k_1 N_C N_B (N_A + \kappa N_R) / V^2 \quad (X-14)$$

or

$$\frac{dN_m}{dt} = k'_a N_B (N_A + \kappa N_R) / V^2 \quad (X-15)$$

where $k'_a = 4N_C k_1$. Eq. (X-15) is a general model for the rate of production of methanol, which along with the material balance and product distribution equations might adequately describe the transesterification reactions.

As was mentioned earlier, κ is equal to 0.5 and, therefore, the model for methanol production according to the competitive-consecutive reaction system is assumed to be:

$$\frac{dN_m}{dt} = k'_a N_B (N_A + 0.5 N_R) / V^2 \quad (X-16)$$

According to this model, which will be referred to as the molecular species model, the product distribution for the mixed ester is given by Eq. (X-17) obtained from Eq. (X-7) with κ equal to 0.5

$$N_R = 2N_A \left[\left(\frac{N_{A_0}}{N_A} \right)^{0.5} - 1 \right] \quad (X-17)$$

while the moles of unreacted DMT when N_m moles of methanol have evolved is given by

$$2N_A \left[\left(\frac{N_{A_0}}{N_A} \right)^{0.5} - 1 \right] + 2(N_A - N_{A_0}) + N_m = 0 \quad (X-18)$$

Eq. (X-18) which is obtained from Eqs. (X-10) and (X-17).

B. Testing of the Molecular Species Model

The adequacy of the molecular species model, Eq. (X-16) was tested by the integral method. In this case, as for the oligomerization model, the integral in Eq. (X-19)

$$Y(N_m) = \int_0^{N_m} \frac{dN_m}{y(N_m)} = k_a' t \quad (X-19)$$

where

$$y(N_m) = N_B(N_A + 0.5N_R) / V^2 \quad (X-20)$$

was evaluated by Simpson's rule using a suitable step size and double precision arithmetic. Equation (X-20) is a function of N_m , the amount of methanol produced up to time t , since N_A , N_B , N_R and V are functions of N_m , which are given by Eqs. (X-18), (X-9), (X-10) and (IX-8), respectively. Newton's algorithm was used in locating the root of Eq. (X-18), namely N_A , required in evaluating $y(N_m)$ of Eq. (X-20). As in the case of the oligomerization model, the numerical techniques used were very satisfactory

and efficient. Testing of the molecular species model was carried out using only isothermal data (Appendix D).

The results of the application of the molecular species model to Fontana's isothermal data are shown in Fig. X.1, in which integral values are plotted against time. The line drawn in this figure is the least squares line

$$Y (N_m) = \hat{\beta}_0 + \hat{\beta}_1 t \quad (X-21)$$

for which some statistics are given in Table X.1. It is clearly evident that the residuals do not show any significant trends and, therefore, the least squares analysis is valid. Since the intercept is not significantly different from zero at 0.01 probability level, Fontana's data are described very well by the competitive, consecutive model assumed for the transesterification reactions.

Figure X.2 shows integral values of the molecular species model plotted against time for Tomita and Ida's set #1. Very significant correlations resulted from the application of this model to the four sets of Tomita and Ida's data, for which some statistics are given in Table X.1. Analysis of residuals showed no significant trends, and since the intercepts are not significantly different from zero the series-parallel model fitted the data extremely well. The line in Fig. X.2 is the least squares line according to Eq. (X-21).

In Fig. X.3 integral values of the molecular species model applied to Peebles and Wagner's data are plotted against time. The figure clearly shows that these values vary linearly with time and least squares analysis confirmed this evidence. Some statistics are given in Table X.1, which show that the intercept of the least squares line is not significantly

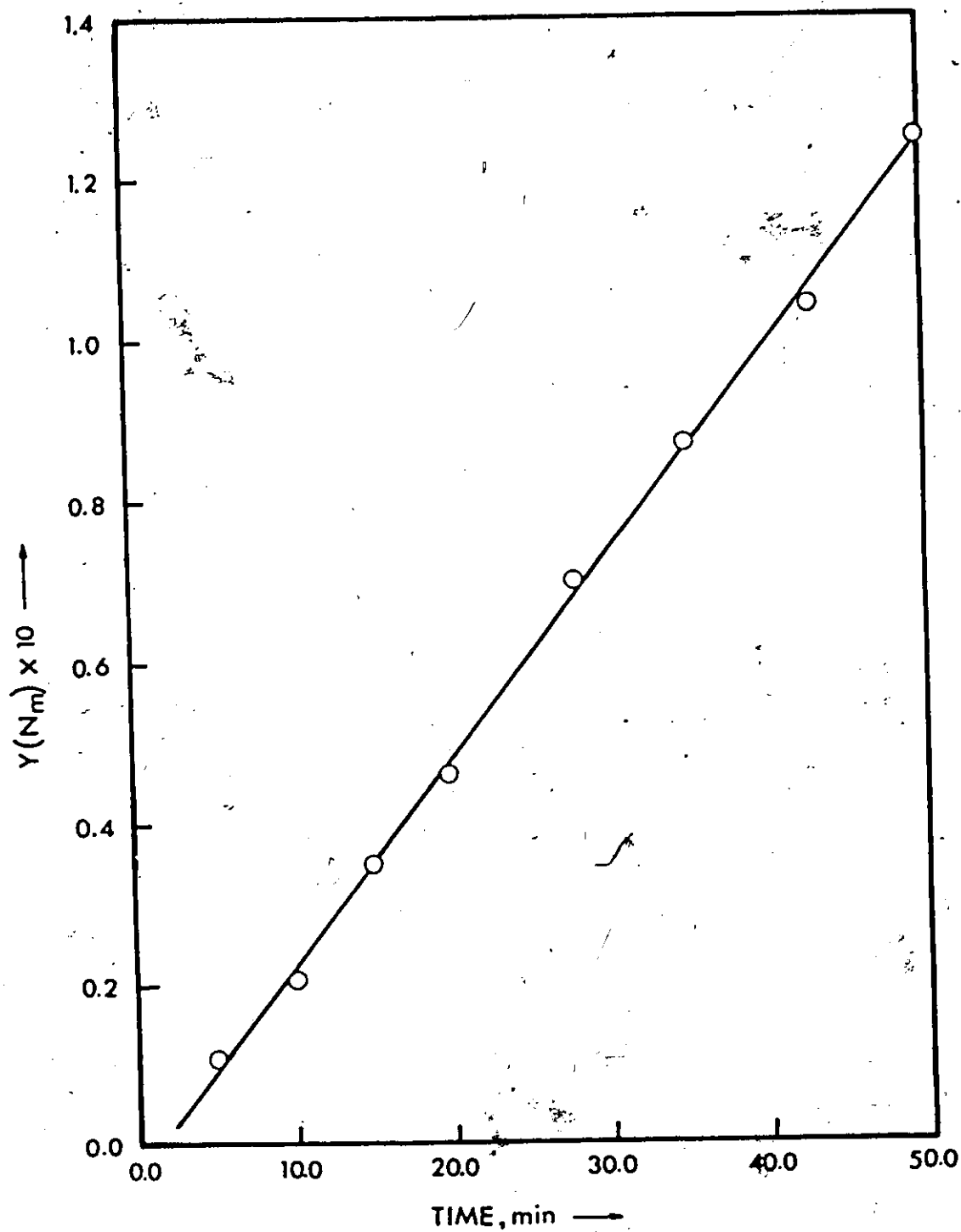


Fig. X.1 Molecular Species Model Applied to Fontana's Data

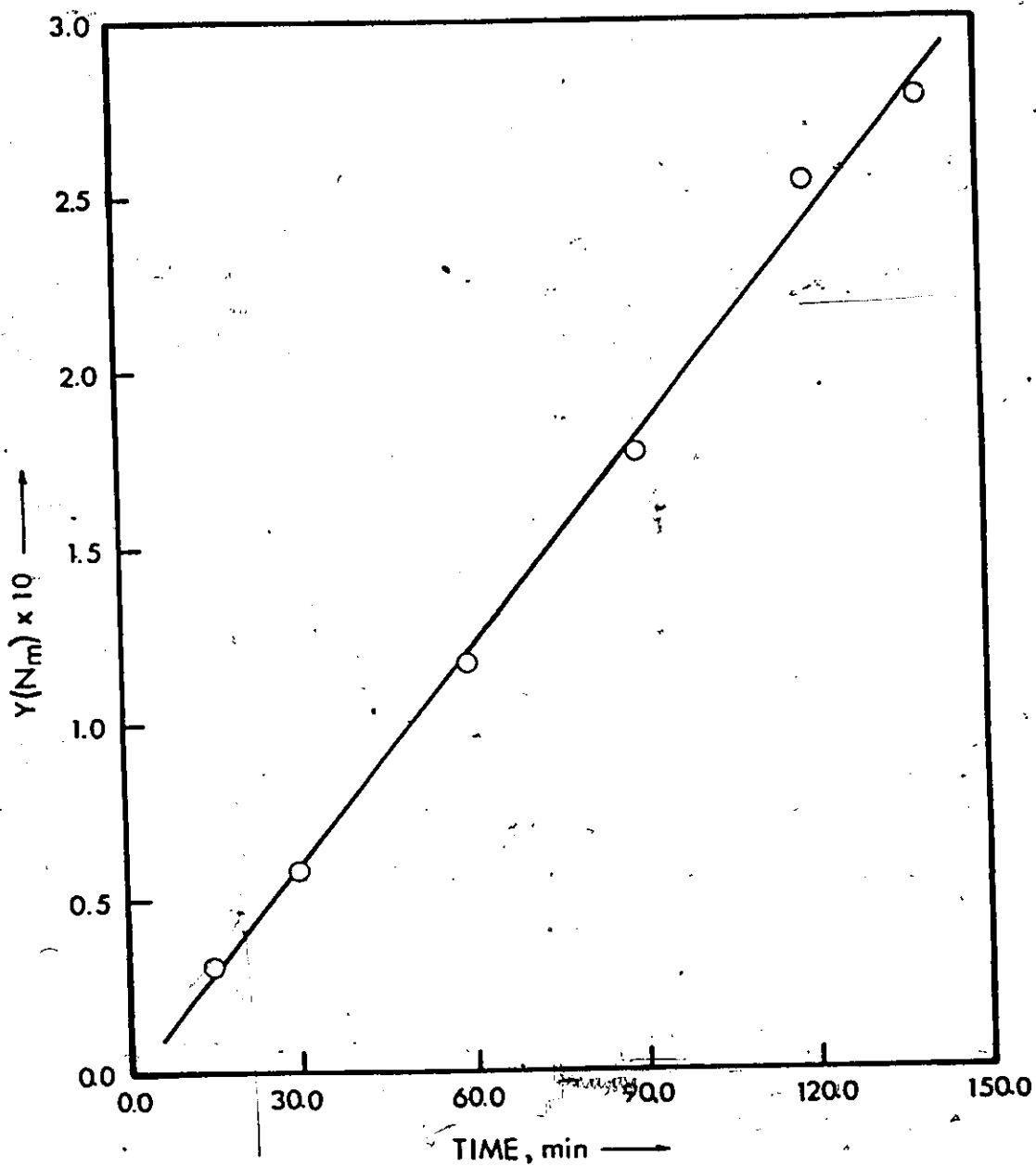


Fig. X.2 Molecular Species Model Applied to Tomita and Ida's Data

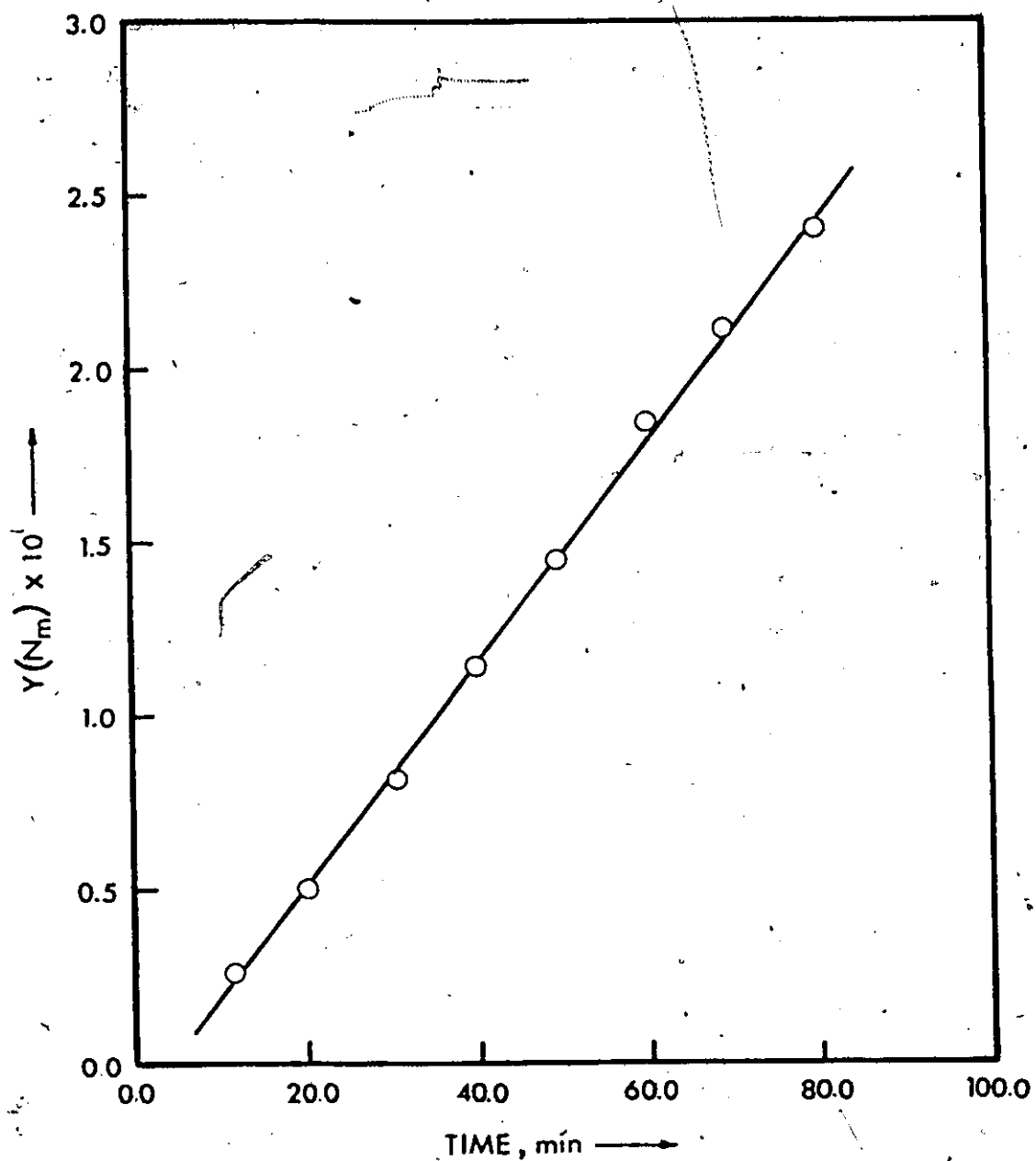


Fig. X.3 Molecular Species Model Applied to Peebles and Warner's Data

different from zero at 0.001 probability level.

The statistics given in Table X.1 and the fact that the assumed model was tested up to about 88% conversion of methyl-ester groups, with Tomita and Ida's and Peebles and Wagner's data, show that the molecular species model adequately describes the DMT transesterification data. Since the model fits the data values for the apparent rate constants, k_a' , which are the slopes of the least squares lines, and for the true rate constants, k_1 , are given in Table X.2. The estimates for the true rate constants are very good and the agreement between the values estimated from Fontana's and Tomita and Ida's data at 180°C is excellent.

The activation energy for the zinc acetate catalyst was estimated to be 8.6 Kcal/mol by fitting the Arrhenius equation to the average values of the true rate constant at 180 and 190°C. The Arrhenius equation of k_1 for zinc acetate is given by the following equation

$$\ln k_1 = -\frac{4335.5}{T} + 10.840 \quad (X-22)$$

The preceding analysis clearly shows that the model assumed for methanol production, namely the model given by equation (X-16), which was derived from a competitive, consecutive model for the monomer ester interchange reactions, along with the product distribution equations, i.e., Eqs. (X-18), (X-9) and (X-10), is, in the light of the available experimental data, an adequate model to describe the kinetics of the transesterification reactions between dimethyl terephthalate and ethylene glycol.

C. Product Distribution

It was mentioned earlier that the molecular species model would

TABLE X.1
Statistics for the
Molecular Species Model

Data	Degrees of Freedom	F-Value	Student's t for β_0
Fontana	6	4357.0 ^a	-2.892
Tomita & Ida #1	4	1089.2 ^a	-0.413
Tomita & Ida #2	4	1801.2 ^a	-0.210
Tomita & Ida #3	5	1951.1 ^a	0.403
Tomita & Ida #4	3	561.3 ^a	0.379
Peebles & Wagner	6	5379.6 ^a	-5.359 ^b

a Very highly significant

b Not significant at 0.001 probability level

TABLE X.2

Rate Constants for
the Molecular Species Model

Data	Catalyst		Reaction Temperature (°C)	Apparent Rate Constant ($k_a \times 10^3$)	True Rate Constant (k_1), $1^2 \text{mole}^{-2} \text{min}^{-1}$
	Compound	Mass (Moles $\times 10^4$)			
Fontana	Zinc Acetate	1.81	180	2.5535	3.527
Tomita & Ida #1	Zinc Acetate	1.00	197	2.0370	5.093
Tomita & Ida #2	Zinc Acetate	0.70	197	1.4187	5.067
Tomita & Ida #3	Zinc Acetate	0.50	197	0.98768	4.938
Tomita & Ida #4	Zinc Acetate	1.00	180	1.4372	3.593
Peebles & Wagner	Zinc Acetylacetonate	5.51	175	3.1787	1.442

generate information on product distribution which could not be furnished by the methyl-ester group model. This information is easily obtained from the model and the appropriate product distribution and material balance equations. Figure X.4 illustrates the product distribution for the experimental conditions of Tomita and Ida's set #1 as given in Appendix D.

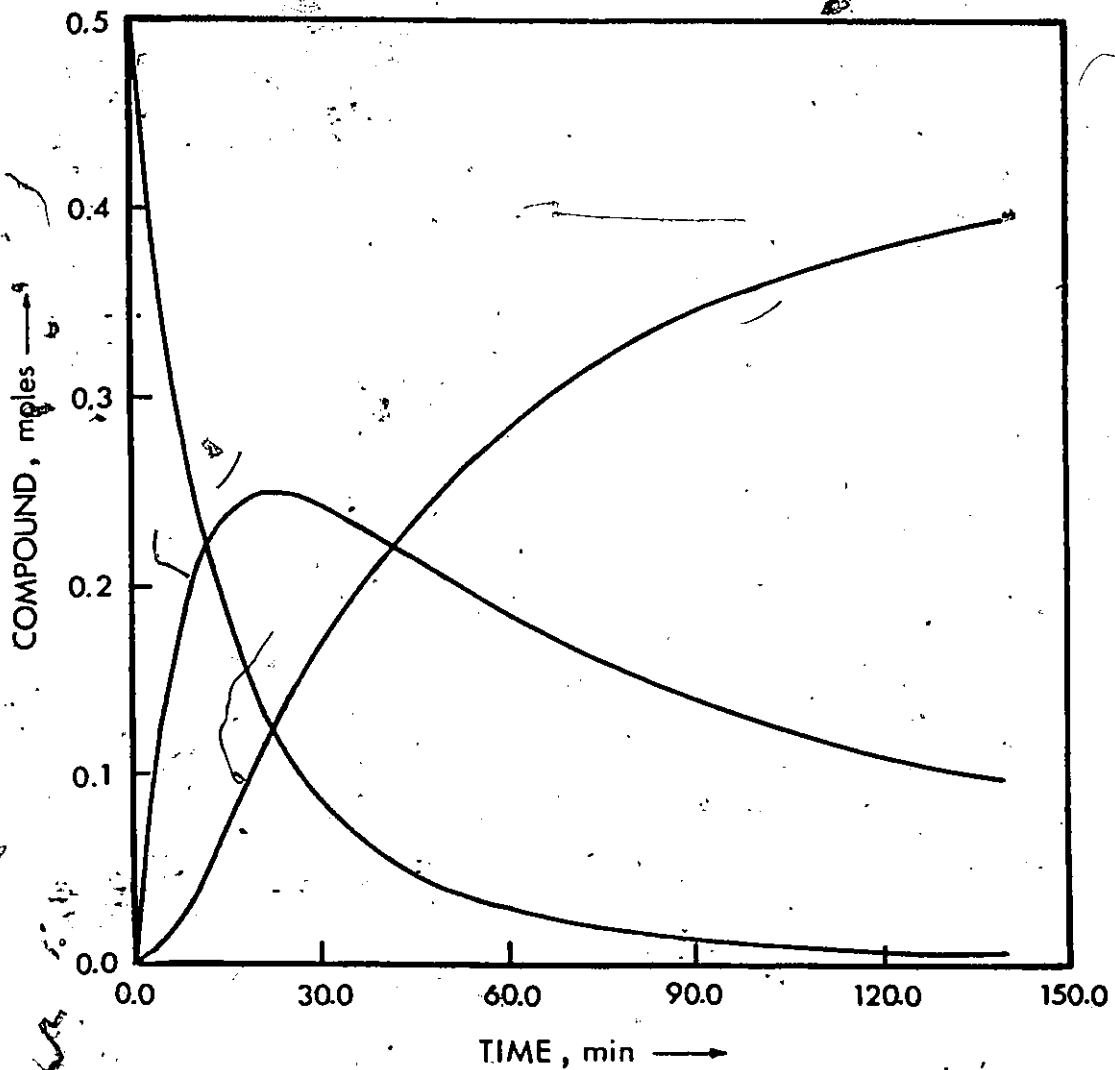


Fig. X.4 Product Distribution (Curves 1, 2, 3 are DMT, MHET and BHET Profiles, respectively)

XI DISCUSSION and CONCLUSIONS

In Ch. VI it was concluded that the transesterification of dimethyl terephthalate catalyzed by Amberlyst 15 is, at the temperature of 146°C, an unselective and inefficient process. This lack of selectivity is brought about by the products of ethylene glycol side reactions which are promoted by the cation exchange resin. Water, an EG dehydration product, hydrolyzes esters while 2-methoxyethanol and oligomers of ethylene glycol actively participate in transesterification and, perhaps, esterification reactions yielding undesirable esters of terephthalic acid. Undesirable products formed to an extent significant enough to warrant discontinuation of the experimental investigation.

On the other hand, investigators of the kinetics of the transesterification reactions catalyzed by homogeneous catalysts and in the temperature range of 175 to 197°C have neither reported ethylene glycol by-products nor obtained data on product distribution. It has been inferred that homogeneous catalysts do not promote EG dehydration, etherification and polymerization reactions to any significant extent. In other words, homogeneous catalysts do not give rise to EG by-products which could transesterify methyl-ester groups producing undesirable terephthalic acid esters.

Therefore, the major difference in the selectivity of Amberlyst 15 and homogeneous catalysts is the extent to which ethylene glycol by-product formation is promoted. Amberlyst 15 is not a selective catalyst while homogeneous catalysts are selective.

The findings of the present study lead to the statements given below where it is recalled that the terms transesterification reactions and pre-

condensation stage reactions are interchangeably used and refer to the reactions which take place during the production of bis-(2-hydroxyethyl) terephthalate from dimethyl terephthalate and ethylene glycol. The latter two compounds are the reactants and are identified by the subscripts A and B, respectively. Subscripts m and R stand for methanol and methyl-(2-hydroxyethyl) terephthalate, respectively, which are two products of the transesterification reactions.

- A. A critical analysis of previously proposed models for the kinetics of the precondensation stage reactions in the presence of homogeneous catalysts showed that they are inadequate.
- B. A study of the transesterification reactions catalyzed by the resin Amberlite IR-120(H⁺ form) showed that the distillate data could be described by the model

$$-\frac{1}{W} \frac{dN_A}{dt} = k C_A C_B \quad (\text{III-6})$$

where the rate constant, k , at the reaction temperature of 142°C, was found to be equal to $3.3 \times 10^{-6} \text{ l}^2/(\text{mole})(\text{min})(\text{g resin})$.

- C. Chemical analysis of the liquid transesterification product was achieved by gas-liquid chromatography after hydroxy compounds were silylated. The quantitatively determined compounds were EG, diethylene glycol, DMT, BHET, and MHET. An experimental procedure for preparing the latter compound was established. The distillate was also quantitatively analyzed for methanol by GLC.

D. A differential recycle reactor was designed and built specifically for this experimental investigation, and, upon testing, was found to operate very smoothly.

E. A mathematical analysis of the differential recycle reactor operated with on-off control of the outlet stream showed that the reactor

1. comes to steady state for irreversible reactions of first and second order,
2. gives rise to a steady state concentration which is equal to that of a continuously operated reactor with the same catalyst mass to feed flow rate ratio,
3. exhibits, in the transient regime, concentration fluctuations the magnitude and frequency of which depend on the ratio of accumulation to discharge time intervals, and
4. has a transient response that lies in between the response of continuously operated reactors with fluid volumes equal to its minimum and maximum volume.

F. The batch reactor transesterification data obtained in the presence of Amberlyst 15 and at the temperature of 146°C did not lead to meaningful mass balances and showed that

1. intraparticle diffusion effects are significant at the reaction temperature and for the resin particle sizes commercially available,
2. dehydration of ethylene glycol is greatly promoted by the cation exchanger. The ethylene oxide, which is likely produced, initiates other reactions which, in total, convert about one third of initial glycol to undesirable products.

3. the ethylene glycol by-products participate in ester interchange reactions and convert a significant fraction of DMT to unwanted esters
 4. the water produced by EG dehydration hydrolyzes esters yielding free carboxylic groups, and,
 5. therefore, the transesterification of dimethyl terephthate with ethylene glycol is, at the aforementioned experimental conditions, an unselective and inefficient process.
- G. Analysis of the kinetics of the transesterification reactions, in the presence of some homogeneous catalysts and in the temperature range of 175°C to 197°C, showed that
1. oligomerization reactions do not proceed to any significant extent, and
 2. the reactivity of hydroxyl groups on half-esterified glycol is negligibly small when compared with the reactivity of the same groups on free ethylene glycol.
- H. Statistical analysis showed that
1. the methyl-ester group model i.e., the rate expression given by Eq. (IX-20)

$$-\frac{dN_E}{dt} = 2k_1 N_C C_E C_B \quad (\text{IX-20})$$

where subscripts C and E refer to catalyst and methyl-ester group, respectively, adequately describes the experimental transesterification data obtained in the presence of some homogeneous catalysts, and

2. the Arrhenius equation for zinc acetate catalyst is

$$\ln k_1 = - \frac{4306.2}{T} + 10.777 \quad (\text{IX-19})$$

with an activation energy of 8.6 Kcal/mole.

- I. Statistical analysis showed that

1. the molecular species model, i.e., the rate expression given by Eq. (X-16)

$$\frac{dN_m}{dt} = k'_a N_b (N_A + 0.5N_R)/V^2 \quad (\text{X-16})$$

where $k'_a = 4 k_1 N_C$ and

$$N_R = 2N_A \left[\left(\frac{N_A^0}{N_A} \right)^{0.5} - 1 \right] \quad (\text{X-17})$$

is an adequate model for the kinetics of the transesterification reactions in the presence of some homogeneous catalysts,

2. the Arrhenius equation for zinc acetate catalyst is

$$\ln k_1 = - \frac{4335.5}{T} + 10.840 \quad (\text{X-22})$$

with an activation energy of 8.6 Kcal/mole, and

3. the molecular species model provides information about product distribution which is not available from the methyl-ester group model.

REFERENCES

1. Process Scan, Brit. Chem. Eng., 14, (February, 1969).
2. New Polyester-Fiber Footings, Chem. Eng., May 3, 1971, p.44.
3. Chem. Eng., July 27, 1970, p.80; Nov.30, 1970, p.18.
4. Isagulyants, V.I., Chem. Abst., 55, 11354d.
5. Vilenchich, R., Technika, 21 (1-4), 322(1966).
6. Kirk-Othmer Encyclopedia of Chemical Technology, 2nd ed., 16, p.144, Interscience Publishers, New York, (1968).
7. Wilfong, R.E., Linear Polyesters, J. Polymer Sci., 54, 385 (1961).
8. Challa, G., Ester Interchange Equilibria from Dimethyl Terephthalate and Ethylene Glycol, Rec. Trav. Chem. Pays-bas, 79, 90 (1960).
9. Griehl, W. and Schnock, G., Zur Katalyse der Polyesterbildung durch Esteraustausch, Faserforsch. Textiltech., 8, 408 (1957).
10. Levenspiel, O., Chemical Reaction Engineering, p.69, J. Wiley & Sons, New York (1962).
11. Mihail, R., Istratoiu, R., Lupu, Al. and Georgescu, E., Acad. rep. populare Romine, studii Cercetari Chem., 1958, pp.161-83.
12. Peebles, L. H., Jr., and Wagner, W.S., The Kinetic Analysis of a Distilling System and its Application to Preliminary Data on the Transesterification of Dimethyl Terephthalate by Ethylene Glycol, J. Phys. Chem., 63, 1206 (1959).
13. Fontana, C. M., Polycondensation Equilibrium and the Kinetics of the Catalyzed Transesterification in the Formation of Polyethylene Terephthalate, J. Polymer Sci., 6, Part A-1, 2343 (1968).
14. Smith, J. M., Chemical Engineering Kinetics, 2nd ed., p.52, McGraw-Hill, New York, (1970).
15. Kramers, H., and Westerterp, K. R., Elements of Chemical Reactor Design and Operation, p.224, Chapman and Hall, London, (1963).
16. Yampol'skaya, M. A., Abloy, A. V., Daydova, S. L. and Platé, N. A., Catalytic Properties of Acetyl-acetonates of Certain Metals in the Transesterification Reaction, Kinetika i Kataliz, 10, No.6, 1382 (1965)(English Transl).
17. Sorokin, M. F. and Chebotareva, N. A., Transesterification of the Dimethyl Esters of Terephthalic Acid by Ethylene Glycol, Tr. Mosk. Khim.-Tekhnol. Inst. 1969, No. 61, 103.

18. Tomita, K. and Ida, H., Studies on the Formation of Poly(ethylene) Terephthalate: 2. Rate of Transesterification of Dimethyl Terephthalate with Ethylene Glycol, Polymer, 14, 55 (Feb. 1973).
19. Vilenchich, R. and Yamanis, J., Kinetics of the Transesterification of Dimethyl Terephthalate with Ethylene Glycol in the Presence of Amberlite IR-120, Can. J. Chem. Eng., 50, 538 (1972).
20. Yamanis, J., Adelman, M. and Vilenchich, R., GLC of Silylated Glycols and Terephthalic Acid Esters, J. Chrom., in Print.
21. Pierce, Alan E., Silylation of Organic Compounds, Pierce Chemical Co., Rockford, Ill. (1968).
22. Sprung, M. M. and Nelson, L. S., Trimethylsilyl Derivatives of Polyols, J. Org. Chem., 20, 1750 (1955).
23. Tornquist, J., Quantitative Analysis of Polyethylene Glycols by Gas Chromatography after Silylation, Acta Chem. Scand., 21, 2095 (1967).
24. Pollard, F. H., Nickless, G. and Uden, P.C., The Application of Gas Chromatography to the Determination of Retention Data of Some Trimethylsilyl Ethers and Trimethylsilyl Thiethers, J. Chrom., 11, 312 (1963).
25. Kudrna, M. and Pavelcova, V., Připrava Dimethyltereftalátu Reesterifikací β, β' -bis-Hydroxyethyltereftalátu Metanolem, Chem. Promysl, 14, (1), 12 (1964).
26. Zahn, H. and Krzikalla, R., Synthese von einheitlichen, linearen Oligoestern vom Poly-glykol-terephthalat-typ, Makromol. Chem., Promysl, 23, 31 (1957).
27. Ettre, L. S. and Zlatkis, A., The Practice of Gas Chromatography, p. 390, Interscience Publishers, New York (1967).
28. Kun, K. A. and Kunin, R., Pore Structure of Some Macroreticular Ion Exchange Resins, Pol. Letters, 2, 587 (1964).
29. Dohse, H., Z. Phys. Chem., Abt. B, 5, 131 (1929); 6, 343 (1930).
30. Hougen, O. A., Reaction Kinetics in Chemical Engineering, Chem. Eng. Monograph Series No. 1, 47, 41 (1951).
31. Perkins, T. K. and Rase, H. F., An Improved Experimental Reactor for Applied Kinetic Studies, A.I.Ch.E. Journal, 4, No. 3, 351 (1958).
32. Boreskov, G. K., Kinetika i Kataliz, 3, 416 (1962) (English Transl.).
33. Korneichuk, G. P., Kinetika i Kataliz, 3, 454 (1962) (English Transl.).

34. Butt, J. B., Bliss, H. and Walker, C. A., Rates of Reaction in a Recycling System-Dehydration of Ethanol and Diethyl Ether, A.I.Ch.E. Journal, 8, No. 1, 42 (1962).
35. Levenspiel, O., op. cit., p.453.
36. Petukhov, B. V., The Technology of Polyester Fibres, p.7, Macmillan, New York (1963).
37. Perry, J. H., Chemical Engineers' Handbook, 4th ed., p. 3-199, McGraw-Hill, New York (1963).
38. Hibbert, H. and Perry, S. Z., Studies of Reactions Relating to Carbohydrates and Polysaccharides. LXI. The Mechanism of Polymerization of Ethylene Oxide, J. Am. Chem. Soc., 62, 2601 (1940)
39. Yamanis, J. and Vilenchich, R., Transient Response of a Differential Recirculation Reactor Subject to Linear Variations of Volume, Chim. Ind. (Milan) In Print.
40. Cunningham, W. J., Introduction to Non-linear Analysis, p.66, McGraw-Hill, New York (1958),
41. Flory, P.J., Principles of Polymer Chemistry, pp.69-105, Cornell University Press, Ithaca (1953).
42. Frost, A. A. and Pearson, R. G., Kinetics and Mechanism, pp.178-184, J. Wiley, New York (1961).
43. Flory, P. J., op. cit., p. 72
44. Lapidus, L., Digital Computation for Chemical Engineers, p. 288, McGraw-Hill, New York (1962).
45. Dixon, W. J., BMD Biomedical Computer Programs X-Series Supplement, pp. 176-186, University of California Press,
46. Challa, G., The Formation of Polyethylene Terephthalate by Ester Interchange. I. The Polycondensation Equilibrium, Makromol. Chem., 38, 105 (1960).
47. Acton, F. S., Analysis of Straight-Line Data, pp.226-8, J. Wiley, New York (1959).
48. Lapidus, L., op. cit., p. 49
49. Weast, R. C., ed., Handbook of Tables for Mathematics, 3rd ed., pp. 539-545, The Chemical Rubber Company, Cleveland (1967).

NOMENCLATURE

a ..	-constant	
A ..	-chemical species	
	-DMT	
	-area	counts
	-integration constant	
b ..	-proportionality factor	
	-constant	
B ..	-EG	
C ..	-chemical species concentration	moles/l
	-catalyst mass	moles
C _v ..	-valve flow coefficient	
d ..	-distillate mass	g
D ..	-capillary diameter	ft
	-integration constant	
e ..	-constant	
E ..	-methyl-ester group	
f ..	-response factor	
F ..	-mass flow rate	moles/min
g ..	-constant	
G ..	-specific gravity	
k ..	-rate constant	
k' ..	-rate constant	
K ..	-polycondensation equilibrium constant	
l ..	-liquid sample mass	g
L ..	-batch reactor mass	g
L ..	-batch reactor mass	g
	-capillary length	

m ..	-methanol	
	-chemical species mass	g
M ..	-initial molar ratio of EG to DMT	
	-initial ratio of EG moles to methyl- ester group equivalents	
n ..	-number of cycles	
N ..	-chemical species mass	moles
	-functional group number	equivalents
P ..	-pressure	lbs/sq ft
	-2-hydroxyethyl group	
Q ..	-volumetric rate of flow	cu. ft./sec
r ..	-reaction rate	moles/(min)(g-resin)-
R ..	-monomer or polymer molecule	
	-MHET	
	-peak area ratio	
S ..	-BHET	
	-component mass withdrawn by sampling	moles
t ..	-time	min
T ..	-absolute temperature	°K
	-constant $\tau_o / (\tau_o + t_a)$	dimensionless
v ..	-molar volume of methanol	l
	-feed flow rate	l/min
V...	-reactor volume	l
w ..	-mass fraction	
W ..	-mass of cation exchange resin	g
x ..	-DMT conversion, $(N_{A_o} - N_A) / N_{A_o}$	

-methyl-ester group conversion, $(N_{E_0} - N_E) / N_{E_0}$

Subscripts

- a .. -accumulation
- apparent
- A .. -DMT
- B .. -EG
- c .. -cycle
- C .. -catalyst
- d .. -discharge
- e .. -equivalents of ethylene glycol
- E .. -methyl-ester group
- f .. -quantity at complete conversion
- g .. -2-hydroxyethyl-ester
- i .. -component index
- j .. -sample index
- m .. -methanol
- methyl-ester
- n .. -cycle index
- R .. -MHET
- s .. -internal standard
- x .. -chemical species
- o .. -base or initial quantity
- index
- 1 .. -index
- 2 .. -index
- 3 .. -index

Superscripts

- f .. -outlet conditions
 o .. -inlet conditions
 ' .. -identification symbol

Greek Letters

- α .. -constant
 .. -ratio of catalyst mass to feed flow rate (g-resin)(min)/l
 β .. -regression coefficient
 .. -ratio of accumulation to discharge time intervals
 .. -constant
 γ .. -constant
 Δ .. -difference
 ϵ .. -fractional change in volume
 θ .. -constant
 .. -temperature °C
 κ .. -rate constant ratio
 μ .. -viscosity lb_m/(ft)(sec)
 ρ .. -density
 σ .. -standard deviation
 τ .. -reactor residence time
 ϕ .. -partial yield, $-(N_x - N_{x_0}) / (N_A - N_{A_0})$

APPENDIX A
GAS CHROMATOGRAPHIC ANALYSIS
CALIBRATION DATA

Calibration curves for the liquid product compounds, namely, ethylene glycol, diethylene glycol, dimethyl terephthalate, methyl-(2-hydroxyethyl) terephthalate, and bis-(2-hydroxyethyl) terephthalate, were established using four synthetic mixtures. The composition of these mixtures was a randomly chosen combination of the four preassigned levels of each compound: Two of the four levels were the extremes of the chosen range for the compound while the other were each about half way from the midrange and one extreme. These samples were dissolved in 5 ml of solvent and aliquots of the resulting solutions were taken for silylation. Silylated solutions were sampled with a 5 μ l syringe, precleaned by means of a syringe cleaner, and chromatographed according to the procedure given in Chapter IV. Each chromatogram yielded individual peak areas in terms of integration module counts from which the component to internal standard peak area ratios were calculated. The component mass levels and the corresponding peak area ratios are given in Tables A.1 and A.2.

The calibration curve for methanol was established using replicated chromatograms at three methanol mass levels. The calibration data are given in Table A.3.

TABLE A.1.
GLC Calibration Data

Ethylene Glycol		Diethylene Glycol		Dimethyl Terephthalate	
Mass, g	Area Ratio	Mass, g	Area Ratio	Mass, g	Area Ratio
0.1098	0.678	0.0102	0.165	0.1091	0.824
	0.666		0.160		0.844
	0.677		0.164		0.831
0.0524	0.323	0.0201	0.314	0.0546	0.416
	0.344		0.322		0.407
	0.355		0.337		0.410
0.0265	0.159	0.0275	0.422	0.0286	0.214
	0.162		0.428		0.212
	0.165		0.424		0.217
	0.166		0.425		0.203
	0.159		0.423		0.202
	0.161		0.430		0.200
	0.169		0.436		0.203
	0.160		0.426		0.202
0.1293	0.797	0.0051	0.083	0.1401	1.063
	0.819		0.083		1.057
	0.812		0.079		1.066
	0.838		0.088		1.082
	0.851		0.080		1.072
	0.829		0.089		1.076
	0.860		0.086		1.081
	0.829		0.090		1.077
			0.079		

TABLE A.2
GLC Calibration Data

Methyl-(2-Hydroxyethyl) Terephthalate		Bis-(2-Hydroxyethyl) Terephthalate	
Mass, g	Area Ratio	Mass, g	Area Ratio
0.1091	0.940	0.0569	0.514
	0.985		0.559
	0.965		0.537
0.0543	0.476	0.1069	0.971
	0.479		1.020
	0.482		0.928
0.0296	0.272	0.0315	0.308
	0.265		0.274
	0.286		0.335
	0.268		0.291
	0.264		0.295
	0.263		0.283
	0.264		0.279
0.260	0.264		
0.1280	1.097	0.1317	1.222
	1.124		1.273
	1.101		1.253
	1.128		1.261
	1.105		1.219
	1.068		1.148
	1.082		1.191
	1.117		1.262
1.109	1.227		

TABLE A.3

Methanol Calibration Data

Mass, g	Area Ratio
0.2387	0.967
	1.007
	0.979
0.1971	0.811
0.1591	0.677
	0.658
	0.650
	0.657

APPENDIX B

FEED FLOW SET-UPS

At first the simple and inexpensive method of pressurizing the feed tank with nitrogen was used to supply the driving force in the feed flow system, a schematic of which is shown in Fig. B.1. A fine metering valve (Nupro^R "S" series, $C_v = 0.004$, 0.031 in. orifice diameter), installed just upstream of the rotameter, was used as the flow control element. When this set-up was tested, it was found totally inadequate due to gas bubbles which frequently traversed the rotameters and made flow setting impossible. The gas bubbles presumably were nitrogen gas which desorbed at the fine metering valve across which a significant pressure drop developed.

It was then decided that the reactants would have to be pumped or constant head tanks should be used to provide the driving force. The latter system would still require pumps for maintaining a constant liquid level, so the former system was chosen, since it required less money and time to set up.

Information about metering pumps showed that these pumps would give rise to pulsating flows, and they were not considered further due to the unknown effects of feed pulsations on the behaviour of the recycle reactor. Pumps which, therefore, could be used were either centrifugal or gear pumps. However, the capacity of the latter pumps was much higher than the required flow rates and this led to the decision to set up by-pass loops from which the feed streams would be taken. This decision was based on the assumption that the delivery end of the pump would, under good temperature control, have stable pressure. Centrifugal pumps were

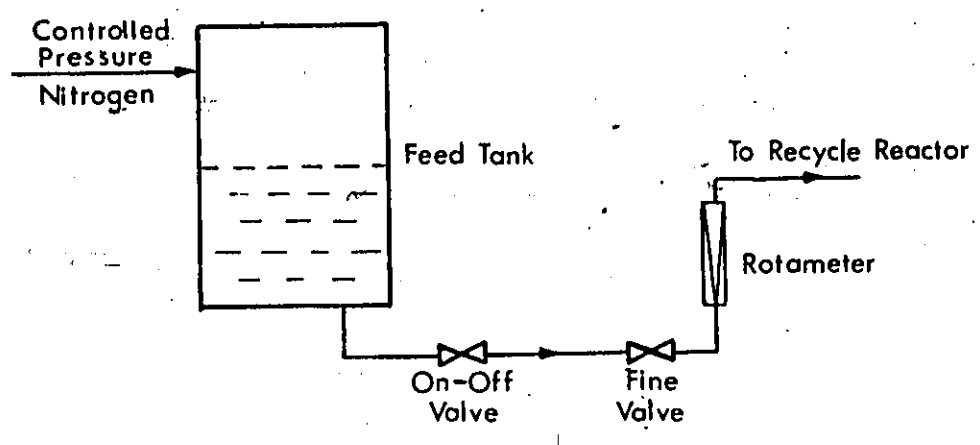


FIG. B.1 Pressurized Tank Feed System

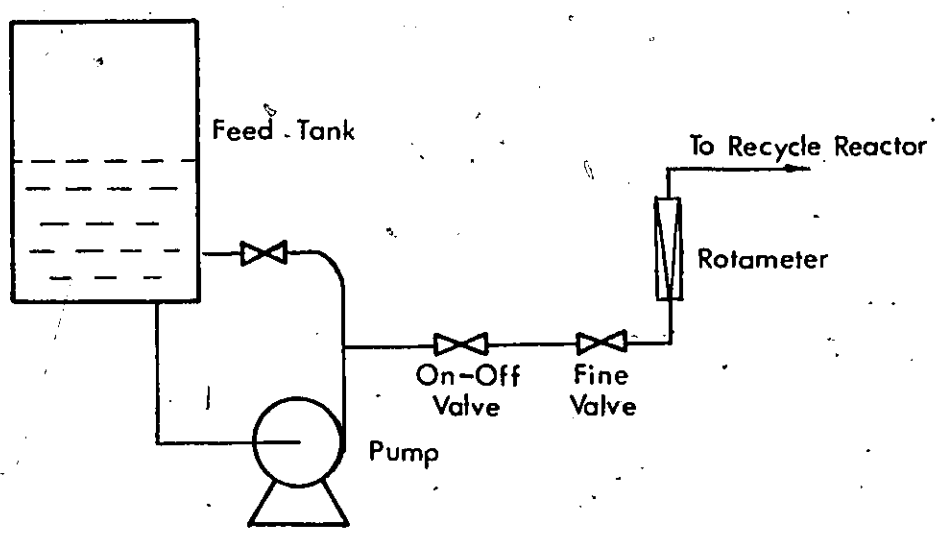


Fig. B.2 By-Pass Loop Feed System

procured, and the feed arrangement shown in Fig. B.2 was set up and tested.

When this feed system was tested with distilled water at room temperature it was found to regulate the flow down to 2.5 g/min very well. However, when it was tested with glycol at 120°C, the flow rate was found to decrease continuously, even after prolonged testing which should have removed transient temperature effects. Trouble-shooting attempts were then aimed at locating the causes of instability, and after lengthy experimentation they were found to be associated with a changing valve orifice and unstable pressure head at the by-pass loop. The variation of the fine metering valve orifice size was presumably caused by deposition of microscopic particles suspended in the feed (the low flow velocity could not sweep them away) and transient temperature effects. The findings of this work suggested that a new, improved feed flow system had to be designed.

The pressure instability could be removed by either installation of a pressure fluctuation damping device in the by-pass loop or by using constant head tanks. The latter solution was chosen since unknown factors in the former gave rise to doubts about its suitability. The problems associated with the flow control element could be eradicated by filtering the fluids and using a new flow control element whose temperature would be regulated by a thermostated bath. The flow control element was to be a composite one made from a new fine metering valve with larger orifice diameter and a piece of glass capillary tubing in series.

APPENDIX C
EXPERIMENTAL DATA

1. Preliminary Data for Amberlite IR-120

The experimental methanol data obtained from transesterification of dimethyl terephthalate with ethylene glycol in the presence of Amberlite IR-120 are given in Table C.1. This table also gives the amounts of reactants and resin used in the corresponding runs.

2. Batch Reactor Data for Amberlyst-15

The experimental data for the batch reactor runs using Amberlyst 15 are given in Tables C.2 through C.8. These tables give the amount of distillate in grams collected between successive sampling times, the liquid sample withdrawn in grams, the solvent volume (as defined in subsection 1 of Ch. IV) used to dissolve the liquid sample, and the peak area ratios for the various components obtained from the gas liquid chromatography of the samples.

The above experimental data were used to calculate the moles of any component converted by reaction, from which the component profiles given in Tables C.9 through C.12 were calculated. The calculations were developed on the assumption that the five components, ethylene glycol (EG), diethylene glycol (DEG), dimethyl terephthalate (DMT), methyl-(2-hydroxyethyl) terephthalate (MHET) and bis-(2-hydroxyethyl) terephthalate, were withdrawn from the reactor only by liquid sampling for which corrections were applied as follows.

The mass m_{ij} of the i th component in the j th sample was obtained from the reverse of the calibration equation (Eq. IV-6), i.e.,

TABLE C.1

Transesterification Data with Amberlite IR-120

$N_{A_0} = 0.2, M = 2$ $W = 18.39 \text{ g}$		$N_{A_0} = 0.2, M = 2.5$ $W = 19.63 \text{ g}$		$N_{A_0} = 0.2, M = 3$ $W = 21.08 \text{ g}$		$N_{A_0} = 0.2, M = 3.5$ $W = 24.21 \text{ g}$	
Time (min)	Methanol (g)	Time (min)	Methanol (g)	Time (min)	Methanol (g)	Time (min)	Methanol (g)
5.3	0.466	4.5	0.415	4.8	0.369	4.0	0.4009
10.9	0.791	9.9	0.870	8.5	0.774	8.1	0.7962
17.4	0.191	15.1	1.248	14.0	1.286	12.0	1.3133
24.0	1.583	18.0	1.593	18.0	1.533	16.0	1.5614
30.1	1.992	26.2	1.993	24.5	1.934	21.6	2.0174
37.8	2.372	32.0	2.398	31.0	2.374	26.2	2.3779
45.9	2.786	39.9	2.786	34.0	2.715	32.0	2.7516
56.0	3.241	48.0	3.222	42.5	3.183	38.2	3.1688
64.1	3.473	55.8	3.563	48.1	3.527	43.9	3.5715
		64.2	4.021	56.5	3.866	50.5	3.9449
						58.5	4.3583
						67.0	4.7104

$$m_{ij} = \frac{1}{\beta_i} \cdot R_{ij} V_j \quad (C-1)$$

where β_i is the regression coefficient of the calibration line (Ch. IV), $R_{ij} = A_{ij}/A_{sj}$ is the peak area ratio and V_j is the solvent used in dissolving the sample. Then the mass fraction, w_{ij} , of component i in the j th sample is

$$w_{ij} = m_{ij}/l_j \quad (C-2)$$

where l_j is the mass of the j th liquid sample. The reactor mass, L_j , at time t_j is

$$L_j = L_1 - \sum_{k=1}^j d_k + \sum_{k=1}^{j-1} l_k \quad (C-3)$$

where d_k is the distillate sample; d_1 and L_1 are equal to zero at time $t_1=0$ and L_1 is the initial reactor mass equal to the sum of the DMT and EG mass weighed. Then, the moles, N_{ij} , of component i at the j th sampling point is

$$N_{ij} = L_j w_{ij} / M_i \quad (C-4)$$

where M_i is the molecular weight of the i th component and the moles converted by reaction are

$$\Delta N = N_{ij} - N_{i1} + S_{ij-1} \quad (C-5)$$

where S_{ij} , the correction for component depletion due to liquid sampling, is given by:

$$S_{ij-1} = \sum_{k=1}^{j-1} l_k w_{ik} / M_i \quad (C-6)$$

Then, the true mole profile TN_{ij} for component i , that is, the mole

profile due to reaction, at time t_j is

$$TN_{ij} = N_{i1} + \Delta N_{ij} \quad (C-7)$$

where N_{i1} is the number of moles of component i initially present in the reactor. The values given in Tables C.9 through C.12 are the true mole profiles. The above corrections were considered desirable in order to avoid bias due to unequal liquid samples.

Further product characterization analyses were carried out only for the left-over mass of run R-113B, and the data obtained are given in Table C.13 for EG and DEG content before and after saponification of product using gas liquid chromatography (Ch. IV); in Table C.14 for total 2-methoxy-ethanol produced during reaction and determined by GLC bracketing technique. The data in Table C.15 are total methyl-ester group content in left-over mass while the data in Table C.16 give the total free carboxylic group content in the same batch. Procedures for the above determinations are described in Ch. IV while calculations are indicated in the Tables or were given previously.

Gas chromatographic analysis of distillate was performed only for run R-116B and the data are given in Table C.17. In this table the methanol content in the sample is calculated from the regression equation given in Ch. IV. Then, the mass fraction is obtained by dividing with the sample mass given in the third column.

Table C.2

Experimental Data of Run R-112B

122.2 g Ethylene Glycol; 194.3 g Dimethyl Terephthalate; Molar Ratio: 1.968 Temperature: 146°C; Mixing Level: 200 rpm 30.0 g Amberlyst 15, -45 + 50 mesh									
Time (min)	Distillate (g)	Liquid Sample (g)	Solvent Volume (ml)	Peak Area Ratio					
				EG	DEG	DMT	MHET	BHET	
22.0	7.82	0.0336	1.0	0.318	*****	0.519	0.210	*****	
50.0	14.04	0.6933	5.0	0.629	0.208	1.220	1.411	0.493	
71.0	8.44	2.5091	20.0	0.421	0.214	0.747	1.275	0.623	
87.0	6.40	0.6560	5.0	0.292	0.209	0.568	1.109	0.614	
101.0	4.58	0.4409	5.0	0.129	0.129	0.292	0.698	0.411	
124.0	5.88	0.6185	5.0	0.128	0.164	0.256	0.725	0.504	

Table C.3

Experimental Data of Run R-113B

122.2 g Ethylene Glycol; 194.2 g Dimethyl Terephthalate; Molar Ratio: 1.969 Temperature: 146°C; Mixing Level: 350 rpm 30.0 g Amberlyst 15, -45 + 50 mesh									
Time (min)	Distillate (g)	Liquid Sample (g)	Solvent Volume (ml)	Peak Area Ratio					
				EG	DEG	DMT	MHET	BHET	
15.0	4.59	0.7812	15.0	0.487	*****	0.944	0.288	*****	
30.0	7.67	3.7721	20.0	0.557	0.032	*****	0.361	0.019	
46.0	8.82	3.1963	20.0	0.966	0.257	1.540	1.564	0.444	
60.0	7.10	2.9332	20.0	0.622	0.244	1.026	1.355	0.520	
75.0	6.86	1.4516	10.0	0.440	0.258	0.732	1.114	0.578	
100.0	9.10	0.8226	10.0	0.126	0.123	0.233	0.550	0.328	
124.0	6.83	2.2682	20.0	0.102	0.143	0.188	0.550	0.369	
				0.112	0.150	0.174	0.487	*****	

Table C.4

Experimental Data of Run R-114B

122.2 g Ethylene Glycol; 194.2 g Dimethyl Terephthalate; Molar Ratio: 1.969 Temperature: 146°C; Mixing Level: 350 rpm 30.0 g Amberlyst 15, -16 + 18 mesh									
Time (min)	Distillate (g)	Liquid Sample (g)	Solvent Volume (ml)	Peak Area Ratio					
				EG	DEG	DMT	MHET	BHET	
22.0	7.00	0.6537	10.0	0.580	*****	1.144	0.346	0.026	
30.0	2.52	0.9732	15.0	0.514	0.044	1.021	0.464	0.057	
60.0	13.41	0.7974	5.0	0.883	0.039	1.450	1.415	0.515	
76.0	6.61	0.7614	5.0	0.643	0.235	1.058	1.369	0.588	
100.0	9.23	1.1860	10.0	0.358	0.201	0.544	0.872	0.385	
				0.337	0.186	0.538	1.034	0.579	
				0.337	0.199	0.549	*****	0.618	
124.0	7.36	1.5105	10.0	0.312	0.245	0.426	0.936	0.597	
				0.308	0.235	0.427	0.924	0.516	

Table C.5

Experimental Data of Run R-115B

122.2 g Ethylene Glycol; 194.2 g Dimethyl Terephthalate; Molar Ratio: 1:969 Temperature: 146°C; Mixing Level: 200 rpm 30.0 g Amberlyst 15, -16 + 18 mesh									
Time (min)	Distillate (g)	Liquid Sample (g)	Solvent Volume (ml)	Peak Area Ratio					
				EG	DEG	DMT	MHET	BHET	
15.0	6.75	1.0151	15.0	0.654	*****	*****	0.270	*****	
30.0	6.46	0.8471	10.0	0.729	0.061	*****	0.600	0.086	
45.0	6.32	1.2914	15.0	0.648	0.094	1.068	0.715	0.136	
60.0	6.17	2.2926	20.0	0.693	0.164	1.088	1.014	0.317	
75.0	5.66	1.5861	10.0	0.771	0.259	1.132	1.337	0.503	
100.0	7.90	1.2220	10.0	0.451	0.222	0.569	0.755	0.271	
124.0	6.32	2.2036	15.0	0.333	0.235	0.465	0.923	0.574	

Table C.6
Experimental Data of Run R-116B
 186.2 g Ethylene Glycol; 145.6 g Dimethyl Terephthalate; Molar Ratio: 4.00
 Temperature: 146°C; Mixing Level: 350 rpm
 30.0 g Amberlyst 15, -35 + 40 mesh

Time (min)	Distillate (g)	Liquid Sample (g)	Solvent Volume (ml)	Peak Area Ratio				
				EG	DEG	DMT	MHET	BHET
15.0	6.42	0.4868	10.0	0.729	0.026	0.599	0.239	*****
30.0	6.87	0.2153	5.0	0.599	0.053	0.395	0.321	0.051
45.0	6.54	0.4606	5.0	1.131	0.191	0.588	0.745	0.266
60.0	5.80	0.5146	5.0	1.170	0.285	0.454	0.866	0.436
75.0	5.00	0.3337	4.0	0.782	0.239	0.242	0.663	0.450
100.0	6.95	0.2822	2.0	1.188	0.555	0.242	0.828	0.708
125.0	5.43	0.3659	2.0	1.431	0.846	0.157	0.812	1.138

Table C.7

Experimental Data of Run R-117B

248.3 g Ethylene Glycol; 48.6 g Dimethyl Terephthalate; Molar Ratio: 16.00 Temperature: 146°C; Mixing Level: 350 rpm 30.0 g Amberlyst 15, -35 + 40 mesh							
Time (min)	Distillate (g)	Liquid Sample (g)	Solvent Volume (ml)	Peak Area Ratio			
				DEG	DMT	MHET	BHET
10.0	1.44	0.2842	2.0	0.107	0.568	0.330	*****
20.0	2.60	0.3452	3.0	0.179	0.286	0.354	0.067
32.0	2.63	0.3989	3.0	0.333	0.184	0.463	0.211
42.0	1.81	0.5974	4.0	0.477	0.135	0.440	0.254
60.0	2.73	0.2859	2.0	0.479	0.131	0.459	0.335
80.0	2.25	0.3940	3.0	0.477	0.124	0.512	0.339
100.0	1.67	0.7136	5.0	0.636	0.051	0.316	0.354
				0.738	*****	0.269	0.590
				0.974	*****	0.189	0.607
				*****	*****	0.185	0.618

Table C.8

Experimental Data of Run R-118B

248.3 g Ethylene Glycol; 48.6 g Dimethyl Terephthalate; Molar Ratio: 16.00 Temperature: 146°C; Mixing Level: 350 rpm 15.0 g Amberlyst 15, -140 # 325 mesh							
Time (min)	Distillate (g)	Liquid Sample (g)	Solvent Volume (ml)	Peak Area Ratio			
				DEG	DMT	MHET	BHET
30.0	3.32	0.1088	1.0	0.119	0.259	0.175	*****
45.0	2.18	0.3054	2.0	0.312	0.230	0.402	0.16
60.0	1.91	0.3931	3.0	0.488	0.118	0.464	0.374
				0.459	0.143	0.486	0.358
				0.456	0.144	0.509	0.371
67.0	0.85	0.4036	3.0	0.445	0.119	0.321	0.177
101.0	3.10	0.2591	2.0	0.582	0.032	0.196	0.250
120.0	1.31	0.1126	1.0	0.549	*****	0.196	0.378

Table C.9

Experimental Component Profiles

	Time (min)	Cumulative Distillate (g)	EG (moles)	DEG (moles)	DMT (moles)	MHET (moles)	BHET (moles)
R-112B	0.0	0.00	1.9687	0.0000	1.0006	0.0000	0.0000
	22.0	7.82	1.4770	*****	0.6421	0.1980	*****
	50.0	21.86	0.6765	0.0532	0.3495	0.3074	0.0886
	71.0	30.30	0.4865	0.0588	0.2298	0.2983	0.1201
	87.0	36.70	0.3175	0.0536	0.1641	0.2431	0.1106
	101.0	41.28	0.2072	0.0484	0.1243	0.2242	0.1083
	124.0	47.16	0.1455	0.0430	0.0775	0.1636	0.0930
	0.0	0.00	1.9687	0.0000	1.0001	0.0000	0.0000
R-113B	15.0	4.59	1.4774	*****	0.7617	0.1771	*****
	30.0	12.26	0.4575	0.0063	*****	0.0600	0.0026
	46.0	21.08	0.8993	0.0563	0.3795	0.2931	0.0682
	60.0	28.18	0.6218	0.0567	0.2705	0.2702	0.0848
	75.0	35.04	0.4411	0.0590	0.1929	0.2204	0.0927
	100.0	44.14	0.2301	0.0484	0.091	0.1866	0.0898
	124.0	50.97	0.1485	0.0409	0.0645	0.1272	0.0719
	0.0	0.00	1.9687	0.0000	1.0001	0.0000	0.0000

Table C.10
Experimental Component Profiles

	Time (min)	Cumulative Distillate (g)	EG (moles)	DEG (moles)	DMT (moles)	MHET (moles)	BHET (moles)
R-114B	0.0	0.00	1.9687	0.0000	1.0001	0.0000	0.0000
	22.0	7.00	1.3903	*****	0.7300	0.1680	0.0106
	30.0	9.52	1.2325	0.0252	0.6511	0.2250	0.0228
	60.0	22.93	0.8253	0.0087	0.3612	0.2668	0.0797
	76.0	29.54	0.6169	0.0529	0.2709	0.2642	0.0932
	100.0	38.77	0.4134	0.0546	0.1748	0.2288	0.1037
	124.0	46.13	0.2888	0.0512	0.1072	0.1715	0.0838
	0.0	0.60	1.9687	0.0000	1.0001	0.0000	0.0000
R-115B	15.0	6.75	1.5150	*****	*****	0.1270	*****
	30.0	13.21	1.3217	0.0261	*****	0.2200	0.0260
	45.0	19.53	1.1334	0.0387	0.4934	0.2524	0.0395
	60.0	25.70	0.8931	0.0498	0.3701	0.2632	0.0674
	75.0	31.36	0.7085	0.0554	0.2741	0.2460	0.0758
	100.0	39.26	0.5295	0.0600	0.1762	0.1767	0.0518
	124.0	45.58	0.3284	0.0516	0.1193	0.1756	0.0882
	0.0	0.60	1.9687	0.0000	1.0001	0.0000	0.0000

g

Table C.11

Experimental Component Profiles for Run R-116B

Time (min)	Cumulative Distillate (g)	EG (moles)	DEG (moles)	DMT (moles)	MHET (moles)	BHET (moles)
0.0	0.00	2.9998	0.0	0.7498	0.0	0.0
15.0	6.42	2.4647	0.0209	0.5396	0.1640	*****
30.0	13.29	2.2417	0.0473	0.3936	0.2431	0.0317
45.0	19.83	1.9373	0.0776	0.2688	0.2583	0.0758
60.0	25.63	1.7617	0.1017	0.1825	0.2639	0.0993
75.0	30.63	1.4303	0.1031	0.1185	0.2450	0.0866
100.0	37.58	1.2570	0.1385	0.0694	0.1771	0.1243
125.0	43.01	1.1470	0.1596	0.0351	0.1319	0.1510

Table C.12
Experimental Component Profiles

	Time (min)	Cumulative Distillate (g)	DEG (moles)	DMT (moles)	MHET (moles)	BHET (moles)	
R-117B	0.0	0.00	0.0000	0.2500	0.0000	0.0000	
	10.0	1.44	0.0267	0.1590	0.0704	*****	
	20.0	4.04	0.0547	0.0980	0.0924	0.0145	
	32.0	6.67	0.0871	0.0542	0.1035	0.0387	
	42.0	8.48	0.1105	0.0339	0.0930	0.0503	
	60.0	11.21	0.1520	0.0140	0.0648	0.0595	
	80.0	13.46	0.1903	*****	0.0595	0.1069	
	100.0	15.13	0.2297	*****	0.0382	0.1015	
	R-118B	0.0	0.00	0.0000	0.2500	0.0000	0.0000
		30.0	3.32	0.0385	0.0939	0.0485	*****
45.0		5.50	0.0715	0.0591	0.0786	0.0267	
60.0		7.41	0.1239	0.0402	0.1099	0.0647	
67.0		8.26	0.1144	0.0343	0.0705	0.0320	
101.0		11.36	0.1538	0.0096	0.0445	0.0465	
120.0		12.67	0.1661	*****	0.0508	0.0802	

Table C.13

Free and Esterified Glycols

Sample Treatment	Sample Mass (g)	Solvent Volume (ml)	Peak Area Ratio		Component* (moles)	
			EG	DEG	EG	DEG
None	5.0	50	0.041	0.077	0.1049	0.0470
Saponification	2.5	50	0.323	0.420	0.8259	0.2548

* In 252 g of left-over mass

Table C.14

Mass of 2-Methoxy-Ethanol

Source	2-Methoxy-Ethanol* (moles)
Liquid Product	0.1128
Distillate	0.0109
Total	0.1237

* In 252 g of left-over mass

Table C.15

Total Carboxylic Groups

Solution	Reagent	Reagent Volume (ml)
Blank	1 N NaOH	50.25
	1 N HCl	50.90
Sample (2.5g)	1 N NaOH	50.25
	1 N HCl	31.0

1 N NaOH for Saponification of 2.5 g Sample =
 $= 50.25 - [31.0 - (50.25 - 50.9)] = 19.9 \text{ ml}$

Total Carboxylic Groups = $\frac{19.9}{1000} \times \frac{252}{2.5} =$
 $= 2.006 \text{ equivalents}$

Table C.16

Total Free Carboxylic Groups

Solution	1 N NaOH (ml)
Blank	6.18
Sample (1.0g)	6.85

1 N NaOH for Free Acid of 1.0 g
Sample = 6.85 - 6.18 = 0.67 ml

Total Free Carboxylic Groups =

$$\frac{0.67}{1000} \times \frac{252}{1} = 0.1688 \text{ equivalents}$$

Table C.17

Methanol Profile for Run R-116B

Time (min)	Distillate (g)	Sample (g)	Peak Area Ratio	Methanol Mass Fraction	Methanol (g)	Cumulative Methanol (moles)
15.0	6.42	0.2428	0.910	0.9070	5.823	0.1816
30.0	6.87	0.2487	0.879	0.8556	5.878	0.3652
45.0	6.54	0.2636	0.787	0.7178	4.694	0.5115
60.0	5.80	0.2514	0.778	0.7489	4.344	0.6470
75.0	5.00	0.2562	0.779	0.7357	3.678	0.7619
100.0	6.95	0.2549	0.782	0.7430	5.164	0.9229
125.0	5.43	0.2585	0.760	0.7118	3.865	1.0433

APPENDIX D

EXPERIMENTAL DATA FOR HOMOGENEOUS CATALYSIS

The experimental methanol data which were used in the analysis of the homogeneously catalyzed transesterification are given below.

One set of non-isothermal data were given by Fontana where the catalyst used was lead oxide. The experimental data are: time, methanol produced and reaction temperature, and they are given in Table D.1 along with the methanol production rates reported by him [Table III of 13]. Also one set of near-isothermal data [Table II of 13] was given by Fontana and presented here in Table D.2. By excluding the initial temperature point and assuming that the reaction temperature varies linearly between successive points, the average reaction temperature, $\bar{\theta}$, for the near-isothermal data was estimated from

$$\bar{\theta} = \frac{\int_5^{60} \theta(t) dt}{\int_5^{60} t dt} \quad (D-1)$$

and found to be 180°. In Eq. (D-1) $\theta(t)$ is the instantaneous reaction temperature as assumed above.

Tomita and Ida did not report any data in tabular form, so the present author had to obtain numerical data by reading off values from the reported graphs [18]. The probable error in doing so is within $\pm 1\%$, and, therefore, the data as read are not considered biased in any respect. Table D.3 reports data obtained from Fig. 2 of [16], while Table D.4 and D.5 report data read off from Fig. 5 of [16]. The data reported in Table D.6 were obtained from Fig. 10 of the same reference.

Peebles and Wagner [12] reported their data of four replicate runs in a single graph, and the data used by the author were read off from Fig. 2 of the reference. The values presented in Table D.7 correspond to the average conversion, visually located, at the indicated time.

Neither Tomita and Ida nor Peebles and Wagner reported values for the reaction volume. Though an attempt was made to estimate the initial and 100% conversion volumes from Tomita and Ida's graphs, it was decided to estimate the reaction volume using the functions reported by Fontana [13] and given by the following equations

$$V_r^t = V_{DMT}^t N_{DMT}^0 + V_{EG}^t N_{EG}^0 - V_M^t N_M^t \quad (D-2)$$

$$V_{DMT}^t = 0.1915[1 + 0.0014(\theta - 140)] \quad (D-3)$$

$$V_{EG}^t = 0.0606[1 + 0.0014(\theta - 140)] \quad (D-4)$$

$$V_M^t = 0.0439[1 + 0.0014(\theta - 140)] \quad (D-5)$$

where V_r^t is the reaction volume at time t , V_{DMT}^t , V_{EG}^t , V_M^t are the molar volumes of DMT, EG and methanol, respectively, at time t , N_{DMT}^0 and N_{EG}^0 are the moles of DMT and EG initially taken, N_M^t are the moles of methanol produced up to time t and θ is the reaction temperature in degrees Centigrade. For the non-isothermal transesterification data, the reaction temperature varies with time, and therefore, the molar volumes become functions of time.

TABLE D.1

Fontana's Non-Isothermal Data

$N_{DMT}^{\circ} = 0.5, N_{EG}^{\circ} = 1.0$ Catalyst: Lead Oxide, $N_C = 2.32 \times 10^{-4}$			
Time, min	Methanol, moles	Rate, (moles / min) $\times 10^2$	Temperature, $^{\circ}C$
0.0	0.058	-	152.2
5.0	0.197	3.2	167.2
10.0	0.365	3.2	173.2
15.0	0.515	2.8	180.1
20.0	0.636	2.4	184.1
25.0	0.755	2.0	193.0
30.0	0.857	1.4	204.0
35.0	0.906	0.9	207.9
65.0	0.999		228.2

TABLE D.2

Fontana's Near-Isothermal Data

$N^{\circ} = 0.5$, $N_{EG}^{\circ} = 1.0$ DMT Catalyst: Zinc Acetate, $N_C = 1.81 \times 10^{-4}$ Average Temperature: 180°C			
Time, min	Methanol, moles	Rate, $\frac{\text{moles}}{\text{min}} \times 10^2$	Temperature, $^{\circ}\text{C}$
0.0	0.035		158.2
5.0	0.172	2.70	180.2
10.0	0.296	2.36	179.2
15.0	0.426	1.90	182.1
20.0	0.504	1.55	179.2
28.0	0.620	1.06	181.2
35.0	0.677	0.82	180.2
43.0	0.721	0.66	174.2
50.0	0.762	0.55	179.2
60.0	0.813	0.48	187.1

TABLE D.4

Tomita and Ida's Data Set #2

$N_{DMT}^{\circ} = 0.5$, $N_{EG}^{\circ} = 1.0$ Catalyst: Zinc Acetate, $N_C = 0.7 \times 10^{-4}$ Temperature: 197°C	
Time, min.	Methanol, moles
10.8	0.182
20.6	0.369
30.4	0.478
51.0	0.623
70.7	0.704
91.4	0.754

TABLE D.3

Tomita and Ida's Data Set #1

$N_{DMT}^{\circ} = 0.5$, $N_{EG}^{\circ} = 1.0$ Catalyst: Zinc Acetate, $N_C = 1.0 \times 10^{-4}$ Temperature: 197°C	
Time, min.	Methanol, moles
15.0	0.381
30.0	0.555
60.0	0.738
90.0	0.820
120.0	0.873
140.0	0.884

TABLE D.5
Tomita and Ida's Data Set #3

$N_{DMT}^{\circ} = 0.5$, $N_{EG}^{\circ} = 1.0$ Catalyst: Zinc Acetate, $N_C = 0.5 \times 10^{-4}$ Temperature: 197°C	
Time, min.	Methanol, moles
12.4	0.166
16.8	0.237
31.3	0.386
39.3	0.461
61.3	0.574
70.5	0.613
99.0	0.692

TABLE D.6

Tomita and Ida's Data Set #4

$N_{DMT}^{\circ} = 0.5$, $N_{EG}^{\circ} = 1.0$ Catalyst: Zinc Acetate, $N_C = 1.0 \times 10^{-4}$ Temperature: 180°C	
Time, min.	Methanol, moles
30.0	0.481
60.0	0.679
90.0	0.782
120.0	0.826
135.0	0.840

TABLE D.7

Peebles and Wagner's Data

N _{DMT} = 0.953, N _{EG} = 3.58 Catalyst: Zinc Acetylacetonate, N _C = 5.51x10 ⁻⁴ Temperature: 175°C	
Time, min.	Methanol, moles
11.3	0.438
20.0	0.762
30.4	1.039
40.0	1.266
49.2	1.414
60.0	1.550
69.6	1.626
80.0	1.683

APPENDIX E
ANALYTICAL INTEGRATION OF METHYL-ESTER
GROUP MODEL

The methyl-ester group model given in terms of conversion by Eq. (IX-12), i. e.

$$\frac{dx}{dt} = k_a C_{E_0} \frac{(1-x)(M-x)}{(1-\epsilon x)^2} \quad (E-1)$$

was integrated by the method of separation of variables.

Equation (E-1) is rewritten as in Eq. (E-2)

$$\frac{(1-\epsilon x)^2}{(1-x)(M-x)} dx = k_a C_{E_0} dt \quad (E-2)$$

which may be integrated for M equal to one and M different from one.

For M different from one, Eq. (E-2) upon expansion becomes

$$k_a C_{E_0} dt = \frac{(1-2\epsilon x + \epsilon^2 x^2)}{[x^2 - (M+1)x + M]} dx \quad (E-3)$$

which, when integrated, yields

$$k_a C_{E_0} t = \int_0^x \frac{dx}{[x^2 - (M+1)x + M]} - 2\epsilon \int_0^x \frac{xdx}{[x^2 - (M+1)x + M]} + \epsilon^2 \int_0^x \frac{x^2 dx}{[x^2 - (M+1)x + M]} \quad (E-4)$$

Now, since,

$$(M+1)^2 - 4M = (M-1)^2 > 0 \quad (E-5)$$

we have [49]

$$\int \frac{dx}{[x^2 - (M+1)x + M]} = \frac{1}{(M-1)} \ln \left(\frac{M-x}{1-x} \right) \quad (E-6)$$

$$\int \frac{x dx}{[x^2 - (M+1)x + M]} = \frac{1}{2} \ln[x^2 - (M+1)x + M] + \frac{(M+1)}{2(M-1)} \ln \left(\frac{M-x}{1-x} \right) \quad (E-7)$$

and

$$\int \frac{x^2 dx}{[x^2 - (M+1)x + M]} = x + \frac{(M+1)}{2} \ln[x^2 - (M+1)x + M] + \frac{(M-1)}{2} \ln \left(\frac{M-x}{1-x} \right) \quad (E-8)$$

Upon substitution of Eqs. (E-6), (E-7) and (E-8) in Eq. (E-4), suitable manipulations and insertion of the integration limits there is obtained

$$k_a C_{E_0} = \epsilon^2 x + \left[\frac{2 - 2(M+1)\epsilon + (M-1)\epsilon^2}{2(M-1)} \right] \ln \left[\frac{(M-x)}{M(1-x)} \right] + \frac{\epsilon}{2} [\epsilon(M+1) - 2] \ln \left[\frac{(1-x)(M-x)}{M} \right] \quad (E-9)$$

or

$$k_a t = \frac{1}{C_{E_0}} \{ \alpha x + \beta \ln \left[\frac{(M-x)}{M(1-x)} \right] + \gamma \ln \left[\frac{(1-x)(M-x)}{M} \right] \} \quad (E-10)$$

where

$$\alpha = \epsilon^2 \quad (\text{E-11})$$

$$\beta = \frac{2 - 2(M+1)\epsilon + (M-1)^2\epsilon^2}{2(M-1)} \quad (\text{E-12})$$

$$\gamma = \frac{\epsilon}{2} [\epsilon(M+1) - 2] \quad (\text{E-13})$$

Eq. (E-10) is the integrated form of the methyl-ester group model when M is different from one, and plotting of the right-hand side versus time should result in a straight line passing through the origin if the assumed model is valid.

For M equal to one Eq. (E-2) becomes

$$k_a C_{E_0} dt = \frac{(1 - 2\epsilon x + \epsilon^2 x^2) dx}{(1-x)^2} \quad (\text{E-14})$$

which upon integration yields

$$k_a C_{E_0} t = \int_0^x \frac{dx}{(1-x)^2} - 2\epsilon \int_0^x \frac{x dx}{(1-x)^2} + \epsilon^2 \int_0^x \frac{x^2 dx}{(1-x)^2} \quad (\text{E-15})$$

The indefinite integrals are as follows [49]

$$\int \frac{dx}{(1-x)^2} = \frac{1}{(1-x)} \quad (\text{E-16})$$

$$\int \frac{x dx}{(1-x)^2} = \frac{1}{(1-x)} + \ln(1-x) \quad (\text{E-17})$$

and

$$\int \frac{x^2 dx}{(1-x)^2} = \frac{(1-x) + 1}{(1-x)} + \ln(1-x) \quad (\text{E-18})$$

and when the above integrals are substituted in Eq. (E-15) and the various operations carried through there is obtained

$$k_a C_{E_0} t = \epsilon^2 x + (\epsilon - 1)^2 \frac{x}{(1-x)} + 2\epsilon(\epsilon - 1) \ln(1-x) \quad (E-19)$$

or,

$$k_a t = \frac{1}{C_{E_0}} [\epsilon^2 x + (\epsilon - 1)^2 \frac{x}{(1-x)} + 2\epsilon(\epsilon - 1) \ln(1-x)] \quad (E-20)$$

which is the integrated form of the methyl-ester group model when M is equal to one. Plotting of the right-hand side of Eq. (E-20) against time should result in a straight line through the origin if the assumed model is adequate.

VITA AUCTORIS

- 1941 Born in Nea Makri, Attica, Greece
- 1959 Graduated from the First High School of Athens, Athens, Greece
- 1964 Received the degree Diploma in Chemical Engineering from the National Technical University of Athens, Athens, Greece
- 1970 Received the degree Master of Engineering in Chemical Engineering from McMaster University, Hamilton, Ontario, Canada
- 1975 Candidate for the degree Doctor of Philosophy in Chemical Engineering from the University of Windsor, Windsor, Ontario, Canada